RICE UNIVERSITY

In vivo analysis of gain-of-function mutations in the Drosophila *eag*-encoded K^+ channel.

by

Robert John Gunn Cardnell

A THESIS SUBMITTED
IN PARTIAL FULFILLMENT OF THE
REQUIREMENTS FOR THE DEGREE

DOCTOR OF PHILOSOPHY

APPROVED, THESIS COMMITTEE:

Michael Stern, Professor
Biochemistry and Cell Biology

Richard Gomer, Professor
Biochemistry and Cell Biology

Mary Ellen Lane, Assistant Professor
Biochemistry and Cell Biology

Kevin MacKenzie, Assistant Professor
Biochemistry and Cell Biology

Michael Kohn, Assistant Professor
Ecology and Evolutionary Biology

HOUSTON, TEXAS

APRIL 2006

Abstract

Neuronal Na^+ and K^+ channels elicit currents in opposing directions and thus have opposing effects on neuronal excitability. Mutations in genes encoding Na^+ or K^+ channels often interact genetically, leading either to phenotypic suppression or enhancement for genes with opposing or similar effects on excitability respectively. For example, the effects of mutations in *Shaker* (*Sh*), which encodes a K^+ channel subunit, are suppressed by loss of function mutations in the Na^+ channel structural gene *para*, but enhanced by loss of function mutations in a second K^+ channel encoded by *eag*.

Here I characterize three novel mutations that suppress the effects of a *Sh* mutation on behavior and neuronal excitability. Recombination mapping localized the mutations to the *eag* locus, and I used sequence analysis to determine that two of the mutations are caused by a single amino acid substitution (G297E) in the S2-S3 linker of Eag. Because these novel *eag* mutations confer opposite phenotypes to *eag* loss of function mutations, I suggest that eag^{G297E} causes an *eag* gain of function phenotype. I hypothesize that the G297E substitution may cause premature, prolonged or constitutive opening of the Eag channels by favoring the "unlocked" state of the channel. The third mutation has two amino acid substitutions in Eag (A259V and E762V) and may also be a gain of function allele of *eag*. Interestingly, these mutations appear to manifest their most obvious phenotypes under conditions that prolong the action potential.

Acknowledgements

I would particularly like to thank my thesis advisor, Dr. Mike Stern, for his invaluable support, guidance and patience through my graduate career. I would also like to thank my thesis committee, Drs. Mary Ellen Lane, Richard Gomer and Kevin MacKenzie, for their guidance.

I would also like to thank some current and former members of the Stern lab for their assistance, often scientific, but some times purely social, namely Dr. Brett Schweers, Dr. Stephen (Fringy) Richards, Dr. Jim Yager, Dr. Yanmei Huang, Dr. Veronica Hall, Eric Howlett, Phil Caldwell, Magdalena Walkiewicz, Will Lavery, Shelly Wells, Rupsa Chadhaury, Matt Fay, Niral Gandhi, Melissa Sanchez and Jeff Blackington.

I would finally like to thank my family and friends for helping me through the tough times and to celebrate the good times. In particular I would like to thank the following friends: Damian Dalle Nogare, Angela Hvitved, Michael Texada, Chuck Throckmorton, Laura Williams, Willie Gordon, Richard Barker, Rachel Schweers and Elisa Johnston.

Table of Contents

List of Figures and Tables

List of Abbreviations

4-AP	4-amino pyridine
bEAG	bovine EAG
Ca^{2+}	calcium ion
DmEag	Drosophila Eag
dsRNA	double-stranded RNA
ejc	excitatory junctional current
ejp	excitatory junctional potential
EMS	ethyl methane sulfonate
GAL4	transcription factor
I	current
I_A	Transient K^+ A current
I_{CF}	Fast Ca^{2+} activated K^+ current
I_{CS}	Slow Ca^{2+} activated K^+ current
I_K	Delayed rectifier K^+ current
K^+	potassium ion
LTF	long term facilitation
mejp	spontaneous mini excitatory junctional potential
Mg^{2+}	magnesium ion
nmj	neuromuscular junction
Na^+	sodium ion
PCR	polymerase chain reaction
PNS	peripheral nervous system

rEAG	rat EAG
RFLP	restriction fragment length polymorphism
RNAi	RNA mediated interference
RT-PCR	reverse transcription PCR
SEM	standard error of the mean
TEA	tetraethylammonium
UAS	upstream activating sequence
$\overline{XX}$	attached X

List of Genes

ala	*CamKII inhibitor peptide*
CamKII	*calcium/calmodulin dependent kinase II*
Cha	*choline acetyl transferase*
eag	*ether-à-go-go* (K^+ channel subunit)
elav	*embryonic lethal abnormal visual system*
Elk	*eag-like* (K^+ channel subunit)
Erg	*eag-related-gene* (K^+ channel subunit)
gli	*gliotactin*
Hk	*hyperkinetic* (K^+ channel subunit)
ine	*inebriated* (Na^+/Cl^- dependent neurotransmitter transporter)
itpr	*inositol-1,4,5-triphosphate receptor*
mle^{nap}	*male-less: no-action-potential*
nap	*no-action-potential*; now known as *mle*
pum	*pummillio* (translational repressor)
para	*paralytic* (Na^+ channel structural subunit)
plc	*phospholipase C*
push	*pushover* (also known as *purity of essence*)
Rap1	GTPase (also known as *roughened)*
Ras1	*Ras* GTPase
Sh	*Shaker* (K^+ channel subunit)
Slo	*slow-poke* (K^+ channel subunit)
VAChT	*vesicular acetylcholine transporter*

Chapter 1: Background

1.1 Significance

1.1.1 K^+ channel disorders

Defects in potassium (K^+) channel function cause a wide range of diseases termed potassium channelopathies. These channelopathies encompass diseases such as episodic ataxia (e.g., D'ADAMO *et al.* 1999), myokymia (DEDEK *et al.* 2001), epilepsy (SCHROEDER *et al.* 1998), arrhythmia (SANGUINETTI 1999), and deafness (VAN HAUWE *et al.* 2000). Furthermore, loss of normal K^+ channel function can enhance tumor growth (MEYER and HEINEMANN 1998; MEYER *et al.* 1999; PARDO *et al.* 1999; SMITH *et al.* 2002; SUZUKI and TAKIMOTO 2004). K^+ channel gain of function mutations have been identified in patients with diseases such a familial atrial fibrillation (CHEN *et al.* 2003) and have also been associated with the low prevalence of diseases such as diastolic hypertension in some populations (FERNANDEZ-FERNANDEZ *et al.* 2004). Consequently, understanding how K^+ channels function, how they are regulated and how they interact with other membrane components is of substantial importance.

1.1.2 Drosophila neuronal excitability

The Drosophila third instar larva provides a unique system to explore the effects of mutant genes upon the excitability of the motor axon. Many genes have been identified as having roles in Drosophila motor axon excitability and a significant proportion of these have human homologues (GANETZKY 2000). This model system thus provides an opportunity to explore possible roles for these genes in humans, with the end goal of the further understanding of human nervous system conditions such as those mentioned in chapter 1.1.1.

1.2 Drosophila larval peripheral nerve

The Drosophila peripheral nerve contains both motor and sensory axons surrounded by peripheral glial cells, which are analogous to mammalian Schwann cells (SEPP *et al.* 2000). A second glial layer, the perineural glia (the perineurium in mammals) wraps both the axons and the peripheral glia. The perineural glia is believed to be mesodermally derived, it is absent in mutants such as *twist* that lack the mesoderm (EDWARDS *et al.* 1993).

The peripheral glia, which is a subset of the surface glia, create the Drosophila equivalent of the blood-brain barrier that is primarily responsible for shielding the nervous system against the high potassium levels of the hemolymph (SCHWABE *et al.*

2005). In peripheral nerves the peripheral glia form a single-cell tube that envelopes the axons and is sealed with septate junctions. These septate junctions are created and maintained at least in part by a G-protein signaling pathway in the peripheral glia. There are a number of genes that appear to be – at least in the peripheral nervous system (PNS) – expressed in only the peripheral glia; these include *gliotactin* (*gli*), *moody*, and *Neuroglian* (*Nrg*) (AULD *et al.* 1995; BAINTON *et al.* 2005; SCHWABE *et al.* 2005)

1.3 The resting potential and action potential

An axon is part of a single cell that is able to convey a uni-directional electrical signal. The resting potential is generated by differences in ionic concentrations across the axonal membrane and the selective permeability of that membrane. At rest, the inside of the axon is negatively charged with respect to outside. Whereas signaling between axons or between axons and other tissues such as muscle is usually chemical in nature, the signal within the axon – the action potential – is a result of a depolarization and subsequent repolarization of the membrane.

The resting potential, or the resting electrochemical potential of the membrane (E_m), is the sum of all the relevant ions individual electrochemical potentials (I_i). The electrochemical potential for each individual ionic species can be calculated using the "Nernst Equation" (Figure 1.1, equation 1). The E_m is found by combining the individual electrochemical potentials for the ionic species that contribute to the membrane potential

The electrochemical potential across a membrane for an individual ionic species:

$$E_i = (E_2 - E_1) = -\frac{RT}{zF}\ln\left(\frac{C_2}{C_1}\right) \qquad \textit{"Nernst Equation"} \qquad (1)$$

Thus for all the ionic species important to neural activity:

$$Em = -\frac{RT}{F}\ln\left(\frac{P_K[K]_o + P_{Na}[Na]_o - P_{Cl}[Cl]_o}{P_K[K]_i + P_{Na}[Na]_i - P_{Cl}[Cl]_i}\right) \qquad \textit{"Goldman Constant Field Equation"} \qquad (2)$$

But as Cl^- ions are distributed passively across the membrane:

$$Em = -\frac{RT}{F}\ln\left(\frac{P_K[K]_o + P_{Na}[Na]_o}{P_K[K]_i + P_{Na}[Na]_i}\right) = \frac{RT}{F}\ln\left(\frac{[Cl]_i}{[Cl]_o}\right) \qquad (3)$$

If:

$$b = \frac{P_{Na}}{P_K} \qquad (4)$$

Then:

$$Em = -\frac{RT}{F}\ln\left(\frac{[K]_o + b[Na]_o}{[K]_i + b[Na]_i}\right) \qquad (5)$$

Figure 1.1 The ionic basis of the membrane resting potential

The membrane potential is a consequence of an uneven balance of ions across a selectively permeable membrane. Potassium (K^+), sodium (Na^+), and chloride (Cl^-) are the major ions involved. Combining their individual membrane potentials, E_i, gives the membrane potential (E_m). Because Cl^- is distributed passively across the membrane, it can be excluded from the calculation. The introduction of b, the relative membrane permeances of Na^+ to K^+, allows a simplified formula. C = concentration, F = Faraday's constant, P = permeability, R = gas constant, T = temperature, $[X]_o$ = concentration outside, $[X]_i$ = concentration inside, z = valence.

(K^+, Na^+ and Cl^-). The formula for Em is called the "Goldman Constant Field Equation" (Figure 1.1, equation 2). In many species, including Drosophila, Cl^- ions are distributed passively across the membrane, allowing the Goldman Constant Field Equation to be simplified to include only K^+ and Na^+ or only Cl^- (Figure 1.1, equation 3). Introducing "b", the ratio of the membrane permeability of Na^+ and K^+ (Figure 1.1, equation 4), allows the Goldman Constant Field Equation to be simplified yet further (Figure 1.1, equation 5). At rest, the membrane is mostly impermeable to K^+ and Na^+, with a higher concentration of K^+ within the axon with respect to outside, and a higher concentration of Na^+ outside. The unequal distribution of K^+ and Na^+ across the membrane is created and maintained by a Na^+/K^+ ATPase pump that transports Na^+ out of the axon and K^+ into the axon. In the absence of the pump, the unequal ionic distribution will gradually decay to equilibrium.

A simplified action potential consists of two major components: a Na^+-driven depolarization, and a K^+-driven repolarization (Figure 1.3). The opening of Na^+ channels in the membrane allows a small current of Na^+ ions to enter the axon, diffusing down their electrochemical gradient (Figure 1.2, equation 2). Consequently "b" increases (Figure 1.2, equation 1), and the relative concentrations of Na^+ change. The result is a rapid increase (i.e., from a very negative potential to a positive one) of the membrane potential as computed by the Goldman Constant Field Equation (Figure 1.1, equations 2 and 6). In response to this depolarization of the membrane, voltage-gated K^+ channels open, allowing a small outward current of K^+ ions. This increases the membrane K^+ conductance, decreasing "b", attenuating the depolarization and starting the

The membrane potential is a function of the internal and external concentrations of K^+ and Na^+, and the relative membrane permeability (b) to these ions. During an action potential, b increases as Na^+ channels open.

$$b = \frac{P_{Na}}{P_K} \tag{1}$$

The current of an ion (I_i) across a membrane can be computed by

$$I_i = G_i(E_m - E_i) \tag{2}$$

Where:

$$G = \frac{I}{R} \tag{3}$$

For a membrane:

$$I_m = I_c - I_i \tag{4}$$

Where:

$$I_c = C_m \frac{dV}{dt} \tag{5}$$

Voltage clamp simplifies analysis by setting:

$$\frac{dV}{dt} = 0 \tag{6}$$

Therefore:

$$I_c = 0$$

$$I_m = I_i \tag{7}$$

Figure 1.2 The ionic basis of the action potential

$_c$ = capacitive, Cm = membrane capacitance, G = membrane conductivity, I = current, $_i$ = ionic, $_m$ = membrane, P = permeability, R = resistance, t = time, V = voltage

repolarization of the membrane. The repolarization of the membrane requires the opening and closing of a series of K^+ channels that open at different rates. The transient inactivation of some channels (both Na^+- and K^+-permeant) following channel closing ensures that the wave of depolarization proceeds uni-directionally along the axon. Before a new action potential can be propagated, enough Na^+ channels must recover from inactivation; this phase during which a new action potential cannot be propagated is called the refractory period.

1.4 Neuronal excitability and ion channel interactions

K^+ channels.

There are many Drosophila K^+ channel subunits, including Shaker (Sh), Ether-á-go-go (Eag), Slowpoke (Slo), Hyperkinetic (Hk), Seizure (Sei), Elk, Ork1, Ir, Shal, Shab and Shaw, (BUTLER *et al.* 1989; ELKINS *et al.* 1986; KAPLAN and TROUT 1969; SALKOFF *et al.* 1987a; SALKOFF *et al.* 1987b; TITUS *et al.* 1997; WANG *et al.* 1997; WARMKE and GANETZKY 1994). K^+ channels fall into four families: voltage gated (K_v) (e.g., *Sh* and *eag*) (WARMKE *et al.* 1991), inward rectifier (K_{IR}) (e.g., *Ir*) (MACLEAN *et al.* 2002), tandem pore region (e.g., *Ork1*) (GOLDSTEIN *et al.* 1996), and Ca^{2+} dependent (e.g., *slo*) (ELKINS *et al.* 1986) channels. Loss-of-function mutations in a K^+ channel subunit typically result in hyperexcitability because the neuron cannot repolarize itself properly. This hyperexcitability often has behavioral phenotypes such as ether-induced leg shaking

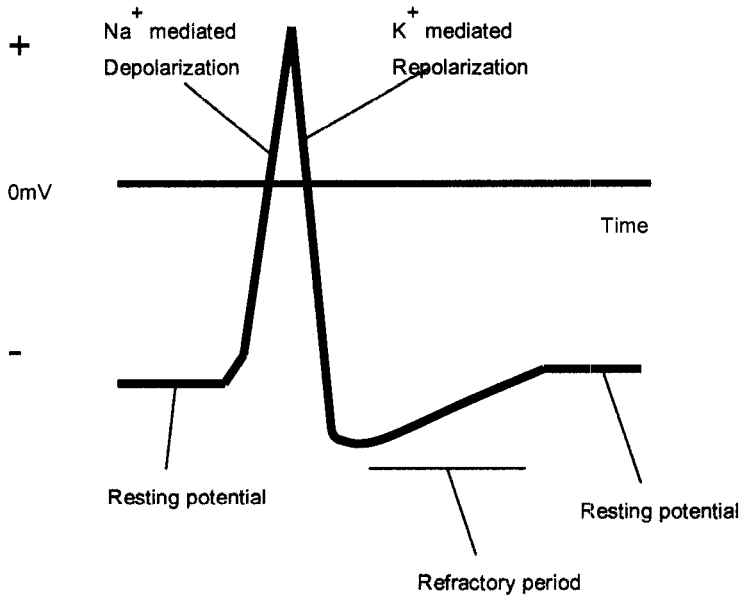

Figure 1.3 Annotated action potential

A simplified action potential. Starting from the negative resting potential, the opening of Na^+ channels causes a depolarization (negative to a positive membrane potential). The opening of voltage gated K^+ channels reverses this depolarization by allowing K^+ ions to leave the axon. The repolarization goes beyond the resting potential causing a hyperpolarization. The axon is then in a brief refractory period during which another action potential cannot be propagated.

(seen in *eag*, *Sh*, and *Hk*) (KAPLAN and TROUT 1969) and electrophysiological phenotypes such as prolonged (*Sh*) or spontaneous (*eag*) action potentials (JAN *et al.* 1977; WU *et al.* 1983). Recently, the *Sh* gene has also been suggested to play a special role in controlling Drosophila sleep (CIRELLI *et al.* 2005).

The loss of a K^+ subunit typically results in the reduction or elimination of one of the K^+ currents in the axon. As discussed in chapter 1.3, K^+ currents are a major contributor to the attenuation of the action potential and the restoration of the resting potential. Electrophysiological analysis of Drosophila larval body wall K^+ currents has revealed that the outward K^+ current (I) consists of multiple parts. These include:

I_A - transient K^+ A current (WU and HAUGLAND 1985).

I_K - delayed rectifier K^+ current (WU and HAUGLAND 1985).

I_{CF} - fast Ca^{2+} activated K^+ current (GHO and MALLART 1986).

I_{CS} - slow Ca^{2+} activated K^+ current (GHO and MALLART 1986).

Na^+ channels.

A number of Na^+ channel subunits have been identified in Drosophila, including Paralytic (Para), DSC1, Ripped pocket (Rpk), and Pickpocket (Ppk) (ADAMS *et al.* 1998; DARBOUX *et al.* 1998; JACKSON *et al.* 1984; SALKOFF *et al.* 1987a; SALKOFF *et al.* 1987b; SUZUKI *et al.* 1971). Na^+ channels fall into two families: voltage-gated (e.g., *para* and

DSC1) and ligand-gated (e.g., *ppk* and *rpk*) channels. The loss of a Na^+ channel subunit such as *para* confers a hypoexcitable phenotype to the neuron. For example, at non-permissive temperatures, the $para^{ts}$ allele confers a reversible paralysis phenotype (SUZUKI *et al.* 1971). Null alleles of *para* are, however, homozygous lethal (GANETZKY 1984).

Reciprocal interactions between channel mutations.

Reciprocal interactions are often observed between excitability mutations, allowing them to either enhance or suppress each others phenotypes (Table 1.1).

Combining mutations in the voltage-gated K^+ channel subunit genes *eag* and *Sh,* which individually confer hyperexcitability signified by ether-induced leg shaking, yields a level of hyperexcitability that is significantly increased over either single mutation. The *eag Sh* double mutant displays exaggerated ether-induced leg shaking, downturned wings, an indented thorax, and an enhancement of the *Sh*-induced electrophysiological phenotypes (GANETZKY and WU 1985; WU and GANETZKY 1986; WU *et al.* 1983). Neurotransmitter release in the double mutant is prolonged by nearly one order of magnitude as compared to either single mutant (WU *et al.* 1983). This strong synergistic interaction between *eag* and *Sh* is not always seen between other pairs of K^+ channel mutations. For example, only additive effects, restricted to their respective defects in I_A and I_{CF}, are observed when mutants of *Sh* and *Slo* are combined (SINGH and WU 1989).

Genotype	Enhances Sh^{133}	Suppresses Sh^{133}
para$^-$		✓
Dp para$^+$	✓	
eag$^-$	✓	

Table 1.1 Genetic interactions among Na^+ and K^+ channel mutations

The hypoexcitable *para* mutations suppress the Sh^{133}-induced leg shaking (STERN *et al.* 1990), whereas hyperexcitable *eag* mutations and *Dp para*$^+$ enhance the Sh^{133}-induced leg shaking (STERN *et al.* 1990). Table adapted from HUANG and STERN (2002)

Regardless of the degree of enhancement of hyperexcitability, however, combining mutations in K^+ channels produces a hyperexcitability greater than seen with either single mutation.

Whereas the combination of hyperexcitable or hypoexcitable mutations results in an exaggerated hyper- or hypo-excitable phenotype respectively, combining a hyperexcitable mutation (Sh^{133}) with a hypoexcitable mutation ($para^{63}$) results in suppression of the Sh^{133} phenotypes (STERN *et al.* 1990). The phenotypes of the two mutations are able to counteract each other and restore nearly normal neuronal function. Interestingly combining the Sh^{133} mutation with a chromosomal duplication of *para* (*Dp* $para^+$) results in an enhancement of the *Sh* mutant-behavioral phenotypes, very similar to the behaviors seen in the *eag Sh* double mutant (STERN *et al.* 1990).

It seems that hyper- and hypo-excitable channel (and other) mutations are able to interact in an additive manner to enhance or suppress each other's phenotypes (Table 1.1). This provides a hypothesis for the interpretation of new channel mutant phenotypes.

1.5 Function and structure of Eag

The first *eag* mutation was identified as a mutation that gave rise to an abnormal leg-shaking phenotype, similar to that of *Sh* (KAPLAN and TROUT 1969). The *eag* locus encodes a K^+ channel subunit of 1174 amino acids (WARMKE *et al.* 1991). Eag is the

founding member of a family of K^+ channel subunits that has three sub-families: Eag, Elk (*eag*-like K^+ channel), and Erg (*eag*-related gene) (WARMKE and GANETZKY 1994).

When measuring the neurotransmitter release at the larval neuromuscular junction of *eag* mutants, it was found that excitatory junctional potentials (ejps) at low Ca^{2+} concentrations were increased in amplitude as compared to wild type and showed a high frequency of spontaneous ejps at high [Ca^{2+}] (Figure 1.4) (WU *et al.* 1983). The spontaneous ejps are similar in time-course to those evoked by nerve stimulation and are blocked by tetrodotoxin suggesting that they are due to repetitive spontaneous firing of the motor axon (WU *et al.* 1983).

Under voltage clamped conditions, it is possible to separate the outward K^+ current from the inward Ca^{2+} current. The absence of extracellular Ca^{2+} eliminates the inward Ca^{2+} current and the Ca^{2+}-dependent K^+ current. The resultant current is biphasic and is blocked by tetraethylammonium (TEA, a voltage-gated K^+ channel blocker) as expected of a K^+ current (WU *et al.* 1983). Analysis of the current-voltage relationship in larval muscles of *eag* mutants identified a large reduction in the amplitude of the I_K component and a smaller reduction in I_A (WU *et al.* 1983; ZHONG and WU 1991; ZHONG and WU 1993). Additionally, when I_A and I_K are pharmacologically blocked, the I_{CF} and I_{CS} currents are also seen to be reduced in *eag* mutant muscles (ZHONG and WU 1991). This demonstrates that Eag contributes to at least four K^+ currents in Drosophila larval muscles, unlike Shaker and Slo, which each contribute to only one current (I_A and I_{CF} respectively) (SINGH and WU 1989; ZHONG and WU 1991). That Eag appears to contribute to a number of currents, and that none of these currents is completely

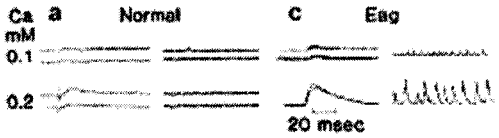

Figure 1.4 Electrophysiological traces from *eag* mutant larvae

Excitatory junctional potentials (ejps) obtained from larval neuromuscular junctions in normal (a) and *Eag* mutant (c) larvae at the Ca^{2+} concentrations indicated. ejps were evoked by stimulating the segmental nerve cut close to the ganglion (left traces) or occurred spontaneously in the same preparation without stimulation (right traces). Spontaneous ejps occurred frequently in *Eag,* but only miniature ejps were seen in normal larvae. (From: WU *et al.* 1983)

eliminated in the absence of Eag, raises the possibility that the *eag* gene contributes a subunit common to a number of different K^+ channels.

The possibility that Eag coassembles with other K^+ channel subunits is supported by the observation that, in contrast to other mutations affecting K^+ channels, the effects of *eag* mutations upon I_A and I_K are temperature sensitive. At 16°C, I_A and I_K are reduced in eag^1, eag^{4PM} and eag^{x6} with respect to wild type, but at 5°C, I_A is increased and I_K is unaltered in eag^1 with respect to wild type (ZHONG and WU 1993). The temperature dependency of the phenotypes indicates a modulatory effect.

Oocyte Expression of eag.

The expression of Drosophila RNA in *Xenopus* oocytes provides an opportunity to explore the action of a particular ion channel in isolation, because oocytes have no K^+ or Na^+ ion channels. It is hard to study individual channels *in vivo* as there are many channels present. Limitations of the oocyte expression technique include possible artifacts due to over-expression and possible improper assembly of channel subunits. It is important to note, for example, that although vertebrate Ca^{2+} and Na^+ channels contain more than one type of subunit *in vivo*, a single subunit, α_1 in Ca^{2+} channels or α in Na^+ channels, can form active, albeit slightly abnormal, channels *in vitro* (AULD *et al.* 1988; MORI *et al.* 1991).

Expression of *eag* RNA in oocytes produces a non-inactivating voltage dependent outward current (BRUGGEMANN *et al.* 1993). Macroscopic currents recorded with conventional voltage clamping have a threshold for activation between –40 and –30 mV. Furthermore, the currents are biphasic with an initial fast rising phase and a second, slower rising phase. These and other observations are consistent with a highly selective K^+ channel such as *Sh* (BRUGGEMANN *et al.* 1993).

An unexpected observation was that the initial slow rising phase of the *eag* channels is due to an inward Ca^{2+} current, as observed with the use of a Ca^{2+} sensitive fluorescent dye (Fluo-3) (BRUGGEMANN *et al.* 1993). Depolarization of voltage clamped oocytes expressing *eag* RNA showed an increase in intracellular fluorescence; this was shown to be quinidine sensitive but not $CdCl_2$ sensitive. Quinidine is known to block certain K^+ channels, whereas $CdCl_2$ blocks Ca^{2+} currents. While it is possible that the Eag channel may be able to conduct Ca^{2+}, there is no suggestion that such a conductance is physiologically relevant; indeed other papers have concluded that Eag channels do not allow a Ca^{2+} flux (e.g., ROBERTSON *et al.* 1996).

It has also been reported that the *eag* encoded channel is sensitive to cAMP. The protein includes a consensus cyclic-nucleotide-binding site (GUY *et al.* 1991), and the addition of the cAMP analogs 8-Br-cAMP or 8-Br-cGMP to the extracellular solution increases the amplitude of the K^+ current and shifts the activation threshold to a more negative voltage (BRUGGEMANN *et al.* 1993). Furthermore, the addition of 2mM cAMP (but not cGMP or ATP) to the extracelluar bath solution significantly increases the

amplitude of the K^+ current. These data are consistent with Eag being a non-inactivating, voltage dependant, cAMP sensitive K^+ channel.

The expression of *eag* RNA in oocytes leads to the production of a functional channel. Given the genetic interactions between *eag* and *Sh*, and the hypothesis that Eag may form heteromultimers, it is obvious to ask if Eag and Sh can coassemble in oocytes. The hypothesis that Eag and Sh coassemble remains controversial. Initial reports indicated that the co-expression of *eag* and *Sh* RNA's produced a current greater than the sum of the currents seen for individual RNA's (non-linear summation), suggesting that a heteromultimer was formed (CHEN *et al.* 1996). Furthermore, the coexpression of Eag (non-inactivating) with Sh (inactivating) appears to significantly decrease the time constant of current decline associated with Sh N-type inactivation (CHEN *et al.* 1996).

This concept of heteromultimerization was subsequently challenged when another group that found the current from *Eag* and *Sh* coexpression to be identical to the summed individual expressions (linear summation) (TANG *et al.* 1998). This group showed that there was no statistical difference in the inactivation time constant for *Sh* expressed alone or in the presence of *Eag*, the conclusion thus being that Eag must form only homomultimers (TANG *et al.* 1998).

Subsequently, it has become apparent that the interaction between Eag and Sh subunits depends upon the expression levels of the two RNAs and how long post-injection the recordings are made (CHEN *et al.* 2000). The expression efficiency of *eag* is

greater than that of *Sh*, hence the interaction is better seen with a lower dose of *eag* RNA relative to *Sh* RNA. For example, measurement at 5 days post-injection of 0.1ng/cell *eag* and 4ng/cell *Sh* gives nonlinear summation (indicating heteromultimers) whereas injection of 0.05ng/cell *eag* and 2ng/cell *Sh* gives linear summation (indicating formation of homomultimers). Additionally the developmental time for Eag currents in oocytes is longer than for Sh; for unknown reasons it takes more time for the Eag current amplitude to develop than the Sh current. This difference in developmental time may explain, at least in part, why adequate development is important for functional interactions among co-expressed Eag and Sh subunits (CHEN *et al.* 2000). In addition to requiring adequate developmental time, the *eag* and *Sh* RNAs must be injected simultaneously for functional interaction. Sequential injection in either order fails to give rise to a functional interaction (CHEN *et al.* 2000). The need for adequate time and co-injection may be significant for *in vivo* assembly and synaptic plasticity.

I hypothesize that Eag forms both homo- and heteromultimers *in vivo*. This could partly explain the extremely diverse responses possible in the nervous system, particularly if the variability contributes to synaptic plasticity. These two types of channels would also explain the contradictory evidence described above.

Regulation of Eag by extracellular Mg^{2+}.

It is known that the ion flux of many ion channels can be influenced by Mg^{2+} ions' entering and blocking the pore. For example, in neuronal tissues, Mg^{2+} blocks the NMDA-receptor at the extracellular side in a voltage dependent manner (MAYER *et al.* 1984; NOWAK *et al.* 1984). Mg^{2+} can interact with the cytoplasmic side of voltage-gated Na^{+} channels (PUSCH 1990), inward rectifier channels (ISHIHARA *et al.* 1989; MATSUDA *et al.* 1987), and delayed rectifier channels (LUDEWIG *et al.* 1993). Additionally, Ca^{2+} channels can be blocked at an extracellular location by Mg^{2+} (LANSMAN *et al.* 1986).

It has also been shown for most members of the Eag subfamily that the kinetics of activation are regulated by extracellular [Mg^{2+}], an effect not observed in other types of voltage-gated K^{+} channels such as Shaker and Kv1.1 channels (STUHMER *et al.* 1988; TERLAU *et al.* 1996). When expressed in oocytes, rat EAG (rEAG), bovine EAG (bEAG) and Drosophila Eag (DmEag) all display [Mg^{2+}] sensitive activation kinetics, whereas channel deactivation and the steady-state current-voltage relationship are insensitive to extracellular [Mg^{2+}] (CHEN *et al.* 2000; FRINGS *et al.* 1998; SILVERMAN *et al.* 2000; TERLAU *et al.* 1996).

The slowing of rEAG channel activation by Mg^{2+} is concentration dependent; increasing [Mg^{2+}] from 0mM to 10mM causes a progressive slowing of the activation kinetics (TERLAU *et al.* 1996). Similar concentration dependency is observed for the bovine and Drosophila channels (FRINGS *et al.* 1998; TANG *et al.* 2000). The slowing of

Eag activation is more pronounced at less negative holding potentials than at more negative potentials, indicating a voltage dependency in the [Mg^{2+}]-dependent slowing of Eag activation kinetics (TERLAU *et al.* 1996).

By expressing mutant forms of DmEag in oocytes, it has been possible to determine how Mg^{2+} ions interact with the channel. It is likely that the Mg^{2+} ion is coordinated by residues D278 in S2 and D327 in S3 (two of the six transmembrane domains in each channel subunit), with D274 also being close to the binding site (SILVERMAN *et al.* 2004; SILVERMAN *et al.* 2000). The D278V mutant channel is insensitive to extracellular [Mg^{2+}] of up to 20 mM (above physiological levels), presumably due to the loss of the interaction between the ion and the negatively charged side chain (SILVERMAN *et al.* 2000). D278E channels are also insensitive to Mg^{2+}, in this case due to either steric hindrance (SILVERMAN *et al.* 2000) or to disruption of the proposed regular octahedral structure of the binding site (SILVERMAN *et al.* 2004). The neutralizing mutant D327A has the same effect as D278V and converting residue 278 to its equivalent in Sh (since it is not [Mg^{2+}] sensitive) (D278F) reduces the effect of Mg^{2+} upon activation kinetics (SILVERMAN *et al.* 2000). D327E, however, retains sensitivity to [Mg^{2+}], indicating a greater degree of flexibility at this site than at position 278. Thus it appears that D278 and D327 coordinate the binding of the of Mg^{2+} ion.

Amino acid substitutions at position 274 yield different results. The neutralizing substitution D274A has similar activation kinetics to wild-type in the presence of extracellular Mg^{2+} as does the Sh mimicking D274E substitution. The kinetics of D274E,

however, recover more slowly than wild-type following the removal of extracellular Mg^{2+}, suggesting that the glutamate side chain can reach and coordinate Mg^{2+} in a manner not seen in wild-type channels (SILVERMAN *et al.* 2000).

A variety of divalent cations (including Zn^{2+}, Mg^{2+}, Mn^{2+}, Co^{2+}, and Ni^{2+}) are able to slow the activation kinetics of Eag (TERLAU *et al.* 1996). It is likely that these ions have a common binding site. The extent to which each cation inhibits activation is proportional to its enthalpy of hydration (SILVERMAN *et al.* 2000). As seen with Mg^{2+}, the D278A channel is insensitive to Mn^{2+} and Ni^{2+}. D278E eliminates Ni^{2+} sensitivity but only reduces Mn^{2+} sensitivity (presumably by decreasing the apparent affinity of the channel for Mn^{2+}). D327A is insensitive to Mn^{2+} but retains some sensitivity to Ni^{2+}, albeit with a reduced affinity (SILVERMAN *et al.* 2004). Both the magnitude of effect of Mn^{2+} upon Eag and the half-maximal concentration are similar to that of Mg^{2+} (SILVERMAN *et al.* 2004). It appears that Mg^{2+} and other ions enter into and bind to a pocket between S2 and S3 to regulate the activation kinetics of Eag.

It is known that in some ion channels, Mg^{2+} acts by blocking the pore. If this is the case in Eag, then the four individual subunits within each channel would not act independently with regard to Mg^{2+} inhibition. The bEAG mutant L322H (analogous to DmEag L342H) shows accelerated activation kinetics, with the channel opening at more negative potentials than wild-type. When dimeric and tetrameric constructs of wild-type and mutant subunits are co-expressed to produce channels with either 0, 1, 2, 3 or 4 mutant subunits in the tetramer, as the number of mutant subunits increases the channel

activation accelerates progressively (SCHONHERR *et al.* 1999). This is consistent with the four bEAG subunits activating independently. Analysis of dose-response data for the Mn^{2+}-dependent slowing of wild-type DmEag activation indicates that Mn^{2+} acts independently in each individual subunit to modulate gating with no co-operativity between the four binding sites (SILVERMAN *et al.* 2004). This presumably holds true for Mg^{2+} binding and is compatible with the conclusions drawn in bEAG, where the divalent cation sensitive slow gating transitions occur independently in each subunit (SCHONHERR *et al.* 1999).

In many voltage-gated channels, hyperpolarizing prepulses can be used to delay the onset of ionic current. Such pulses delay the onset, but do not affect the time course of the activation, providing evidence that such channel proteins transit through a number of closed conformations prior to opening (TANG *et al.* 2000). Like these other voltage channels, oocyte expressed DmEag displays delayed channel opening and dramatically slowed kinetics of evoked ionic currents following hyperpolarizing prepulses. This suggests that DmEag also goes through a series of closed states and that the transition between hyperpolarized states is rate limiting (TANG *et al.* 2000).

In the presence and absence of hyperpolarizing prepulses, extracellular Mg^{2+} slows the kinetics of ionic current activation (TANG *et al.* 2000). The interaction between extracellular Mg^{2+} and hyperpolarizing prepulses is complex and particularly prominent during the initial phase of activation. This interaction suggests that Mg^{2+} slows rate limiting gating transitions that occur between closed states that are populated at

hyperpolarized potentials (TANG *et al.* 2000). Furthermore, it does not appear that the final opening transition is the rate-limiting step in DmEag opening. Whereas Mg^{2+} does appear to modulate the kinetics of channel opening, channel deactivation is insensitive to Mg^{2+}, indicating that Mg^{2+} does not influence the transition between the open state and the most accessible closed state.

Analysis of DmEag gating currents when ionic currents are blocked with TEA showed that the slow component of the charge movement in ON gating is more prominent in the presence of extracellular Mg^{2+}, suggesting that the gating transitions modulated by Mg^{2+} occur slowly or involve relatively little charge or both (TANG *et al.* 2000). The effects of extracellular Mg^{2+} on gating current kinetics and opening kinetics suggest that Mg^{2+} does not act upon S4 (the voltage sonsor) (TANG *et al.* 2000).

Mg^{2+} binds the resting channel.

If Mg^{2+} is modulating transitions between closed states, then presumably Mg^{2+} must bind Eag when the voltage sensor (S4) is in its resting (closed) position. To determine if extracellular ions can access the binding site in closed channels, it was determined whether Ni^{2+} can access its binding site when the D274A mutant channel is closed.

At potentials of -80mV and -120mV, the probability of the D274A channel's being open is very low (the midpoint of activation is +25mV). By applying Ni^{2+} at

different potentials, it is apparent that Ni^{2+} is able to access its binding site from the extracellular solution when the channel is at rest (SILVERMAN *et al.* 2004). Furthermore, Ni^{2+} cannot effectively prevent the opening of the D274A channel if the voltage sensor is activated before the Ni^{2+} is added, and Ni^{2+} can also dissociate from its binding site when the channel is at rest (SILVERMAN *et al.* 2004). This suggests that the ion binding site is accessible when the channel is at rest, which is not compatible with the "paddle" model that has been proposed from the crystal structure of KvAP (the voltage-dependent K^+ channel from *Aeropyrum pernix*) (JIANG *et al.* 2003a; JIANG *et al.* 2003b). Whereas Mg^{2+} coordinating residues are typically 2.7-3.4 Å apart, the paddle model has the equivalent of D278 and D327 approximately 17 Å apart, which is too far for Mg^{2+} coordination (SILVERMAN *et al.* 2004). The structure of the isolated voltage sensor (S2-S4) in the open conformation (i.e. not a conformation in which Mg^{2+} can bind) of KvAP has these residues approximately 10.8 Å apart (JIANG *et al.* 2003a; SILVERMAN *et al.* 2004). If the larger aspartic acid side chains are substituted for the corresponding valine and glycine, then, with some minor changes, these residues in the isolated voltage sensor become close enough together to conceivably bind Mg^{2+} (SILVERMAN *et al.* 2004). Interestingly, the D278 equivalent in KvAP (G101) is near a break in the secondary structure of S3 caused by P99 (P325 in DmEag). This may impart flexibility to S3 that may be important in channel opening (SILVERMAN *et al.* 2004). It thus seems likely that Ni^{2+}, and presumably all divalent cations, can bind Eag to regulate activation when the voltage sensor is at rest, and that either the paddle model is incorrect or that voltage gating mechanism of Eag is different to that of KvAP. More recent complete structures of Kv1.1

and KvAP in their open state suggest that S2 and S3 may be close enough together to allow Mg^{2+} coordination (LEE *et al.* 2005; LONG *et al.* 2005).

Gating mechanism.

It seems likely that the Mg^{2+} controlled events occur independently of and prior to the voltage-controlled events in Eag channel activation. Several gating mechanisms have been proposed for the opening and closing of Eag channels. These mechanisms involve Mg^{2+} sensitive transitions between two or more closed states that occur independently in each subunit; once all four subunits are in the most accessible closed (i.e., closest to open) all four subunits proceed simultaneously through the final voltage-dependent opening transition (SCHONHERR *et al.* 2002; SILVERMAN *et al.* 2004).

The voltage dependency of accessibility from the extracellular solution to S4 of bEAG1 is consistent with the substantial outward movement of S4 from a gating canal seen in Na^{+} and Sh channels (BAKER *et al.* 1998; WANG *et al.* 1999; YANG *et al.* 1996). With this mode of voltage activation in mind, it has been proposed that Mg^{2+} acts to cross-bridge S2 and S3, holding the gating canal in a narrow "locked" conformation and that for S4 to move to its activated position, Mg^{2+} must first dissociate, allowing the canal to change to a wider "unlocked" conformation (SCHONHERR *et al.* 2002). This model is shown as Figure 1.5.

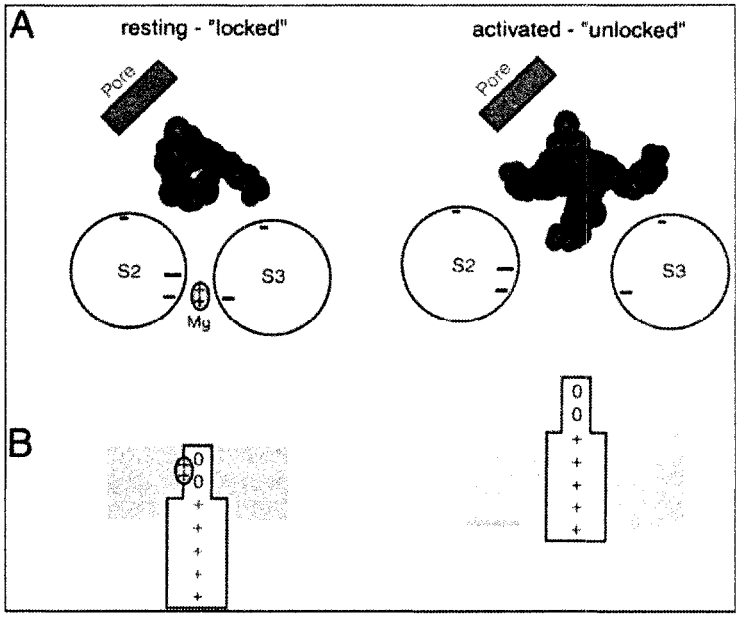

Figure 1.5 Mg^{2+}-Dependent Canal Rearrangement Proposed to Lock and Unlock S4 in the Resting State

(Left) Mg^{2+} coordination between Eag specific negative residues in S2 and S3 (black) proposed to lock the canal in a narrow configuration. (Right) Entry of S4's wider section into the canal upon activation requires the "unlocking" motion or S2/S3 (arrows) prior to S4 activation. (A) Top view from the extracellular side shows space-filled side chains for S4's high-impact charge residues (blue) facing S2's and S3's conserved negative residues and high-impact S4's hydrophobic residues (magenta) facing the pore domain. Only high-impact residues located in the canal in the resting (left) or activated state (right) are shown. The activated topology is reached by a 9 residue helical screw motion along the pitch of the threads. (B) Mg^{2+} binding in the canal at rest and unbinding in the activated state would give the canal a constant net charge and could explain the need for stronger hyperpolarization to push S4 into the resting conformation at low [Mg^{2+}]. (Taken from: SCHONHERR *et al.* 2002).

Phosphorylation of Eag.

Calcium/calmodulin dependent kinase II (CaMKII) is a regulator of neuronal excitability and plasticity (GRIFFITH *et al.* 1994). Genetic interactions between *eag* and the CaMKII inhibitory peptide *ala* transgene suggest that CaMKII may regulate Eag (GRIFFITH *et al.* 1994). Biochemical and electrophysiological studies have demonstrated that current amplitude is regulated by the phosphorylation of Eag T787 by CaMKII, possibly when held in a complex with the Camguk/CASK adaptor protein (MARBLE *et al.* 2005; WANG *et al.* 2002). Conversely, there is evidence that Eag activates CaMKII in the absence of Ca^{2+}, but only when an Eag/CaMKII complex is formed (SUN *et al.* 2004). Residues 773-794 of Eag appear to be the binding site responsible for this interaction (Figure 1.6), and this direct binding of CaMKII to Eag does not appear to affect the phosphorylation of T787 (SUN *et al.* 2004). Loss of function mutations such as eag^1 appear to be phenocopied by the overexpression of *ala* (Figure 1.7), which is presumably equivalent to a reduction in CaMKII activity (GRIFFITH *et al.* 1994).

It seems possible that there is a positive feedback loop where CaMKII phosphorylates Eag to enhance its activity, which in turn activates CaMKII which again phosphorylates Eag.

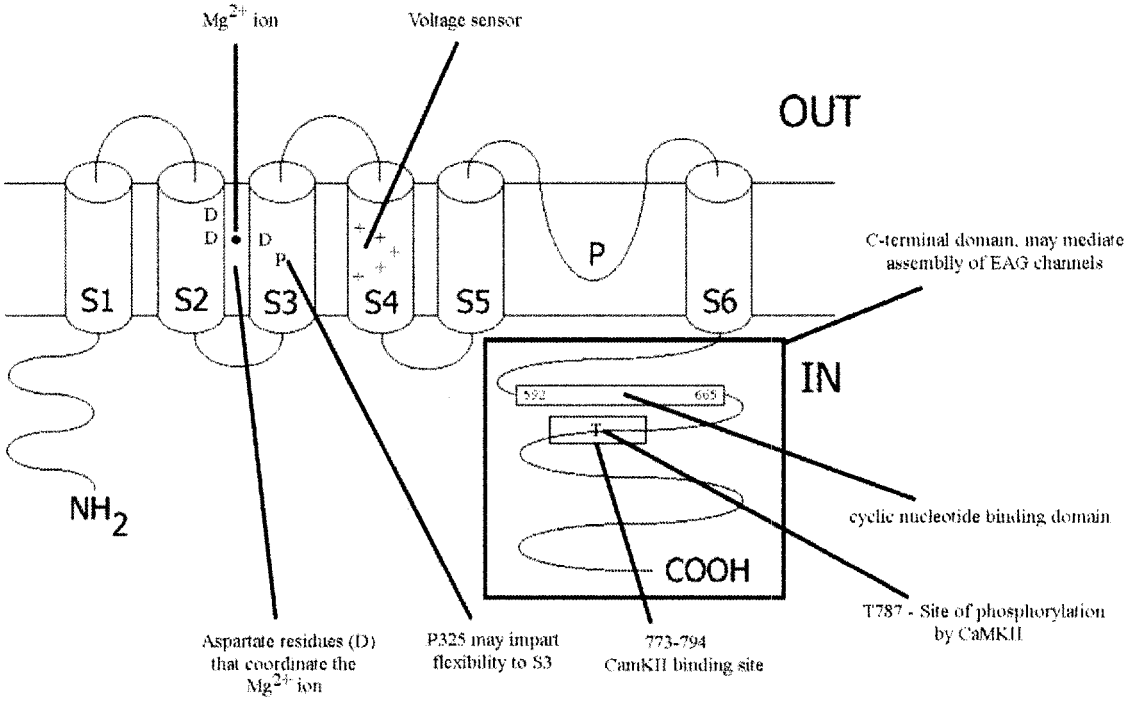

Figure 1.6 Annotated topological diagram of Eag

Schematic depicting the topology of the Eag protein. S1 through S6 represent the six transmembrane domains, and P, the pore domain. Indicated in red are some domains and individual residues of note: the positive charges of the voltage sensor, the Mg^{2+} ion and its coordinating residues, a putative source of flexibility for gating, the site of regulation by cyclic nucleotides, CaMKII phosphorylation, and the domain important for channel assembly. Residue numbers correspond to DmEag. (GUY *et al.* 1991; LUDWIG *et al.* 1997; SILVERMAN *et al.* 2004; SUN *et al.* 2004; WANG *et al.* 2002)

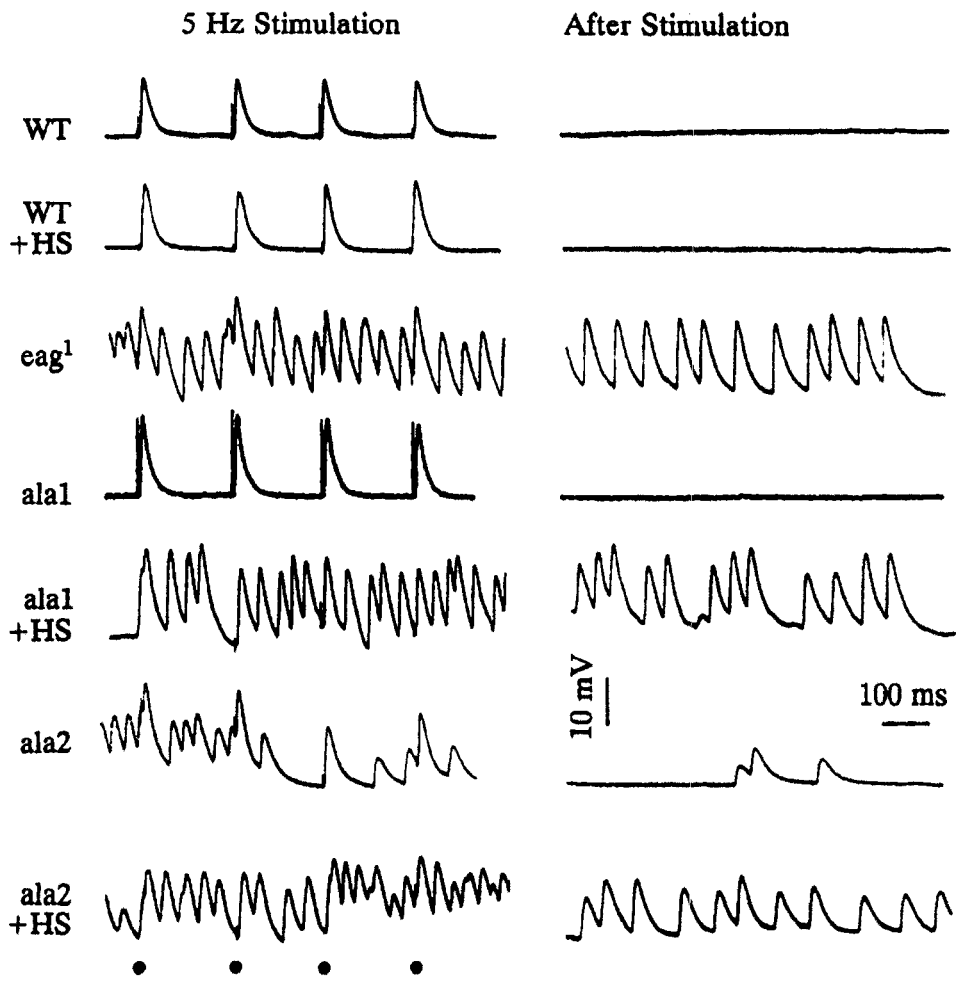

Figure 1.7 Overexpression of *ala1* phenocopies *eag*^{1}

ejps recorded from larval nmjs of *eag*^{1}, *ala1* with or without heat shock (HS), *ala2* homozygotes with or without heat shock, and Canton-S controls (wild-type, WT). Stimulus artifacts are indicated by filled circles. (*Left*) High-frequency supernumary discharges seen with 5-Hz stimulation in *ala* and *eag*^{1} flies. Supernumary discharges were never observed in controls and were not seen in all heat-shocked *ala1* larvae. (*Right*) Continued activity after stimulation ceased. This activity could last up to 10 seconds after cessation of stimulation. (Taken from: GRIFFITH *et al.* 1994)

1.6 Inebriated

The *inebriated* (*ine*) gene was identified in a screen for mutations that had a behavioral interaction with the *Sh* mutation. Like the *eag Sh* double mutant, mutations in *ine* were identified for their ability to enhance *Sh*, producing downturned wings and an indented thorax in adult Drosophila (STERN and GANETZKY 1992). In an otherwise wild-type background, *ine* flies do not display any mutant behavioral phenotypes; they do not exhibit ether-induced leg shaking, temperature-sensitive paralysis, or sensitivity to mechanical shock (STERN and GANETZKY 1992). However, the *ine* mutation was, like the K^+ channel blocking agent dideoxy forskolin (DDF), able to potentiate the effects of quinidine on synaptic transmission (STERN and GANETZKY 1992).

Further electrophysiological analysis showed that the ine^1 mutation increases the rate of onset of long term facilitation (LTF) (HUANG and STERN 2002), indicating that the loss of Ine increases neuronal excitability.

Mapping and cloning of the *ine* gene identified a cDNA encoding an open reading frame of 658 amino acids that bears significant similarity to members of the Na^+/Cl^- dependent neurotransmitter transporter family (SOEHNGE *et al.* 1996). Members of this family have been shown to catalyze the reuptake of neurotransmitters such as glycine, dopamine, 5HT, NE and, GABA, as well as metabolites or osmolytes such as taurine, betaine, β-alanine, and creatine (SOEHNGE *et al.* 1996).

Northern blot and sequence analysis showed two *ine* transcripts of 2.3kb (*ine-RB*) (SOEHNGE *et al.* 1996) and 3.6kb (*ine-RA*) (BURG *et al.* 1996). The smaller transcript encodes a protein of 658 amino acids called Ine-P2, and the longer, a protein of 943 amino acids called Ine-P1 or RosA (BURG *et al.* 1996; SOEHNGE *et al.* 1996). Ine-P1 and Ine-P2 are identical except that Ine-P1 has an additional N-terminal tail (HUANG and STERN 2002) (Figure 1.8).

Overexpression of a *UAS-ine-RA* transgene with either *gli*-GAL4 or *MZ1580* (both peripheral glia GAL4 drivers) rescued both the LTF phenotype in a ine^{1} background and the downturned wing phenotype in a *Sh;* ine^{1} mutant background (HUANG and STERN 2002). The same *UAS-ine-RA* construct driven with the neuronal *elav*-GAL4 driver produced only a partial rescue of either phenotype (HUANG and STERN 2002). *MZ1580* driven *UAS-ine-RB* was not able to fully rescue either the LTF or downturned wing phenotypes; only a partial rescue was observed suggesting the two isoforms of Ine have different efficiencies (HUANG and STERN 2002).

The overexpression of Ine-P1 (also called $Overine^{+}$) with either *MZ1580* or *gli*-GAL4 confers a number of phenotypes. First, in a *Sh* mutant background, suppression of the characteristic ether-induced leg-shaking is observed; a similar effect is seen with *para* mutations (STERN *et al.* 1990) and, more recently, with an *eag* gain-of function allele (see Chapter 3). Second, in an otherwise wild-type background, $Overine^{+}$ confers reduced excitability as assayed by the onset rate of LTF. In $Overine^{+}$ larvae, the onset rate of LTF is decreased; as in eag^{84} (a gain-of-function mutation, see chapter 3), facilitation is not

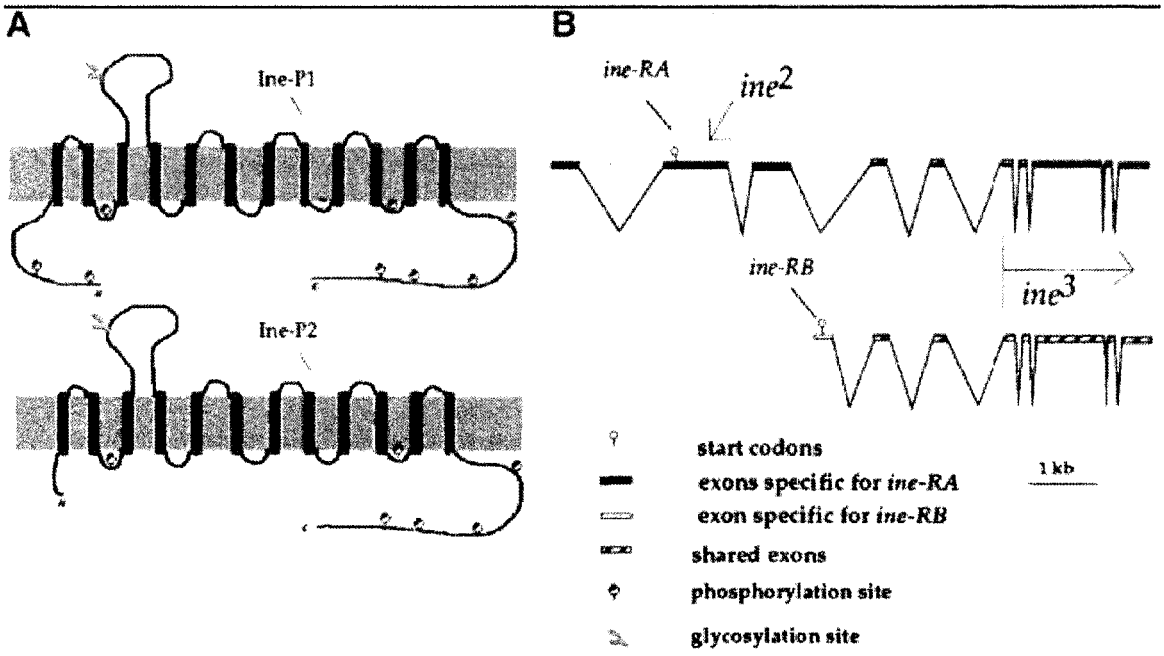

Figure 1.8 Organization of Ine and *ine*

(A) The putative membrane topology of the two Inebriated protein isoforms. The two isoforms are identical except that Ine-P1 (encoded by *ine-RA*) contains an N-terminal intracellular region that is ~300 amino acids longer than the corresponding region in Ine-P2, encoded by *ine-RB*. This 300-amino-acid extension, unlike the region common to both proteins, has no similarity to other transporters. Potential sites of N-linked glycosylation and phosphorylation are indicated. (B) Map of the *ine* region showing the exons of the two *ine* isoforms and the location of two identified mutations. The ine^2 mutation is a nonsense mutation at codon 126 of *ine-RA*, whereas ine^3 is a deletion that removes most of the open reading frame common to both transcripts and begins at codon 293 of *ine-RA*. Although ine^1 has not been localized, it was previously shown by Northern blot analysis that transcripts of both *ine* isoforms are undetectable in the ine^1 mutant (SOEHNGE *et al.* 1996). (Taken from: HUANG *et al.* 2002)

observed at 5Hz stimulation (HUANG and STERN 2002). Third, like *para, tipE,* and *mle*^{nap} mutations that decrease sodium channel activity, *Overine*$^{+}$ causes a temperature sensitive paralysis phenotype. A synergistic relationship is observed between *Overine*$^{+}$ and *para*^{63}; the double mutant displays a much stronger temperature sensitive paralysis phenotype than either single mutation. Fourth, there is an increased number of failures to evoke neurotransmitter release at the neuromuscular junction in response to nerve stimulation in *Overine*$^{+}$ larvae; a similar phenotype is seen in *para*^{63} larvae. No alteration in the amplitude of spontaneous mini-excitatory junctional potentials is observed, indicating a normal muscle response to neurotransmitter and a normal quantal content of neurotransmitter.

It is known that decreasing the number of sodium channels (e.g., by mutating them as with *para*^{63}) confers neuronal hypoexcitability and that increasing sodium channels (as in *Dp para*$^{+}$) confers hyperexcitability. It has also been shown that *eag* loss-of-function mutations (e.g., *eag*^{1}) confer neuronal hyperexitability and that gain-of-function mutations (e.g., *eag*^{G297E}) confer hypoexcitability. It appears that a similar effect is seen with *ine*, where loss of Ine (*ine*^{1}) confers neuronal hyperexcitability and the over-expression of Ine-P1 (*Overine*$^{+}$) confers hypoexcitability. It is thus reasonable to postulate that Ine somehow regulates sodium channels in the axonal membrane, and that the Ine-P1 isoform rather than Ine-P2 is responsible for the control of excitability.

Osmotic stress response.

There were two observations that suggested that *ine* might be involved in osmolyte transport and thereby affect the Drosophila stress response. First, both isoforms of Ine are robustly expressed in the kidney analogue (the Malpighian tubule, hindgut, and anal plate) (SOEHNGE *et al.* 1996); second, other members of the same transporter family as *ine* such as BGT1 transport osmolytes in the mammalian renal medulla (BURG 1995). If Ine performs osmolyte transport in the Malpighian tubules and midgut, then *ine* mutants would be defective in such transport and would be expected to be more sensitive to osmotic stress than wild-type flies (HUANG *et al.* 2002). When maintained on media with elevated [NaCl] (0.2M) for 4 days, ine^1 and ine^3 mutants exhibit significantly increased lethality than either wild-type or ine^2 mutants (HUANG *et al.* 2002). Similar results were observed with elevated sorbitol and KCl confirming that the reduced viability was due to a response to hypertonicity and not altered sensitivity to NaCl (HUANG *et al.* 2002).

The ine^1 and ine^3 mutants most likely produce null phenotypes; ine^3 is a deletion mutation that eliminates most of the ORF, and ine^1 mutants produce undetectable levels of either mRNA transcript (SOEHNGE *et al.* 1996). The ine^2 mutation is a nonsense mutation in codon 125 of the Ine-P1 isoform; this mutation is therefore expected to eliminate Ine-P1 but not Ine-P2 (HUANG *et al.* 2002).

Two isoforms with different functions?

The stress response experiments indicate that the shorter Ine-P2 isoform is mainly responsible for the transport of osmolytes in the Malphagian tubules and midgut, with Ine-P1 having very little involvement. The electrophysiological and behavioral assays suggest that absence or excess of Ine-P1 is the main mediator of the phenotypes observed. It is thus possible that the additional N-terminal region of Ine-P1 is responsible for the regulation of neuronal excitability.

1.7 GAL4/UAS system

The GAL4/UAS system, adapted from yeast, uses the expression of the GAL4 gene under the control of endogenous promoters, such as *gliotactin*, *elav*, and *actin 5*, to drive the expression of the UAS-transgene (BRAND and PERRIMON 1993). The UAS promoter is only active when bound by GAL4 thus producing temporal and spatial control of transgene expression.

Transgene expression.

The *p*UAST expression vector is part of the GAL4/UAS system in Drosophila that allows for the selective activation of a transgene in a temporal and spatial specific manner (BRAND and PERRIMON 1993).

RNAi

For many applications dsRNA can be injected directly into cells to induce RNA mediated gene interference (RNAi). This is not, however, suitable for the heritable tissue specific silencing of a target gene. The GAL4/UAS system in Drosophila allows for heritable, tissue specific RNAi. Initially plasmids were created that place a gene fragment and its complement in series behind a UAS component to create a UAS-inverted repeat. Expression of the UAS-inverted repeat gives rise to a hairpin dsRNA molecule (KENNERDELL and CARTHEW 2000). Subsequent improvements involved the creation of cDNA-genomic combinations to avoid problems with homologous recombination within the construct (KALIDAS and SMITH 2002). Finally a vector was created whereby RNAi is triggered by the symmetrical transcription of a transgene (GIORDANO *et al.* 2002).

Chapter 2: Materials and Methods

2.1 Drosophila genetics

All fly stocks were maintained on standard cornmeal/agar Drosophila media at room temperature in either half pint bottles or vials. Vials were transferred approximately every four weeks.

Fly husbandry was performed as described previously (GREENSPAN 1997).

2.2 *p*UAST expression vector

The *p*UAST expression vector (BRAND and PERRIMON 1993) (Figure 2.1) contains 5 UAS (GAL4 binding) sites followed by the *hsp70* TATA box and a transcriptional start site. This region is followed by a polylinker containing restriction sites for EcoRI, BglII, NotI, XhoI, KpnI and XbaI which is followed by a polyadenylation site. The vector also contains P3' and P5' p-element insertion sites, and the *mini-white* gene to act as a heritable *in vivo* marker. *p*UAST is bases upon the pUC vector which provides ampicillin resistance and an origin of replication for selection and replication in *Escherichia coli*.

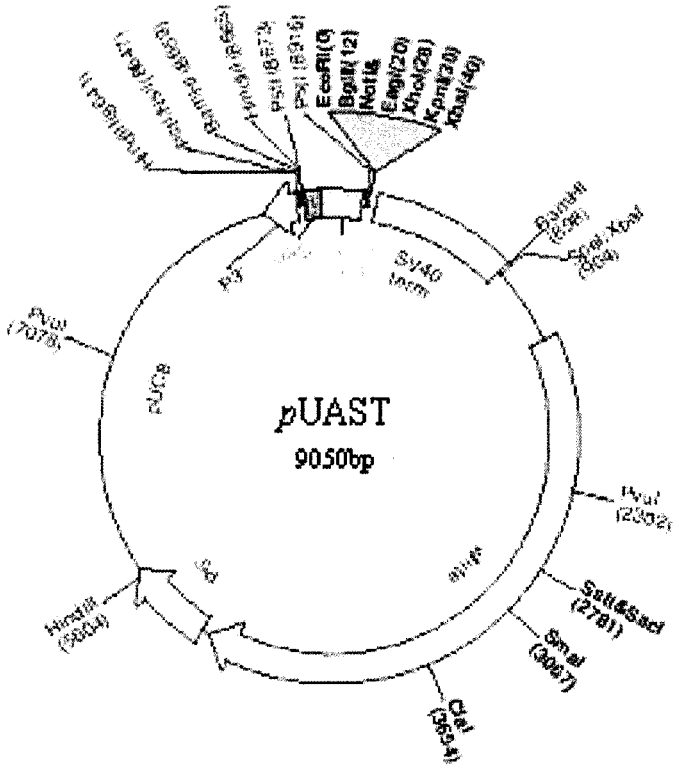

Figure 2.1 *p*UAST expression vector

pUAST consists of five tandemly arrayed optimized GAL4 binding sites (red) followed by the *hsp70* TATA box and transcriptional start (blue), a polylinker (green) containing unique restriction sites for EcoRI, BglII, NotI, Xho, KpnI and XbaI and the SV40 small t intron and polyadenylation site. These features are included in a P-element vector (pCaSpeR3) containing the P element ends (P3' and P5') and the white gene which acts as a marker for successful incorporation into the Drosophila genome (BRAND and PERRIMON 1993).

Image from: http://www.gurdon.cam.ac.uk/~brandlab/reagents/pUAST.html

2.3 *sym-p*UAST RNAi vector

The symmetrical transcription plasmid (*sym-p*UAST) (Figure 2.2) contains two UAS arrays and two SV40 polyadenylation sites. This arrangement drives the transcription of a single insert corresponding to the target gene in two directions, giving both the sense and anti-sense strands. Thus the dsRNA molecule can be made by the cell.

2.4 Making *sym-p*UAST-*eag*

To make a UAS RNAi transgene targeting the *eag* K^+ channel, a 509nt fragment of genomic DNA corresponding to the 5'UTR and most of exon 1 of *eag* was amplified by PCR (forward primer: ATATAAGAATTCGAAAGAGAGTGAGACAGC, reverse primer: ATATAAAGATCTGCATGATGATGTTCTCCGAGG). The PCR product was TA-cloned into the pGEM-T vector (Promega). An EcoRI/BglII double digest was then used to transfer the PCR product into the *sym-p*UAST plasmid. The new plasmid, named *sym-p*UAST-*eag*, was sequenced to ensure accurate cloning prior to being micro-injected into Drosophila embryos.

The fragment of *eag* used as the trigger for RNAi shows no significant homology to other genes as determined by a BLAST search of all Drosophila sequences.

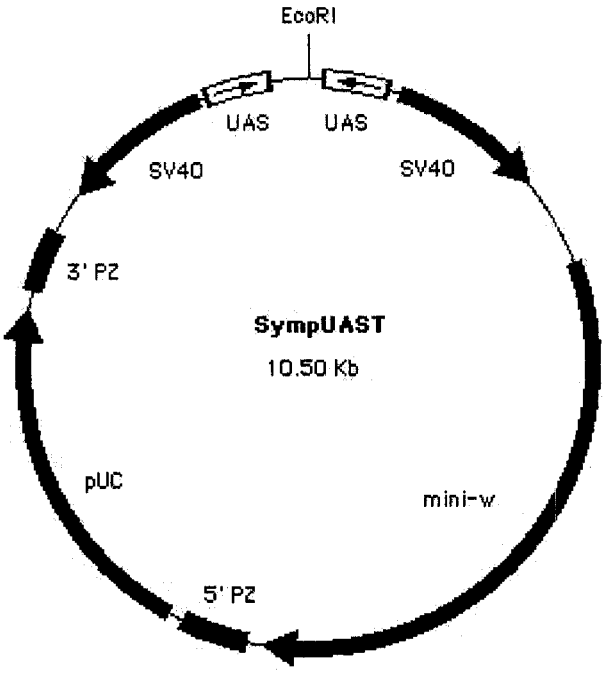

Figure 2.2 *sym-p*UAST RNAi vector

Contains an EcoRI site for the insertion of the trigger fragment. The *mini-w* gene is a selectable marker for followowing insertion into the fly genome. pUC carries an Amp^R gene for selection in E.coli. 3'PZ and 5'PZ are p-element insertion sites. UAS (upstream activation sequence) is a promoter and the SV40 is a polyA terminator (GIORDANO *et al.* 2002).

All other *sym-p*UAST plasmids (see chapter 7.3) were created in a similar manner to *sym-p*UAST-*eag*. Primer details are included in chapter 7.3.

2.5 Sequencing of *eag*

As recombination and RFLP mapping had demonstrated that the suppressor mutations were within the *eag* locus, I undertook the sequencing of all 15 exons from the three suppressors and appropriate controls. PCR primers (listed in table 2.1) were designed at the beginning and end of either each exon, or pair of exons. If an individual exon was too large to easily amplify it was amplified in two parts.

Genomic PCR products were separated by gel electrophoresis and the appropriate band excised and gel extracted using the Montage DNA Gel Extraction Kit (Millipore, MA) as per the manufacturer's instructions. The extracted band was purified using the QIAquick PCR Purification Kit (Qiagen, MD) as per the manufacturer's instructions. The PCR product was then sequenced using both PCR primers and occasionally with additional internal primers. Putative mutations were resequenced from repeat PCR reactions as confirmation.

Name	Direction	Sequence (5'→3')
eag exon 1F	F	GAAAGAGAG TGAGACAGC
eag exon 1F-2	F	GGGAGAAAGAGAGTGAGACAGCATC
eag exon 1R	R	GGATGATGTTCTCGAGG
RC-EAG-EX1R	R	TTGAACTTGGTACACC
eag exon 1R-2	R	CCGGATGATGTTCTCGAGGAATGTG
RC-EAG-EX2F	F	GGTGAAGAGGTGAATC
RC-EAG-EX2R	R	CGATTATTGAAACGC
RC-EAG-EX3F	F	GCATTCTGGCATTC
RC-EAG-EX3F-3	F	TCTTCTGGCATCTCCTG
RC-EAG-EX3R-2	R	CTTTTGCATAGCAGG
RC-EAG-EX3R-3	R	CGACTTTGATTTGGGTATAGC
RC-EAG-EX4F	F	CACCAGCGAGTATC
RC-EAG-EX4R	R	CCAAGACACGTTAG
4R-2	R	CCAAGACACGAATCG
RC-EAG-EX5F	F	GCATCTCTGGTGTTC
RC-EAG-EX5R	R	TTCATCAGGCAACC
EX6F	F	GTGTGCGTGTACCC
RC-EAG-EX6F	F	CTAAAGGATCCCACGAAGCAGTCCAATTTGGC
RC-EAG-EX7R	R	GTTGCATACCTCGAC
RC-EAG-EX8F	F	TTCCAGGTGCCATAC
RC-EAG-EX9R	R	CCCATTATCCGCATCG
RC-EAG-EX10F	F	GATCCAATACAGCTG
10F-2	F	CGATGCGGATAATGG
EX11R	R	CTGCAATGATCATC
RC-EAG-11R-2	R	CACCTGCAATGATGATCATC
RC-EAG-IN11F-1	F	AAAGCTAGGCCATCC
IN11F-2	F	CGTGAGAAAACTGCC
RC-EAG-IN11R-1	R	CGTGAGAAAATGCC
MF-EAG-EX12F	F	CTCTGCTGTATGCC
12F-2	F	GCTCTGCTGTATGCC
EAG-EX12F	F	CTCTGCTGTATGCCACGATCTTTGGTCACG
MF-EAG-EX12R	R	CTTCTCGGTATCCAG
12R-2	R	CCTTCTCGGTATCCAG
EAG-EX12R	R	CTTGGTCATGGCCCAGGTGGAGACGACATAGTCC
RC-EAG-EX13F	F	GGTACTAAACTATTGTCCG
RC-EAG-EX13R	R	CCAATATTGCCAC
RC-EAG-EX14F	F	TTACAGGCAAGGG
RC-EAG-14F-2	F	CAGTAAGGAGCTCGTC
RC-EAG-EX14R	R	CTTAGTTCGCTCCACC
RC-EAG-IN14R	R	CAACGAGCATAAGTCAC
ex15F	F	GATAACCATTTCATCGCC
RC-EAG-EX15F-2	F	CATCCGCATCTCC
RC-EAG-15F-3	F	CACACCCACAACACAGG
ex15R	R	TTCATCCAAAACTCCACTAC
RC-EAG-EX15R-2	R	GATCCTGATGCTCC
RC-EAG-15R-3	R	GCGATTGATCTGCCG

Table 2.1 Primers used in genomic sequencing of *eag*

Primers used for PCR amplification and/or sequencing of PCR products. All sequences presented 5'→3'.

Some regions that proved difficult to amplify from genomic DNA were amplified from cDNAs and sequenced as above. The cDNAs were created by extracting RNA from adult flies using the TRIzol Reagent protocol (GibcoBRL) and performing RT-PCR (Superscript III First-Strand Synthesis System for RT-PCR (Invitrogen)). PCR reactions were subsequently performed on the cDNA, and were analyzed as above.

2.6 Larval micro-dissection

Wandering third instar larvae were grown in uncrowded half pint bottles and collected 1 or 2 days after the appearance of the first wandering third instar larva. Larval dissections and muscle recordings were made as described previously (GANETZKY and WU 1982; HUANG *et al.* 2002; JAN and JAN 1976; STERN *et al.* 1995; STERN and GANETZKY 1989). Ventral lateral longitudinal peripheral nerves that innervate the body wall muscles were cut immediately posterior to the ventral ganglion (see Figure 2.3) and were captured and stimulated using a suction electrode (see Figure 2.4). Intracellular muscle recordings were made using a microelectrode pulled on a Flaming/Brown micropipette puller to tip resistances of 30-60 MΩ and filled with 3M KCl. All dissections and recordings were performed at room temperature in standard saline solution (JANs buffer) (0.128M NaCl, 2.0mM KCl, 4.0mM $MgCl_2$, 0.34M sucrose, 5.0mM Hepes pH 7.1 and $CaCl_2$ as specified in the text) unless otherwise indicated. Ventral longitudinal muscle cell 6 (also known as muscle L2) was used for the recording

A.

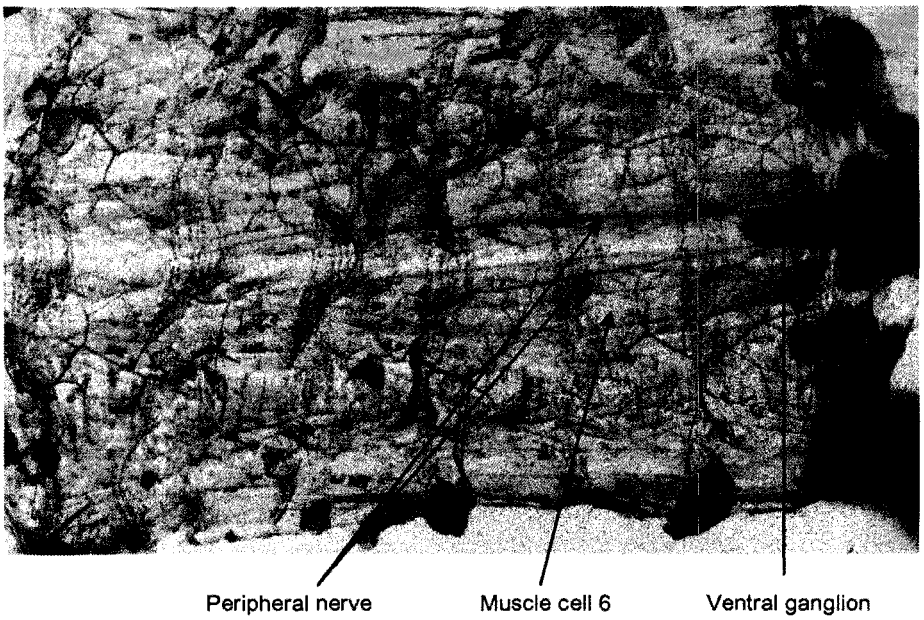

B.

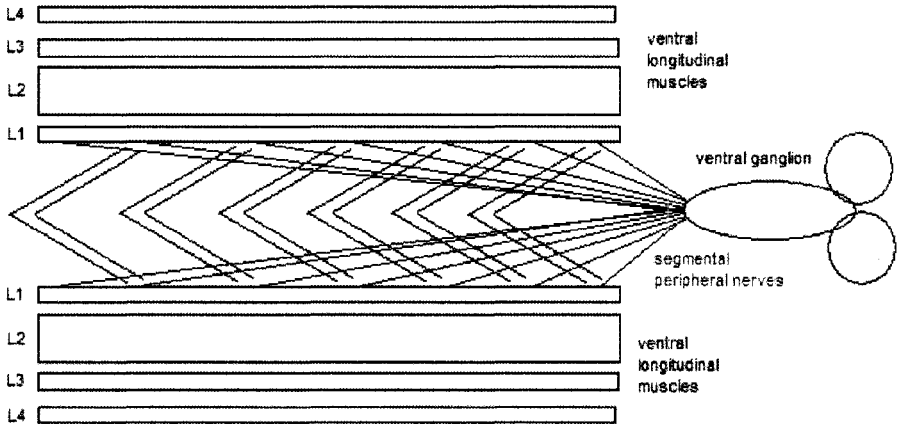

Figure 2.3 Wandering 3rd instar larval preparation

A. Light micrograph of a filleted wandering third instar larva. B. Schematic of a filleted wandering third instar larva. The ventral lateral longitudinal peripheral nerves (red) are cut immediately posterior of the ventral ganglion. Each peripheral nerve innervates the section of longitudinal muscle posterior to where the nerve contacts the muscle. Muscle cell 6 (L2) is used for recordings where the amplitude or duration of the response will be assayed.

of all electrophysiological parameters. Quinidine, 4-Aminopyridine (4-AP) and tetraethylammonium (TEA) were applied following dissection as described previously (JAN *et al.* 1977; SINGH and WU 1989).

2.7 ejp amd mejp recordings

The mean amplitude and duration was typically calculated from 5 evoked excitatory junctional potentials (ejps) for each larva and data was collected from at least 3 larvae for each genotype under each set of conditions. The number of larvae tested is presented as the n-value. Duration of the ejp was measured as the interval from half-maximal response to half-maximal response. The amplitude of spontaneous mejps was determined similarly.

2.8 Voltage clamping and ejc recordings

To voltage clamp, larvae were dissected as for ejp recordings and a nerve was captured as before. Two electrodes were introduced into muscle cell 6, one to act as the current electrode the second as the voltage electrode (see Figure 2.5). To obtain voltage a variable current is applied through the current electrode to hold the muscle at the desired holding potential (-60 mV in my experiments). The muscle potential is monitored by the voltage electrode.

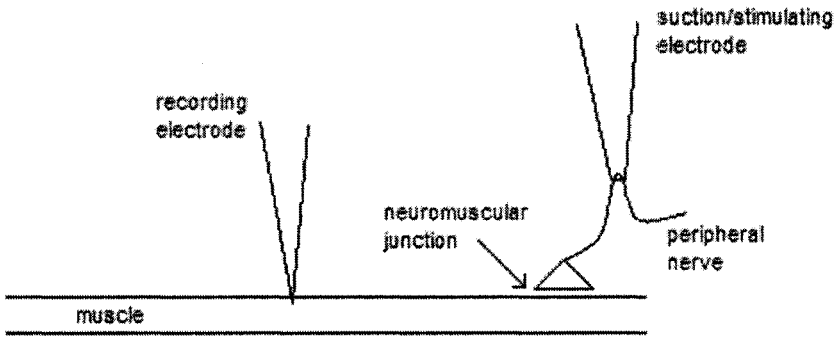

Figure 2.4 Standard larval nmj preparation

A loop of peripheral nerve is captured with a suction electrode. The electrode is then positioned such that no strain is placed upon the nerve. An intracellular recording electrode is then inserted into a muscle cell (typically muscle cell 6). The nerve is then stimulated through the suction electrode at the desired frequency. The muscle response is recorded via the recording electrode and digitized.

An excitatory junctional current (ejc) is the change in the current applied to maintain the muscle potential at -60mV in response to an evoked action potential in the innervating nerve. Several ejcs were recorded per larva and the average ejc amplitude was calculated for each larva.

2.9 Long term facilitation

LTF, also known as augmentation, is a phenomenon exhibited at the Drosophila larval nmj. Following repetitive stimulation at frequencies typically between 3 and 10 Hz, an excitation threshold is reached, and subsequent stimulations elicit a facilitated response of increased magnitude and duration (JAN and JAN 1978; WANG *et al.* 1994). Certain mutations that decrease neuronal excitability (such as *para* (MIKE STERN, UNPUBLISHED DATA)) result in delayed onset of LTF; those that increase excitability (such as *Dp para*$^{+}$, *Hk*, *frq* and *pumilio* (RIVOSECCHI *et al.* 1994; SCHWEERS *et al.* 2002; STERN *et al.* 1995; STERN and GANETZKY 1989)) result in faster onset of LTF.

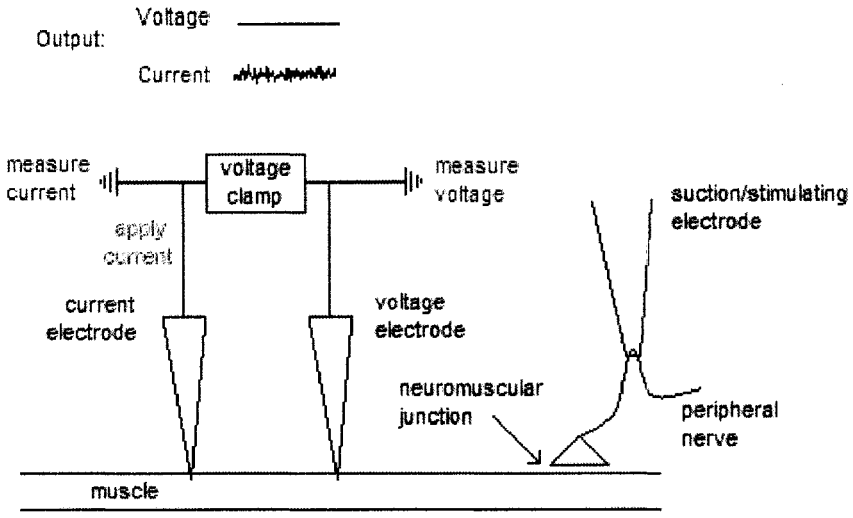

Figure 2.5 Larval nmj voltage clamp setup

As shown in Figure 2.4, a nerve is captured and stimulated. To voltage clamp the muscle, two intracellular electrodes are introduced into the same muscle cell. The voltage electrode monitors the muscle potential, as described in Figure 2.4. The output from the voltage electrode is recorded and also feeds into the voltage clamp. The current electrode applies a current. The current applied to maintain the desired muscle potential is recorded simultaneously to the muscle potential (voltage).

Chapter 3: Suppressors of *Shaker*

3.1 Mutagenesis

To identify novel mutations that suppress the leg-shaking phenotype of *Sh*-mutants, males carrying Sh^{133} were mutagenized with EMS, crossed to $\overline{XX}$ *ywf* females, and their sons scored for an absence of leg-shaking. Of 35,000 sons tested, nine failed to shake their legs when etherized. Five of these suppressor mutations have previously been shown to be new alleles of *para,* which encodes a sodium channel subunit (STERN *et al.* 1990).

Five alleles of para.

The characterization of these alleles provides the basis for my hypotheses for the characterizing of the remaining suppressors. The new alleles of *para* are known as 60, 63, 74, 103 and 141. The allele $para^{74}$ has been characterized molecularly to be a methionine to isoleucine substitution within the third S6 domain (PITTENDRIGH *et al.* 1997).

The remaining 4 suppressors.

One of these lines was lost with time leaving only three (Sup^{39}, Sup^{84} and Sup^{146}) to be further characterized.

3.2 Mapping: recombination and RFLP

Initial recombination mapping, by Mike Stern, using the leg-shaking phenotype placed *Sup*^{39}, *Sup*^{84}and *Sup*^{146} between the *garnet* (12B4-6) and *scalloped* (13F) loci and then to a region between two P[*ry*$^{+}$]-elements at positions 12E and 13B/C.

Damian Dalle Nogare used restriction fragment length polymorphism (RFLP) analysis to localize *Sup*^{146} centromere-proximal to a PstI polymorphism in exon 1 of *ether-a-go-go* (*eag*). The frequency of cross-over between the leg-shaking suppression phenotype and the RFLP suggested that *Sup*^{146} is approximately 30Kb from *eag* exon 1, which would place it within the *eag* locus (see Figure 3.1A).

3.3 Genomic sequencing

To test the possibility that *Sup*^{39}, *Sup*^{84} and *Sup*^{146} are new alleles of *eag*, I sequenced genomic DNA from the 15 exons of *eag* from the suppressor mutations as well as from isogenic *Sup*$^{+}$ flies. The *eag* sequence of *Sup*^{39} yielded only a single amino acid substitution: a glycine to glutamate change at position 297 (G297E, see Figure 3.1B). Interestingly, the *eag* sequence from *Sup*^{146} flies showed the identical G297E mutation as well as two additional mutations (A1088T and I1142T). To test the possibility that these

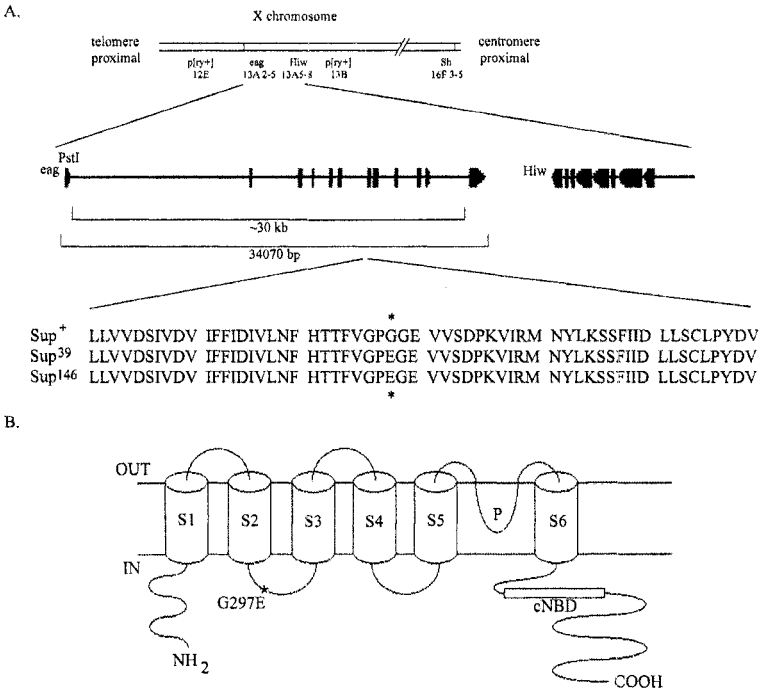

Figure 3.1 Map position of the *Sup*^{39} *and Sup*^{146} mutations

(A) Mapping of the suppressor mutations between P[ry^{+}]-elements at positions 12E and 13B. Direct genomic sequencing of *Sup*^{39} and *Sup*^{146} identified the substitution of a glutamate for a glycine at position 297, indicated by the pair of asterisks. *Sup*$^{+}$ represents sequence from *eag*$^{+}$ *para*^{63} and *eag*$^{+}$ *para*^{141}*f. para*^{63} and *para*^{141} are siblings of *Sup*^{39} and *Sup*^{146}, respectively generated by mutagenesis from the same isogenic wildtype X chromosome. (B) Schematic depicting the topology of the Eag protein. S1 through S6 represent the 6 transmembrane domains, P the pore domain and cNBD the cyclic nucleotide binding domain. The asterisk indicates the location of the G297E substitution identified in *Sup*^{39} and *Sup*^{146}. Having shown *Sup*^{39} and *Sup*^{146} to be mutations in *eag*, I have subsequently renamed them *eag*^{G297E}.

two additional mutations were generated after the mutagenesis, while the fly line was being maintained, I sequenced these regions from a second Sup^{146} stock, which was split off from the first stock about 6 months after Sup^{146} was obtained. I found that the G297E mutation was retained in this second Sup^{146} stock, but that the two additional mutations were absent. I conclude that Sup^{146}, like Sup^{39}, is a G297E mutation in *eag*; I shall now refer to them as eag^{G297E}. I am not aware of any previous study that has assigned a function to G297.

Genomic sequencing of Sup^{84} revealed two substitutions: A259V and E762V (Figure 3.1B); I have renamed this allele eag^{84}. It remains unclear as to whether one or both of these substitutions is responsible for the phenotypes observed.

3.4 Gain-of-function hypothesis

Previous studies have shown that *eag* loss of function mutations enhance the phenotypes of Sh^{133} mutation (WU *et al.* 1983). In contrast eag^{G297E} and eag^{84} suppress the phenotypes of the Sh^{133} mutation. I thus hypothesize that eag^{G297E} is a gain of function allele (Table 3.1). eag^{84} may also be a gain of function allele of *eag*.

An alignment of the Eag protein sequence from several species (Figure 3. 2) indicates that position 297 and the surrounding residues are highly conserved in all members of the Eag channel sub-family, but not in the Eag-like (Elk) or Eag-related

Genotype	Enhances Sh^{133}	Suppresses Sh^{133}
para^{-}		✓
Dp para^{+}	✓	
eag^{-}	✓	
eag^{G297E}		✓
eag^{84}		✓

Table 3.1 Genetic interactions among Na^+ and K^+ channel mutations

The hypoexcitable *para* mutations suppress the Sh^{133}-induced leg shaking (STERN *et al.* 1990), whereas hyperexcitable *eag* mutations and *Dp para*$^{+}$ enhance the Sh^{133}-induced leg shaking (STERN *et al.* 1990). eag^{G297E} and eag^{84} suppress the Sh^{133}-induced leg shaking, leading me to hypothesize that eag^{G297E} and eag^{84} are gain of function mutations. Table adapted from HUANG AND STERN (2002)

(Erg) sub-families. Interestingly this region of Eag is close to the site at which Mg^{2+} ions interact with the channel to regulate its activity, a phenomenon not seen in either the Elk or Erg sub-families (TANG *et al.* 2000).

3.5 Suppression of the Sh^{133}-induced ejp by eag^{G297E} at low [$CaCl_2$]

In Sh^{133} mutants, motor axon excitability is increased, which leads to action potential triggered Ca^{2+} influx in the nerve terminal that is larger and more prolonged than in wild-type (JAN *et al.* 1977). This increased Ca^{2+} influx, in turn, leads to increased neurotransmitter release from the motor neuron and subsequent muscle depolarization that is increased in amplitude and duration compared to wild type. I hypothesize that eag^{G297E} suppresses the Sh^{133}-induced leg shaking phenotype by reducing neuronal excitability, which would compensate for the increased excitability conferred by Sh^{133}. If so, then eag^{G297E} might suppress the increased neurotransmitter release conferred by Sh^{133}. To test this possibility I used the larval neuromuscular junction (nmj) preparation (JAN *et al.* 1977) to compare synaptic transmission at the larval nmj in eag^{G297E} Sh^{133} and eag^{+} Sh^{133}. With this preparation an action potential is induced in the motor axon and the consequent neurotransmitter release at the nmj elicits a depolarization in the muscle called an excitatory junctional potential (ejp) which is monitored with an intracellular recording electrode.

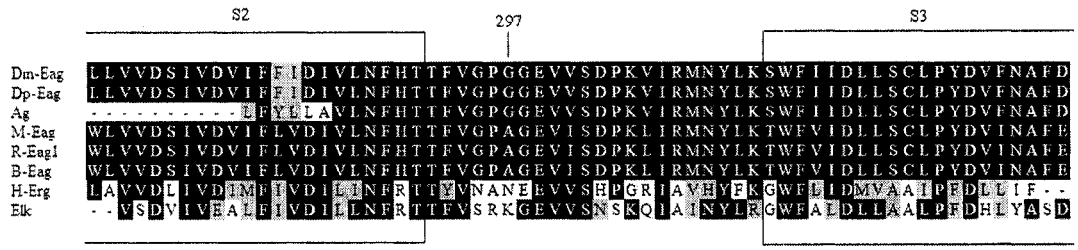

Figure 3.2 Sequence conservation in the S2-S3 loop of Eag

An alignment of the amino acid sequences corresponding to the S2 domain, the S3 domain and the S2-S3 loop of Eag from a number of species. The S2 and S3 domains are boxed. Also indicated is Dm-Eag position 297. Dm-Eag, *Drosophila melanogaster* (WARMKE *et al.* 1991); Dp-Eag, *Drosophila pseudoobscura* (RICHARDS *et al.* 2005); M-Eag, Mouse (WARMKE and GANETZKY 1994); R-Eag1 (LUDWIG *et al.* 1994), Rat; B-Eag, *Bos Taurus* (Bovine) (FRINGS *et al.* 1998); Ag-Eag, *Anopheles gambiae* (mosquito) (MONGIN *et al.* 2004), H-Erg, Human Eag related gene (WARMKE and GANETZKY 1994); Elk, Human Eag like K^+ channel (WARMKE and GANETZKY 1994). The Eag family has three branches – Eag, Erg and Elk, all with slightly different properties. At the position indicated within the S2-S3 linker, a residue with a small, non-polar side chain is conserved with the Eag sub-family.

As neurotransmitter release is dependent upon Ca^{2+} influx into the nerve terminal, at low external [Ca^{2+}] (such as 0.1mM) at most only a single quantum of neurotransmitter is released into a wild-type neuromuscular junction following nerve stimulation. As a consequence, only failures or low amplitude ejps are observed (JAN and JAN 1976). The Sh^{133} mutant exhibits a prolonged nerve terminal depolarization, leading to prolonged neurotransmitter release and an ejp of increased duration and amplitude even at low [Ca^{2+}] (JAN *et al.* 1977).

To determine if eag^{G297E} can suppress the defects in synaptic transmission conferred by the Sh^{133} mutation, I compared ejps from eag^{+} Sh^{133} with ejps from eag^{G297E} Sh^{133} (Figure 3.3). I found that the eag^{G297E} allele from either the Sup^{39} or Sup^{146} lines partially suppress the Sh^{133} phenotype in a dosage dependent manner. Significant decreases in both ejp amplitude ($p<0.001$) and duration ($p<0.001$ for eag^{G297E} from Sup^{39} and $p<0.05$ for Sup^{146}) were observed when the suppressor mutations were homozygous. When heterozygous, a moderate decrease in the Sh^{133}-induced ejp amplitude, but not ejp duration, was observed ($p<0.02$ for Sup^{146}, Figure 3.3). The smaller suppressive effect in the heterozygotes indicates that dosage of eag^{G297E} controls the degree of suppression observed.

Similar suppression of Sh^{133}-induced phenotypes has been observed previously by mutations in *para* and mle^{nap}, which decrease the number of Na^{+} channels (GANETZKY and WU 1985; STERN *et al.* 1990) and thus create hypoexcitable neurons. These

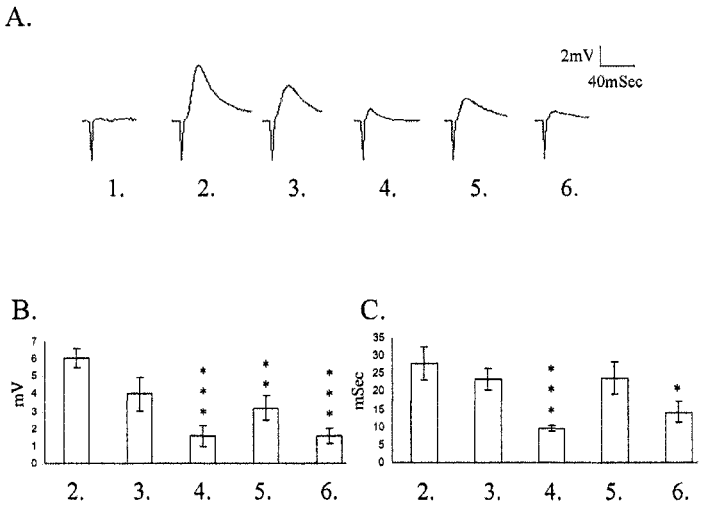

Figure 3.3 Dosage dependent suppression of Sh^{133} by eag^{G297E}

(A) Averaged intracellular muscle recordings from larvae of the indicated genotypes in response to nerve stimulation. (B) Average amplitudes of ejps evoked by nerve stimulation in the presence of low bath [Ca^{2+}] (0.1mM) in larvae of the genotypes indicated. Under these low [Ca^{2+}] conditions most successful wild type ejps result from the release of at most a single vesicle of neurotransmitter. (C) Average duration of evoked ejps. Values are presented as the mean ± SEM, data collected from at least 5 larvae for each genotype.

1. eag^{+} Sh^{+}; 2. eag^{+} Sh^{133}; 3. eag^{G297E} (from Sup^{39}) Sh^{133} / eag^{+} Sh^{133}; 4. eag^{G297E} (from Sup^{39}) Sh^{133}; 5. eag^{G297E} (from Sup^{146}) Sh^{133} / eag^{+} Sh^{133}; 6. eag^{G297E} (from Sup^{146}) Sh^{133}. *p<0.05 by student's t-test, **p <0.02 by student's test, ***p <0.01 by student's t-test versus eag^{+} Sh^{133}.

observations support the hypothesis that eag^{G297E} reduces neuronal excitability, a phenomenon that is presumably the result of conferring a gain of function phenotype on the Eag channels. A suppression of Sh^{133} could possibly be produced by increasing the number of Eag channels in the neuronal membrane; similar to the enhancement of Sh^{133} seen with *Dp para*$^{+}$ (table 3.1). An alternative possibility is that this gain of function phenoptype is the result of premature, prolonged or constitutive opening of the Eag channels.

3.6 No suppression of the Sh^{133}-induced ejp by eag^{G297E} at higher $[CaCl_2]$

When performed at higher $[CaCl_2]$ (0.4mM), eag^{G297E} does not decrease the amplitude or duration of Sh^{133} mutant ejps (Figure 3.4). This result is not unexpected as the evoked ejp at this $[CaCl_2]$ is not significantly different in *Sh* mutants as compared to wild type (JAN *et al.* 1977). The absence of an effect by eag^{G297E} in the presence of high $[CaCl_2]$ does suggest that muscle is not impaired in its response to neurotransmitter at the nmj.

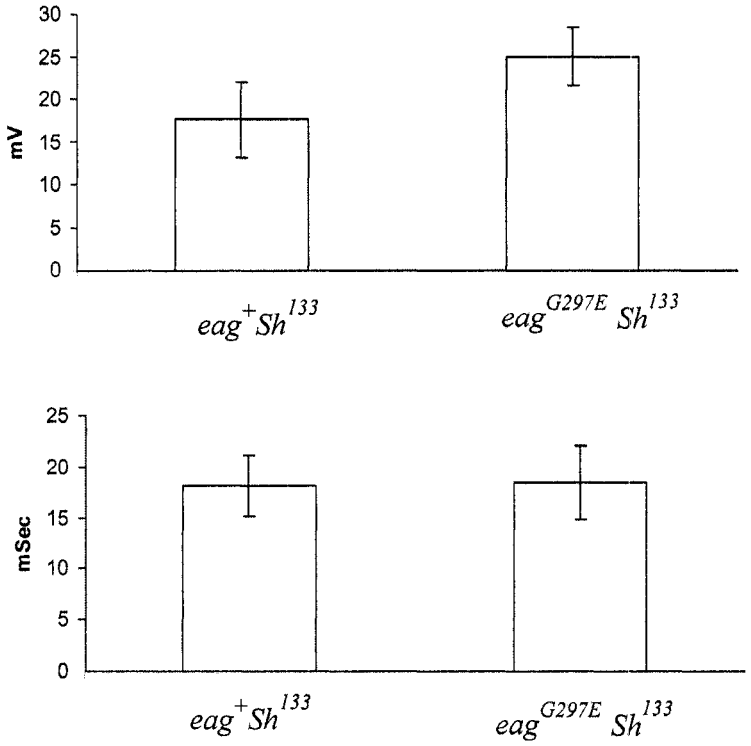

Figure 3.4 No suppression of Sh^{133} at high [$CaCl_2$]

Mean amplitudes and durations of excitatory junctional potentials (ejps) evoked by nerve stimulation in the presence of high bath [Ca^{2+}] (0.4mM) in larvae of the genotypes indicated. Values are presented as the mean ± SEM, data collected from at least 4 larvae for each genotype.

3.7 Suppression of the quinidine enhanced Sh^{133}-induced increase in neurotransmitter release by eag^{G297E}

The addition to the extracellular bath of 0.1mM quinidine, a drug that selectively blocks I_K in Drosophila larval muscles (SINGH and WU 1989), enhances the amplitude and duration of the action potential-evoked ejp in Sh^{133} mutant larvae (WU *et al.* 1989). To determine if eag^{G297E} is able to suppress this enhancement of the Sh^{133} phenotype, ejp recordings were performed at 0.1mM [Ca^{2+}] and in the presence of 0.1mM [quinidine]. As shown in Figure 3.5, when homozygous eag^{G297E} is able to partially suppress the quinidine enhanced Sh^{133} ejp phenotype.

If 0.1mM [quinidine] blocks I_K completely, how can eag^{G297E} reduce the sensitivity of the motor neuron to quinidine? There are several possible explanations. First, while it is known that 0.1mM [quinidine] nearly eliminates I_K in Drosophila larval body wall muscles (SINGH and WU 1989), it is not clear if it blocks I_K specifically and completely in the motor neuron. Second, the G297E mutation might render Eag less sensitive to quinidine than eag^+. This possibility is supported by the observation that mutations in human Eag can alter the binding characteristics of quinidine and other antiarrhythmic agents (GESSNER *et al.* 2004). Third, the K^+ channels distinct from I_K in which Eag participates (I_A, I_{CS} & I_{CF} (GANETZKY and WU 1983; WARMKE *et al.* 1991; WU *et al.* 1983; ZHONG and WU 1991)) are not sensitive to quinidine, and it is possible that Eag^{G297E} exerts its effects through one of these channels.

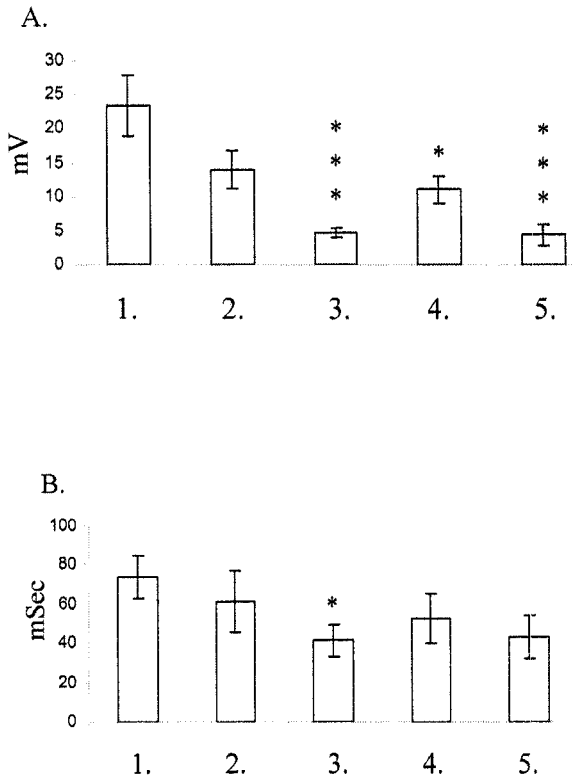

Figure 3.5 Suppression of the *Sh*^{133}-induced increase in neurotransmitter release by *eag*^{G297E}: effects of quinidine

Mean amplitudes and durations of excitatory junctional potentials (ejps) evoked by nerve stimulation in the presence of low bath [Ca^{2+}] (0.1mM) and 0.1mM [quinidine] in larvae of the genotypes indicated. Values are presented as the mean ± SEM, data collected from at least 4 larvae for each genotype.

1. *eag*$^{+}$ *Sh*^{133}; 2. *eag*^{G297E} (from *Sup*^{39}) *Sh*^{133} / *eag*$^{+}$ *Sh*^{133}; 3. *eag*^{G297E} (from *Sup*^{39}) *Sh*^{133}; 4. *eag*^{G297E} (from *Sup*^{146}) *Sh*^{133} / *eag*$^{+}$ *Sh*^{133}; 5. *eag*^{G297E} (from *Sup*^{146}) *Sh*^{133}. *p<0.05, ***p <0.01 versus *eag*$^{+}$ *Sh*^{133}.

3.8 Suppression of the Sh^{133}-induced ejp by eag^{G297E} is not allele specific

The eag^{G297E} mutation does not appear to produce any obvious behavioral abnormality in an otherwise wild type background. No temperature sensitive paralysis is observed, the flies appear well coordinated and flight appears normal. To determine if eag^{G297E} confers a defect in synaptic transmission in an otherwise wild type background, I made measurements of ejp amplitude and duration at 0.15mM [$CaCl_2$]. No significant decrease in either ejp amplitude or duration was observed (data not shown). Similarly, the onset rate of long term facilitation (JAN and JAN 1978) was also unaffected by eag^{G297E} (see chapter 3.12). The observation that eag^{G297E} conferred no detectable excitability phenotype in a Sh^{+} background raised the possibility that the suppression of Sh^{133} by eag^{G297E} might be an allele-specific restoration of Sh function. This possibility is supported by the observation that Eag and Sh subunits can co-assemble in a channel complex (CHEN *et al.* 1996; CHEN *et al.* 2000). To test this possibility I examined the effects of eag^{G297E} on the hyperexcitability conferred by the K^{+} channel blocking drug 4-aminopyridine (4-AP) which is a specific Sh channel blocker (GANETZKY and WU 1983; YAMAMOTO and SUZUKI 1989).

I found that the amplitude of ejps evoked at 0.1mM [$CaCl_2$] and 2mM [4-AP] was significantly suppressed by eag^{G297E} (Figure 3.6). This suppression of the increased ejp conferred by 4-AP suggests that the G297E mutation is increasing the activity of the

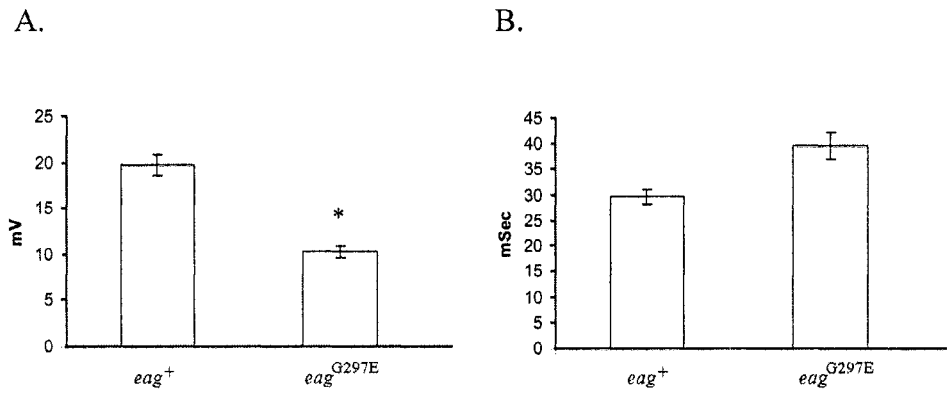

Figure 3.6 Suppression of Sh^{133} by eag^{G297E} is not allele specific

Mean amplitudes and durations of excitatory junctional potentials (ejps) evoked by nerve stimulation in the presence of low bath [Ca^{2+}] (0.1mM) and 2mM [4-AP] in larvae of the genotypes indicated. Values are presented as the mean ± SEM, data collected from at least 5 larvae for each genotype. *$p<0.05$, versus eag^{+}.

voltage-gated K^+ channels that remain active following the addition of 4-AP, and thus that the suppression of the *Sh*-induced increased ejp is not allele specific.

3.9 eag^{G297E} suppresses the effect of TEA

Having shown that eag^{G297E} suppresses the effect of 4-AP on synaptic transmission, I tested the effects of eag^{G297E} on the hyperexcitability conferred by a second K^+ channel blocking drugs tetraethylammonium (TEA), which is a more general voltage-gated K^+ channel blocker (GANETZKY and WU 1983; YAMAMOTO and SUZUKI 1989).

I found that the large amplitude and prolonged ejp's evoked at 0.1mM [$CaCl_2$] by addition of 10mM [TEA] were easily evoked in all wild type larvae; in contrast in eag^{G297E} larvae it was possible to evoke such an ejp in only about half of the larvae tested (data not shown). Furthermore as shown in Figure 3.7, even when an ejp was successfully elicited, eag^{G297E} reduced the amplitude and duration of the ejp in comparison to eag^{+}. This suppression of the increased ejp conferred by TEA further suggests that the G297E mutation is increasing the activity of the voltage-gated K^+ channels that remain active following the addition of either 4-AP or TEA. Interestingly, it appears that eag^{G297E} manifests its most obvious phenotypes under conditions that prolong the action potential.

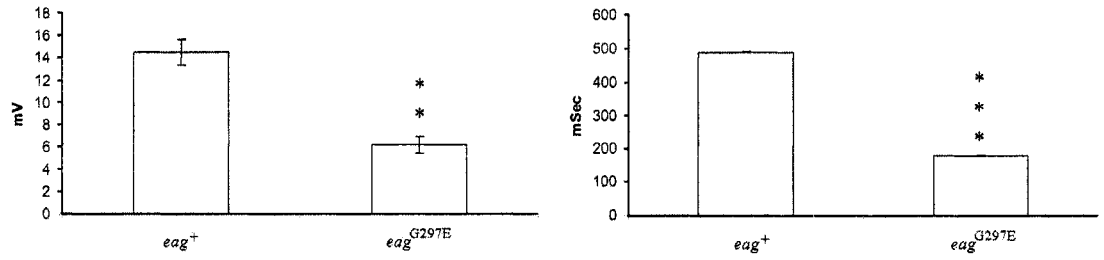

A. B.

Figure 3.7 *eag*^{G297E} suppresses the effect of TEA

Mean amplitudes and durations of excitatory junctional potentials (ejps) evoked by nerve stimulation in the presence of low bath [Ca^{2+}] (0.1mM) and 10mM [TEA] in larvae of the genotypes indicated. Values are presented as the mean ± SEM, data collected from at least 4 larvae for each genotype. **p<0.02, ***p <0.01 versus *eag*$^{+}$.

3.10 eag^{G297E} acts presynaptically to suppress Sh^{133}

The suppression of the Sh^{133}-induced increased amplitude ejp conferred by eag^{G297E} could be a consequence of a suppression of the increased neurotransmitter release of Sh^{133} mutants, of reduced sensitivity of the muscle membrane glutamate receptors to the neurotransmitter L-glutamate, or increased voltage-dependent or voltage-independent K^+ currents in the muscle membrane. To distinguish among these possibilities I monitored synaptic transmission while holding the muscle membrane potential to -60mV with a voltage clamp, which prevents the opening of voltage-gated ion channels such as Eag and Sh in the muscle membrane. If the eag^{G297E}-dependent suppression of the Sh^{133}-induced increase in ejp size is due to suppression of the increased neurotransmitter release, then I expect that excitatory junctional currents (ejcs) of reduced amplitude will be observed in eag^{G297E} Sh^{133} compared with eag^{+} Sh^{133}. In contrast, if the suppression of the ejp amplitude phenotype is a result of altered muscle voltage-dependent K^+ currents then ejc amplitude in eag^{G297E} Sh^{133} is expected to be the same as eag^{+} Sh^{133}. Figure 4 shows that the ejc in eag^{G297E} Sh^{133} is significantly smaller than in eag^{+} Sh^{133}, which is consistent with the notion that eag^{G297E} acts pre-synaptically to suppress Sh^{133} phenotypes by decreasing the amount of neurotransmitter released. The proportional reduction in ejc amplitude (69%) is similar to the proportional reduction in ejp amplitude (73%).

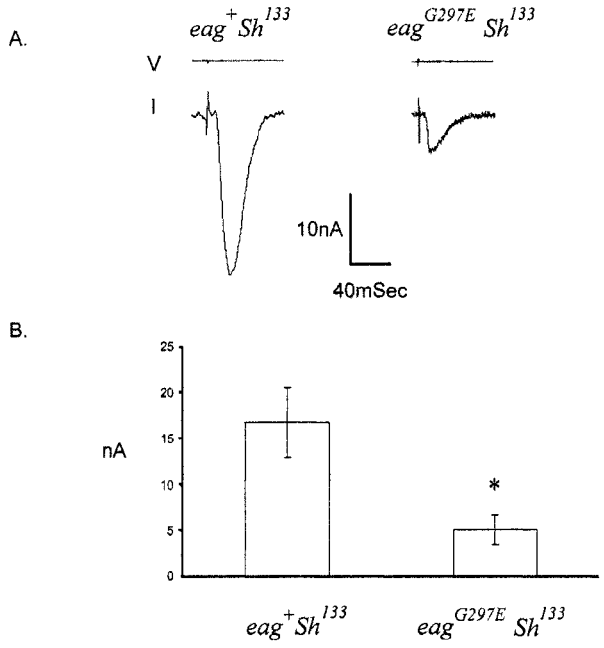

Figure 3.8 The *eag*^{G297E} mutation acts pre-synaptically to suppress the phenotypes of *Sh*^{133}

(A) Typical excitatory junctional currents (ejcs) in response to nerve stimulation in the presence of 0.1mM [Ca^{2+}]. Holding potential was -60mV. Simultaneous intracellular recording of voltage (V) and current (I) were performed. (B) Average amplitude of evoked ejcs. *eag*^{G297E} from *Sup*^{39}. Values presented as mean ± SEM, n = 4. *$p<0.05$ by student's t-test.

To exclude the possibility that an altered voltage-independent current or altered sensitivity to L-glutamate is responsible for the suppression of the ejp phenotypes I compared the amplitude of spontaneous miniature ejps (mejp) in eag^{+} Sh^{133} and eag^{G297E} Sh^{133}. If the eag^{G297E}-dependent suppression of the Sh^{133}-induced increased ejp amplitude is due to decreased muscle response to the neurotransmitter L-glutamate or increased voltage-independent K^{+} currents, then mejps of reduced amplitude will be observed in eag^{G297E} Sh^{133} compared to eag^{+} Sh^{133}. I found that the mejp amplitudes recorded in eag^{G297E} Sh^{133} and eag^{+} Sh^{133} are almost identical (0.79mV ±0.11 and 0.81mV ±0.14 respectively), suggesting eag^{G297E} does not affect voltage-independent currents or the muscle response to L-glutamate. I conclude that eag^{39} acts pre-synaptically to suppress the effects of Sh^{133}.

3.11 Suppression by eag^{G297E} of the Sh^{133}-induced increase in neuronal excitability requires extracellular Mg^{2+}

The S2 and S3 transmembrane domains of Eag contain three aspartic acid residues that coordinate the binding of a Mg^{2+} ion when the channel is in its closed state (SCHONHERR *et al.* 2002; SILVERMAN *et al.* 2000; TANG *et al.* 2000). Mg^{2+} ions slow channel activation in a concentration- and voltage-dependent manner in bovine, mouse and Drosophila Eag (SCHONHERR *et al.* 1999; SILVERMAN *et al.* 2000; TANG *et al.* 2000; TERLAU *et al.* 1996). The observation that the G297E substitution falls within the highly

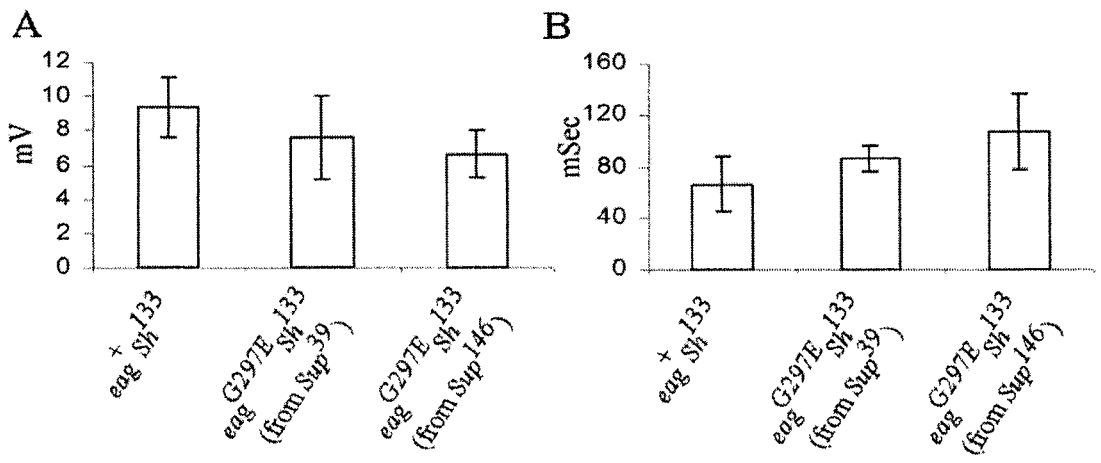

Figure 3.9 Suppression of the *Sh*^{133}-induced increase in neurotransmitter release by *eag*^{39} and *eag*^{146} requires extracellular Mg^{2+}

Mean amplitudes and durations of ejps evoked by nerve stimulation in the absence of extracellular $MgCl_2$ and in the presence of low bath [Ca^{2+}] (0.1mM) in larvae of the genotypes indicated. Values are presented as the mean ± SEM, data collected from at least 4 larvae for each genotype.

conserved S2-S3 linker raised the possibility that G297E acts by eliminating or reducing the effect of Mg^{2+}. If so, then in the absence of extracellular Mg^{2+}, neuronal excitability is predicted to be the same in eag^{G297E} and eag^{+}. To test this possibility, ejp recordings were performed in eag^{G297E} Sh^{133} and eag^{+} Sh^{133} at low [Ca^{2+}] in the absence of extracellular Mg^{2+} (table 4). Table 4 shows that the ejp amplitude and duration are not significantly different in eag^{+} Sh^{133} as in eag^{G297E} Sh^{133}. This observation supports the hypothesis that the regulatory effects of Mg^{2+} upon Eag have been lost in eag^{G297E} and is consistent with the possibility that eag^{G297E} increases Eag activity by reducing the affinity of Eag for Mg^{2+}.

The model of Mg^{2+} action upon Eag proposed by Schönherr et al. (2002) suggests that Mg^{2+} is involved in the switch between the resting ("locked") and activated ("unlocked") states (Figure 1.5). I suggest that the G297E mutation alters the configuration of the channel such that it favors the "unlocked" over the "locked" state. Studies of this mutant channel in ooctyes would be required to test this possibility.

3.12 eag^{84}, but not eag^{G297E}, produces a hypoexcitable LTF phenotype

Like eag^{G297E}, eag^{84} does not confer decreased ejp amplitude in an otherwise wild-type background. Similarly, no temperature sensitive paralysis or other behavioral phenotypes are observed. However, unlike eag^{G297E}, the rate of onset of LTF in eag^{84} is decreased as compared to wild-type (Figure 3.10). Delayed facilitation was observed

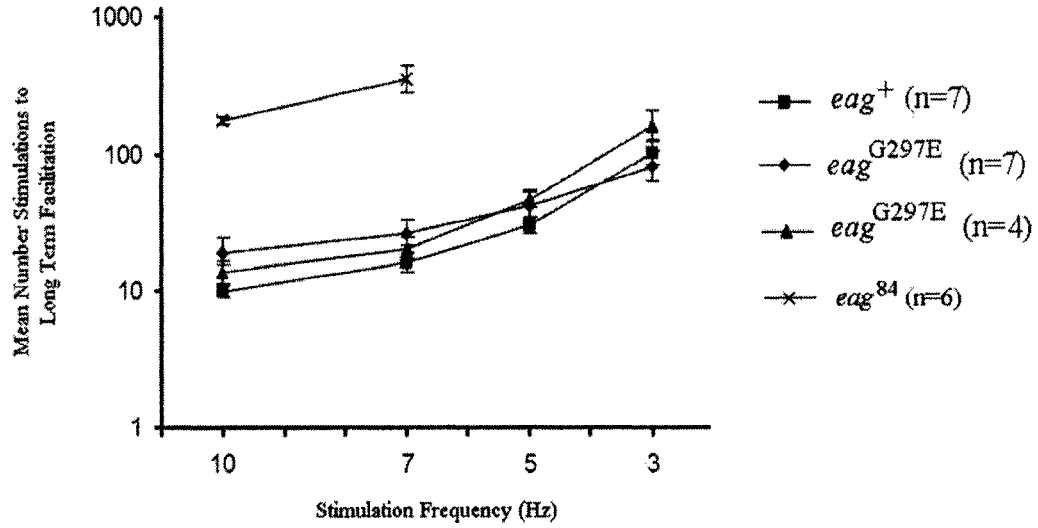

Figure 3.10 *eag*^{84} delays the onset of long term facilitation

Average number of stimulations required to elicit the facilitative response at the stimulation frequencies tested (10, 7, 5 and 3 Hz). No facilitation observed in *eag*^{84} at 5 or 3 Hz stimulation. Both *eag*^{G297E} alleles from *Sup*^{146}. Values presented as mean ± SEM, n-values as indicated.

following stimulation at 10Hz and 7Hz, but no facilitation was seen in eag^{84} larvae at 5Hz or 3Hz, unlike wild-type that facilitated at all frequencies tested. This indicates a significant decrease in neuronal excitability in eag^{84}.

3.13 eag^{84} suppresses the effects of 4-AP and TEA on motor neuron excitability

To determine if eag^{84} could suppress the hyperexcitability conferred by 4-AP, I compared the amplitude and duration evoked ejps in the presence of 4-AP in eag^{84} and eag^{+} larvae. Like eag^{G297E}, eag^{84} significantly reduced the amplitude of ejps evoked at 0.1mM [$CaCl_2$] and 2mM [4-AP] in an otherwise wild-type background (Figure 3.11). This suggests that eag^{84} is also likely to suppress the Sh^{133}-induced ejp.

I was unable to elicit the typical TEA-induced exaggerated response seen in wild-type larvae in any of the eag^{84} larvae tested (n=4). This indicates that eag^{84} is increasing the activity of K^+ channels that retain activity in the presence of either 4-AP or TEA.

3.14 Aberrant phosphorylation hypothesis

I suggested in chapter 1.5 that there is a positive feedback loop in which CaMKII phosphorylates Eag to enhance its activity, which in turn further activates CaMKII. I

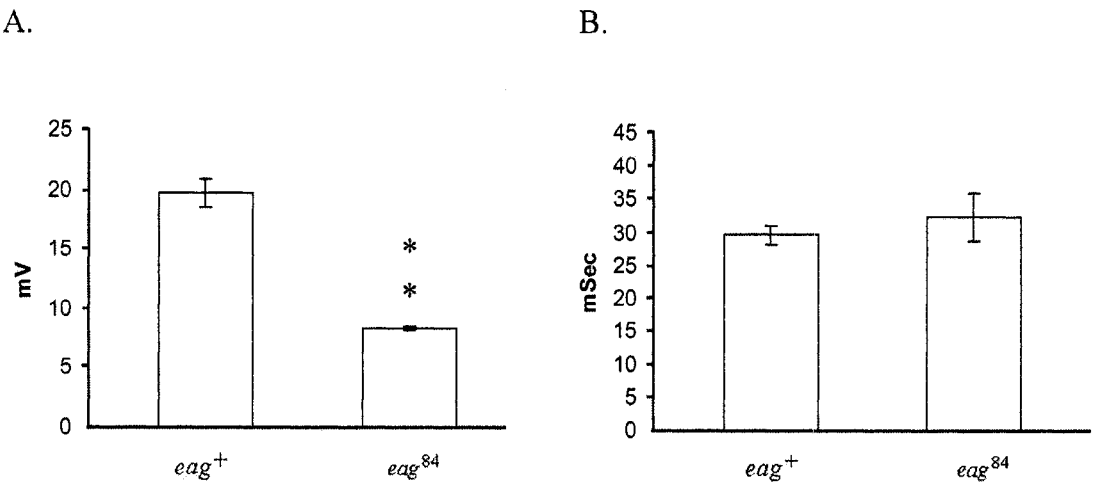

Figure 3.11 Suppression of the effects of 4-AP by *eag*^{84}

Mean amplitudes and durations of excitatory junctional potentials (ejps) evoked by nerve stimulation in the presence of low bath [Ca^{2+}] (0.1mM) and 2mM [4-AP] in larvae of the genotypes indicated. Values are presented as the mean ± SEM, data collected from at least 4 larvae for each genotype. **$p<0.02$, versus *eag*$^{+}$.

hypothesize that as one of the substitutions in eag^{84} (E762V) is close to the CaMKII phosphorylation site (T787) and the CaMKII binding site (residues 773-794), the gain-of-function characteristics of eag^{84} are due to aberrant phosphorylation. A mutation that makes Eag easier to phosphorylate would cause an increased level of Eag phosphorylation and thus an increased level of Eag activity. Additionally, altering a phosphorylation mechanism may explain why eag^{84} produces a LTF phenotype where eag^{G297E} does not.

3.15 Phenocopying of eag^{G297E} and eag^{84} with a UAS transgene

To show that the identified mutations are truly responsible for the phenotypes observed, I attempted to create UAS-*eag* transgenes carrying the mutations. Previous attempts to create UAS-*eag* transgenes have been unsuccessful; my strategy was to create a transgene with no UTRs as this had not previously been tried. While obtaining a cDNA I learnt that another group had made transgenic flies carrying the wild-type construct that I was trying to make (LESLIE GRIFFITH, PERSONAL COMMUNICATION). As this group has not been able to make the transgene functionally express, there is no purpose served in creating the mutant transgenes. A potential solution is to use homologous recombination to replace the wild-type gene in control line with a mutant copy.

3.16 Conclusions

eag^{G297E}

The results shown here demonstrate that the leg-shaking and electrophysiological phenotypes caused by the Sh^{133} mutation are suppressed in a dosage dependent manner by eag^{G297E}. Because phenotypes of eag^{G297E} are opposite to those of *eag* loss-of-function mutants (BRUGGEMANN *et al.* 1993; WARMKE *et al.* 1991; WU *et al.* 1983) I propose that these new mutations confer a gain-of-function phenotype to the Eag channels. Thus, *eag* activity regulates neuronal excitability: reduction in *eag* activity confers a hyperexcitable neuron, whereas increases in *eag* activity confer a hypoexcitable neuron. A similar phenomenon occurs with the *para*-encoded Na^+ channel: decreasing or increasing channel number produces hypoexcitable or hyperexcitable neurons respectively (STERN *et al.* 1990). Given that eag^{G297E} acts pre-synaptically, I hypothesize that the neuronal hypoexcitability effect is mediated by the premature, prolonged or constitutive opening of the Eag channels in the motor neuron membrane, resulting in an attenuation of the action potential. Furthermore, the experiments raise the possibility that the reduction or elimination of the response to extracellular Mg^{2+} may be responsible for this gain of function phenotype of eag^{G297E}.

Polymorphisms such as eag^{G297E}, if they exist in humans, might be of particular therapeutic importance because an individual carrying such a polymorphism might exhibit no overt abnormalities, and yet show an aberrant sensitivity to particular

therapeutic drugs. The identification of a gain of function mutation in a K^+ channel gene that can be further studied both *in vivo* and *in vitro* provides a unique opportunity to obtain new knowledge in K^+ channel regulation.

***eag*^{84}**

I propose that *eag*^{84} also confers a gain of function phenotype to Eag channels. The mode of action of *eag*^{84} appears to be different to *eag*^{G297E}. It seems possible that the gain of function phenotype may be conferred through a phosphorylation dependent mechanism, although this hypothesis remains to be tested. Like *eag*^{G297E}, it appears that the phenotypes of *eag*^{84} are best observed under conditions that prolong the action potential such as in the presence of drugs such as quinidine and 4-AP.

3.17 Future Work

Future experiments that may be considered either in the Stern lab or in other labs include: analysis of the current voltage relationship in larval muscles, ooctye expression and single channel analysis of channel activation kinetics and Mg^{2+} dependence, biochemical analysis of channel phosphorylation, and the replacing of wild-type *eag* with mutant forms *in vivo* using homologous recombination.

Chapter 4: Tissue specificity of *eag*

4.1 Introduction

Neuronal function is in large part regulated by K^+ ion channels. The loss of a K^+ channel such as the Drosophila *eag*-encoded voltage gated K^+ channel results in increased neuronal excitability, that is, an increase in the propensity for a neuron to generate and propagate an action potential in response to synaptic activity. Loss of function mutations in K^+ channel subunit genes such as *eag, Sh,* and *Hk* confer electrophysiological phenotypes such as spontaneous or prolonged action potentials, which lead to behavioral phenotypes such as ether-induced leg shaking (GANETZKY and WU 1983; WARMKE *et al.* 1991; WU *et al.* 1983; ZHONG and WU 1991). For example, the first *ether-à-go-go (eag)* mutation was identified by its ether-induced leg shaking phenotype (KAPLAN and TROUT 1969); these were later found to be caused by spontaneous action potentials (WU *et al.* 1983).

While many of the characteristics of Eag have been studied *in vivo* and in heterologous systems, no definitive data exist to confirm in which tissues the normal function of Eag is necessary for correct neuronal function. Recent work using a truncated, dominant negative, *eag* transgene has shown that the expression of this transgene in motor neurons is sufficient to replicate the degree of ether-induced leg shaking observed in eag^1 mutant flies (BROUGHTON *et al.* 2004). It has not, however, been determined if this dominant negative transgene can also recapiulate the other phenotypes of *eag*

mutations, such as the observation of spontaneous ejps at the larval neuromuscular junction or the enhancement of the *push*^{1}-induced thickening of the larval perineural glia. Concern also remains that the dominant negative transgene is producing a phenotype via some secondary mechanism rather than by only preventing the proper formation of channels containing the Eag subunit.

The aims of this study are to confirm that the loss of Eag function in neuronal tissues is sufficient to confer neuronal hyper-excitability, to demonstrate that the UAS-*eag*$^{\Delta 1932}$ transgene disrupts Eag function and not some other intracellular process, and to determine in which tissue(s) the loss of Eag function acts to enhance the *push*^{1}-induced thickening of the perineural glia.

4.2 Methods

Drosophila stocks: All fly stocks were maintained on standard cornmeal/agar Drosophila media at room temperature. The *push*^{1} allele is a recessive *push* allele described previously (RICHARDS *et al.* 1996; YAGER *et al.* 2001) that causes neurophysiological defects, sterility, and a thickening of the perineural glia. The UAS-*eag*$^{\Delta 1932}$ line carries a truncated form of *eag* that produces a dominant negative effect that behaviorally mimics the *eag*^{1} mutation (BROUGHTON *et al.* 2004).

UAS-*eag*^{RNAi} transgenic flies: The RNAi transgene targeting the *eag*-encoded K^+ channel was created by amplifying a 509bp fragment of genomic DNA corresponding to the 5'UTR and most of exon 1 of *eag* was amplified by PCR (primers: forward: ATATAAGAATTC-GAAAGAGAGTGAGACAGC; reverse: ATATAAAGATCT-GCATGATGATGTTCTCCGAGG). The PCR product was TA-cloned into the pGEM-T vector (Promega). An *EcoR*I/*Bgl*II double digest was then used to transfer the PCR product into the *sym-p*UAST plasmid (GIORDANO *et al.* 2002). Finally, the transgene was introduced into Drosophila using P-element mediated transformation. The fragment of *eag* used as the trigger for RNAi shows no significant homology to other Drosophila genes as determined by a BLAST search of all Drosophila sequences.

Behavioral tests: *Leg-shaking*: Ether-induced leg shaking was assayed by exposing young adult flies to ether for about 10 seconds. Under these conditions, wild-type flies are immobilized except for occasional tarsal twitches; *Sh*^{133}-mutant flies exhibit a rapid shaking of all six legs.

Electrophysiology: Larval dissections and muscle recordings were performed as described previously (GANETZKY and WU 1982; HUANG and STERN 2002; JAN and JAN 1976; STERN *et al.* 1995; STERN and GANETZKY 1989). Ventral lateral longitudinal peripheral nerves that innervate the body wall muscles were cut immediately posterior to the ventral ganglion and were stimulated using a suction electrode. Intracellular muscle recordings were made using a microelectrode pulled on a Flaming/Brown micropipette puller to tip resistances of 30-60 MΩ and filled with 3M KCl. All dissections and

recordings were performed at room temperature in standard saline solution (0.128M NaCl, 2.0 mM KCl, 4.0 mM $MgCl_2$, 0.34 M sucrose, 5.0 mM HEPES pH 7.1 and $CaCl_2$ as specified in the text). Quinidine was applied following dissection as described previously (JAN *et al.* 1977; SINGH and WU 1989)

Semi-quantitative PCR: Semi-quantitative PCR was performed on RNA extracted from the heads of 20 flies. Flies were manually decapitated, and RNA was extracted using the TRIzol® Reagent Protocol (GIBCOBRL). Oligo$(dT)_{20}$-primed cDNAs were prepared using the SuperScript III First-Strand Synthesis System (Invitrogen).

Western blotting: Western blots were performed on total protein extracted from heads of 20 flies. The flies were decapitated as described above and protein extracted using standard methods and probed using an anti-Eag antibody.

Transmission electron microscopy: Tissue sections were prepared as described previously (YAGER *et al.* 2001). Wandering third instar larvae were grown in uncrowded half-pint bottles at room temperature and were collected 1-2 days after the first third instar larva appeared. Larvae were dissected, fixed with glutaraldehyde and paraformaldehyde, stained with both 0.5% OsO_4 and 2% uranyl acetate, and embedded in an eponate 12-araldite mixture. Ultrathin cross-sectional slices (pale gold, 75-125 nm thick) were captured, poststained with uranyl acetate and Reynolds lead citrate, and analyzed using a transmission electron microscope. The thickness of the perineural glial layer for a given nerve was determined by averaging the distance from the edge of the

nerve to the boundary of the axon containing lumen at 8 different positions equally spaced around the nerve. Measurements were not taken when a perineural glial cell nucleus was encountered.

4.3 Results

An RNAi transgene targeting the *ether-à-go-go* (*eag*) gene was created for use in the GAL4/UAS system (BRAND and PERRIMON 1993) to create larvae and adults with increased neuronal excitability. Enhancer trap GAL4 lines were used to drive the expression of the RNAi transgene (UAS-eag^{RNAi}, see methods) to enhance neuronal excitability. The GAL4 lines were chosen for their particular expression patterns in regions previously implicated in Eag function. The tissues tested by these GAL4 lines include post-mitotic neurons (*elav*-GAL4 (SCHUSTER *et al.* 1996)) and motor neurons (D42 (YEH *et al.* 1995)).

4.3.1 Neuronal expression of UAS-eag^{RNAi} confers neuronal excitability

The overexpression of a novel, dominant negative, truncated *eag* K^+ channel in motor neurons enhances their excitability (BROUGHTON *et al.* 2004). To determine if the knockdown of the *eag* transcript by RNAi could also enhance neuronal excitability, we made intracellular muscle recordings in third instar larvae of the genotypes *elav*-GAL4/Y; eag^{RNAi}/+, a*ct5C*-GAL4/UAS-eag^{RNAi} and *elav*-GAL4/Y; UAS-eag^{RNAi}.

Spontaneous ejps in the presence of 0.4 mM [$CaCl_2$], characteristic of *eag* mutants (WU *et al.* 1983), were only observed in the *elav*-GAL4/Y; UAS-eag^{RNAi} larvae (Figure 4.1), indicating that with two copies of the RNAi transgene, the knockdown of *eag* in neurons is sufficient to phenocopy loss-of-function mutations in *eag*. Similarly, *elav*-GAL4/Y; UAS-eag^{RNAi} adults displayed ether-induced leg shaking, whereas a single copy of the RNAi transgene driven by either *elav*-GAL4 or *act5C*-GAL4 was unable to do so. This provides independent verification of the finding that the loss of Eag function in motor neurons is sufficient to elicit the characteristic *eag* mutant behavioral phenotype (BROUGHTON *et al.* 2004) and indicates that the effect of the dominant negative transgene is to disrupt Eag function specifically.

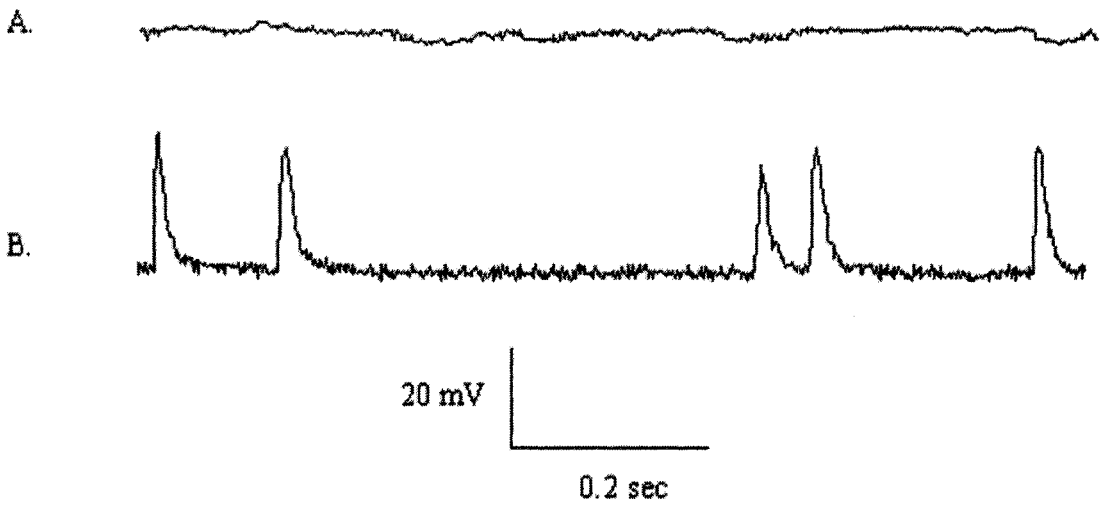

Figure 4.1 RNAi knockdown of neuronal *eag* elicits spontaneous ejps

Example intracellular recordings obtained from larval neuromuscular junctions in A. wild-type and B. *elav*-GAL4/y; UAS-eag^{RNAi} larvae in the presence of 0.4 mM [$CaCl_2$]. Spontaneous ejps are observed in *elav*-GAL4/Y; UAS-eag^{RNAi} larvae (B.), whereas only miniature ejps were observed in wild-type larvae (A.).

4.4 Future work

4.4.1 Is disruption of *eag* in motor neurons sufficient to phenocopy eag^1?

To show that the dominant negative and RNAi constructs confer the same affect upon neuronal excitability, recordings should be made at the larval nmj of *elav*-GAL4; UAS-$eag^{\Delta 932}$ larvae in the presence of 0.4 mM [$CaCl_2$]; spontaneous ejps will confirm the existing data. If driving the dominant negative transgene with D42, which drives transgene expression in motor neurons, produces the same result, then the effect can be considered specific to motor neurons.

4.4.2 Are mRNA and protein levels decreased in *elav*-GAL4; UAS-eag^{RNAi} heads?

To determine the efficiency of the disruption of *eag* expression, I propose to compare *eag* mRNA and Eag protein levels in adult heads from *elav*-GAL4; UAS-eag^{RNAi} and wild-type flies. The *eag* mRNA levels in adult heads will be assayed by semi-quantitative PCR. Protein levels will be measured using Western blotting with an anti-Eag antibody.

4.4.3 Does neuronally driven $eag^{\Delta 932}$ enhance $push^{1}$ nerve thickness?

Whereas the eag^{1} mutation alone has no effect upon the thickness of the perineural glia in the third instar larval peripheral nervous system, the eag^{1} mutation confers a significant enhancement of the $push^{1}$-induced increase in perineural glial thickness (YAGER *et al.* 2001). I propose to determine in which tissue(s) the loss of Eag function is sufficient to affect perineural glial thickness. Since two copies of the UAS-eag^{RNAi} construct are needed to produce a neurophysiological phenotype, and only one copy of the UAS-$eag^{\Delta 932}$ transgene is sufficient to mimic the eag^{1} mutation (BROUGHTON *et al.* 2004), I propose to use the dominant-negative transgene rather than the RNAi transgene. I predict that neuronal expression of the UAS-$eag^{\Delta 932}$ transgene will produce an enhancement of the $push^{1}$-induced thickening of the perineural glial layer.

Chapter 5: A dominant-negative *inebriated* transgene

5.1 Introduction

The control of neuronal excitability, the propensity for a neuron to generate and propagate an action potential in response to synaptic activity, is in large part regulated by ion channels, that themselves are affected by other proteins and neurotransmitters. Such affects can be direct, as in the enhancement and suppression of the Sh^{133} mutation by mutations in other ion channels (CARDNELL *et al.* 2006; STERN *et al.* 1990), or indirect, as observed with the *in vivo* manipulation of the Drosophila neurotransmitter transporter encoded by *inebriated (ine)* (HUANG and STERN 2002).

The *ine* mutation was first identified for its increased neuronal excitability that enhanced the Sh^{133}-mutant behavioral phenotypes (STERN and GANETZKY 1992). Flies defective in both *ine* and *Sh*, which encodes a voltage gated K^+ channel subunit, display a downturned wing and indented thorax phenotype, a phenotype identical to that seen in *eag Sh* double mutants (STERN *et al.* 1990). Two isoforms of *ine* are transcribed in Drosophila, a long form (*ine-RA*) and a short form (*ine-RB*) (BURG *et al.* 1996; SOEHNGE *et al.* 1996). These two isoforms encode two proteins that differ only at the N-terminus, at which the long form (Ine-P1) has an additional domain that is not present in the short form (Ine-P2); this N-terminal extension of Ine-P1 bears no significant homology to any other known protein domains.

Whereas the *UAS-ine-RA* construct was able to fully rescue the excitability phenotypes of ine^{1}, *UAS-ine-RB* was only able to partially rescue the phenotypes (HUANG and STERN 2002). These results suggest that the unique N-terminal domain of Ine-P1 is important for some aspects of neuronal excitability regulation. I hypothesize that the over expression of the N-terminal 313 amino acids of the long isoform of Inebriated will create a dominant negative phenotype conferring neuronal hyper-excitability by preventing the N-terminal domain of endogenous full-length Ine-P1 from interacting with its intracellular partners.

5.2 Methods

Drosophila stocks: All fly stocks were maintained on standard cornmeal/agar Drosophila media at room temperature, except where indicated for viability assays. The Sh^{133} allele is a dominant *Sh* allele described previously (JAN *et al.* 1977; KAPLAN and TROUT 1969) that produces a rapid leg-shaking phenotype when under ether anesthesia. The $push^{1}$ allele is a recessive *push* allele described previously (RICHARDS *et al.* 1996; YAGER *et al.* 2001) that causes neurophysiological defects, sterility, and a thickening of the perineural glia.

UAS-$ineP1^{1\text{-}313}$ transgenic flies: The truncated UAS-$ineP1^{1\text{-}313}$ transgene was created by amplifying a 939bp genomic fragment starting at the ATG start codon of *ine-RA* with PCR (primers: forward: GAATTC-ATGGCGGAGAACAAAGCAG, reverse:

GGTACC-TGGTGGCGTCTGCGATTG). This fragment of *ine-RA* was cloned into pGEM-T. We then used the *EcoR*I and *Kpn*I restriction sites to transfer this fragment into *p*UAS-T. Finally, the transgene was introduced into Drosophila using P-element mediated transformation.

Behavioral tests: *Leg-shaking*: Ether-induced leg shaking was assayed by exposing young adult flies to ether for about 10 seconds. Under these conditions, wild-type flies are immobilized except for occasional tarsal twitches; Sh^{133}-mutant flies exhibit a rapid shaking of all six legs.

Electrophysiology: Larval dissections and muscle recordings were performed as described previously (GANETZKY and WU 1982; HUANG and STERN 2002; JAN and JAN 1976; STERN *et al.* 1995; STERN and GANETZKY 1989). Ventral lateral longitudinal peripheral nerves that innervate the body wall muscles were cut immediately posterior to the ventral ganglion and were stimulated using a suction electrode. Intracellular muscle recordings were made using a microelectrode pulled on a Flaming/Brown micropipette puller to tip resistances of 30-60 MΩ and filled with 3M KCl. All dissections and recordings were performed at room temperature in standard saline solution (0.128 M NaCl, 2.0 mM KCl, 4.0 mM $MgCl_2$, 0.34 M sucrose, 5.0 mM HEPES pH 7.1, and $CaCl_2$ as specified in the text). Quinidine was applied following dissection as described previously (JAN *et al.* 1977; SINGH and WU 1989)

Viability assays on hypertonic media: Flies were grown in uncrowded half-pint bottles and collected during the first four days following the initial eclosions. Following etherization, flies were aliquoted into groups of 20 and placed into vials for 1 day to allow recovery from the etherization. The flies were then transferred into vials containing instant medium (Carolina) prepared according to the manufacturer's instructions, except that salt solutions of the appropriate concentrations were substituted for water. Fly manipulations and assays were performed at 18°C and 70% relative humidity, and fly viability on salt media was assayed every day for 10 days.

Transmission electron microscopy: Tissue sections were prepared as described previously (YAGER *et al.* 2001). Wandering third instar larvae were grown in uncrowded half-pint bottles at room temperature and were collected 1-2 days after the first third instar larva appeared. Larvae were dissected, fixed with glutaraldehyde and paraformaldehyde, stained with both 0.5% OsO_4 and 2% uranyl acetate, and embedded in an eponate 12-araldite mixture. Ultrathin cross-sectional slices (pale gold, 75-125 nm thick) were captured, poststained with uranyl acetate and Reynolds lead citrate, and analyzed using a transmission electron microscope. The thickness of the perineural glial layer for a given nerve was determined by averaging the distance from the edge of the nerve to the boundary of the axon containing lumen at 8 different positions equally spaced around the nerve. Measurements were not taken when a perineural glial cell nucleus was encountered.

5.3 Results

A transgene based upon the *inebriated* (*ine*) gene was created for use in the GAL4/UAS system (BRAND and PERRIMON 1993) to create larvae and adults with increased neuronal excitability. Five enhancer-trap GAL4 lines were used to drive the expression of a novel truncated *ine* transgene (UAS-*ineP1*$^{1\text{-}313}$; see methods) to enhance neuronal excitability. The GAL4 lines were chosen for their particular expression patterns in regions previously implicated in Ine function. The tissues tested by these GAL4 lines include post-mitotic neurons (*elav*-GAL4 (SCHUSTER *et al.* 1996)), motor neurons (D42 (YEH *et al.* 1995)), and peripheral glia (*gli*-GAL4 and MZ709 (ITO *et al.* 1995; SEPP and AULD 1999)), alongside a GAL4 line expressed in all tissues at all times (*act5C*-GAL4 (PIGNONI and ZIPURSKY 1997)).

5.3.1 Neuronal expression of UAS-*ineP1*$^{1\text{-}313}$ confers neuronal hyperexcitability

The loss of Ine function confers a number of phenotypes, including a neuronal excitability phenotype manifested at the neuromuscular junction (nmj) of wandering third instar larvae. Wild-type Drosophila larvae nmjs exhibit a phenomenon termed long term facilitation (LTF), also known as augmentation. Following repetitive stimulation at frequencies typically between 3 and 10 Hz, an excitation threshold is reached, and subsequent stimulations elicit a facilitated response of increased magnitude and duration (JAN and JAN 1978; WANG *et al.* 1994). Certain mutations that decrease neuronal excitability (such as *para* (MIKE STERN, UNPUBLISHED DATA) and *eag*^{84} (ROBERT

CARDNELL, UNPUBLISHED DATA)) result in delayed onset of LTF; those that increase excitability (such as *Dp para*$^{+}$, *Hk, frq* and *pumilio* (RIVOSECCHI *et al.* 1994; SCHWEERS *et al.* 2002; STERN *et al.* 1995; STERN and GANETZKY 1989)) result in faster onset of LTF. The *ine*^{1} mutation also confers an increased rate of onset of LTF that is rescued by the expression of a UAS-*ine-RA* transgene.

To determine if the overexpression of the N-terminal domain of Ine-P1 could increase neuronal excitability, we made measurements of the onset rate of LTF in the presence of 0.15 mM [$CaCl_2$] and 0.1 mM [quinidine]. Figure 5.1 shows that the rate of onset of LTF is dramatically increased when the truncated *ine* transgene is expressed in neurons. Unexpectedly, despite both being considered peripheral glia drivers, *gli*-GAL4 and MZ709 driven UAS-*ineP1*$^{1\text{-}313}$ gave different outcomes. MZ709 driven expression of the transgene gave a rate of onset of LTF similar to that of the neuronal driver suggesting that MZ709 expresses GAL4 in neurons in addition to the peripheral glia.

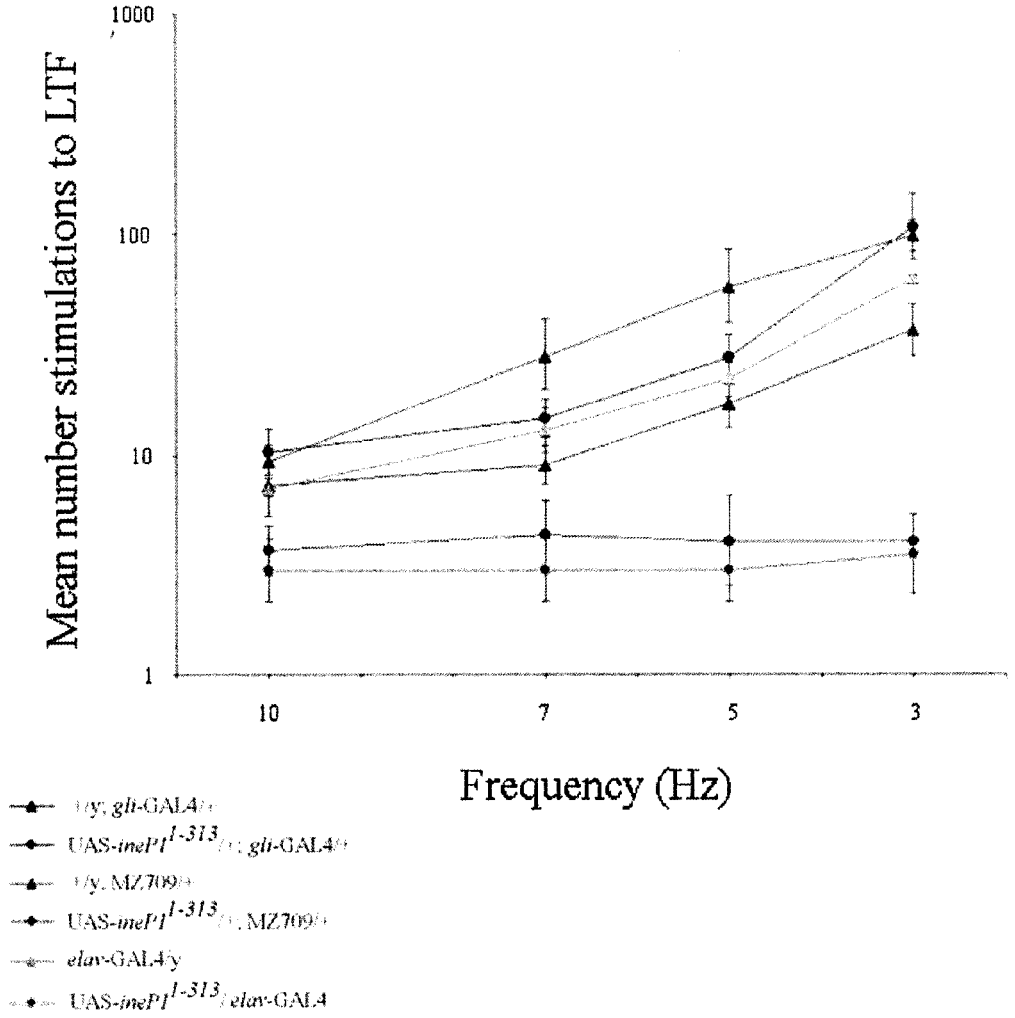

Figure 5.1 Neuronally driven UAS-*ineP1*$^{1-313}$ increases the rate of onset of LTF

Average number of stimulations required to elicit the facilitative response at the stimulation frequencies tested (10, 5, 7 and 3 Hz). An accelerated rate of onset of facilitation is observed in larvae when UAS-*ineP1*$^{1-313}$ is driven by *elav*-GAL4 or MZ709. Values presented as mean ± SEM, n ≥2.

5.4 Future work

5.4.1 Does neuronal expression of UAS-*ineP1*$^{1\text{-}313}$ truly confer neuronal hyperexcitability?

The n-values for the data presented in Figure 5.1 must be increased to confirm the phenotypes observed. Additionally, the rate of onset of LTF should be determined when the UAS-*ineP1*$^{1\text{-}313}$ construct is expressed in motor neurons (D42) and when constitutively expressed (*act5C*-GAL4).

5.4.2 Does neuronal expression of UAS-*ineP1*$^{1\text{-}313}$ enhance the *Sh* mutant behavioral phenotype?

The *ine*^{1} mutation was isolated in a mutant screen in which it enhanced the ether-induced leg shaking behavior of *Sh*^{133} adults to produce exaggerated leg shaking, down-turned wings and an indented thorax (STERN and GANETZKY 1992). Since many factors can increase the rate of LTF onset, to confirm that the increased neuronal excitability seen with neuronally expressed UAS-*ineP1*$^{1\text{-}313}$ is due to the loss of Ine function, I will express the UAS-*ineP1*$^{1\text{-}313}$ in the presence of the *Sh*^{133} mutation. The observation of exaggerated ether-induced leg shaking, down-turned wings and an indented thorax in the presence of the *Sh*^{133} mutation (i.e., a phenocopy of the *Sh*^{133}; *ine*^{1} double mutant) would indicate that the loss of Ine function is responsible for the observed neuronal hyperexcitability.

I predict that expression of UAS-*ineP1*$^{1\text{-}313}$ in the motor neurons will enhance *Sh*^{133} to produce down-turned wings, and an indented thorax, showing that the expression of the dominant negative transgene in motor neurons is sufficient to phenocopy the neuronal excitability phenotypes of the *ine*^{1} mutation.

5.4.3 Does the UAS-*ineP1*$^{1\text{-}313}$ transgene affect osmotic tolerance?

Both isoforms of Ine are expressed in the Drosophila kidney analogue (the Malpighian tubule and midgut) (SOEHNGE *et al.* 1996) and other members of the same transport family, such as BGT1, perform osmolyte transport in the mammalian renal medulla (BURG 1995). As would be expected of an osmolyte transporter, *ine* mutants display reduced tolerance of hypertonicity. The *ine*^{1} and *ine*^{3} null mutations that produce neither isoform of Ine confer significantly increased lethality when maintained on media with elevated [NaCl] (HUANG *et al.* 2002). The *ine*^{2} mutation, which is expected to eliminate only Ine-P1 and not Ine-P2, also confers an increased sensitivity to hypertonicity. All the *ine* mutations can be rescued by the overexpression of Ine-P2, raising the question as to whether or not the N-terminal domain of Ine-P1 is involved in osmoregulation. To test the possibility that the N-terminal domain of Ine-P1 is not important for the osmotic stress response, I propose to assess the viability of flies expressing the UAS-*ineP1*$^{1\text{-}313}$ transgene on hypertonic media. I predict that when driven by *elav*-GAL4 or *gli*-GAL4 the transgene will have no effect upon osmotolerance. When expressed ubiquitously with *act5C*-GAL4, if the N-terminal domain does play a role in

the osmotic stress response, then decreased viability in response to hypertonicity will be observed.

5.4.4 Does neuronal expression of the UAS-*ineP1*$^{1\text{-}313}$ transgene phenocopy the enhancement of perineural glial growth observed in *ine*^{1} mutants?

Whereas the *ine*^{1} mutation alone has no effect upon the thickness of the perineural glia in the third instar larval peripheral nervous system, it does confer a significant enhancement of the *push*^{1}-induced increase in perineural glial thickness (YAGER *et al.* 2001). Since this enhancement of the *push*^{1} thickened perineural glia is rescued by the overexpression of Ine-P1, and since a similar enhancement is produced by the *eag*^{1} mutation (YAGER *et al.* 2001), I propose to test the possibility that the overexpression of UAS-*ineP1*$^{1\text{-}313}$ might also affect perineural glial thickness. I predict that neuronal expression of the UAS-*ineP1*$^{1\text{-}313}$ transgene will produce an enhancement of the *push*^{1}-induced thickening of the perineural glial layer, mimicking that produced with *ine*^{1}.

Chapter 6: Literature Cited

ADAMS, C. M., M. G. ANDERSON, D. G. MOTTO, M. P. PRICE, W. A. JOHNSON *et al.*, 1998 Ripped pocket and pickpocket, novel Drosophila DEG/ENaC subunits expressed in early development and in mechanosensory neurons. J Cell Biol **140:** 143-152.

AULD, V. J., R. D. FETTER, K. BROADIE and C. S. GOODMAN, 1995 Gliotactin, a novel transmembrane protein on peripheral glia, is required to form the blood-nerve barrier in Drosophila. Cell **81:** 757-767.

AULD, V. J., A. L. GOLDIN, D. S. KRAFTE, J. MARSHALL, J. M. DUNN *et al.*, 1988 A rat brain Na+ channel alpha subunit with novel gating properties. Neuron **1:** 449-461.

BAINTON, R. J., L. T. TSAI, T. SCHWABE, M. DESALVO, U. GAUL *et al.*, 2005 moody encodes two GPCRs that regulate cocaine behaviors and blood-brain barrier permeability in Drosophila. Cell **123:** 145-156.

BAKER, O. S., H. P. LARSSON, L. M. MANNUZZU and E. Y. ISACOFF, 1998 Three transmembrane conformations and sequence-dependent displacement of the S4 domain in shaker K+ channel gating. Neuron **20:** 1283-1294.

BRAND, A. H., and N. PERRIMON, 1993 Targeted gene expression as a means of altering cell fates and generating dominant phenotypes. Development **118:** 401-415.

BROUGHTON, S. J., T. KITAMOTO and R. J. GREENSPAN, 2004 Excitatory and inhibitory switches for courtship in the brain of Drosophila melanogaster. Curr Biol **14:** 538-547.

BRUGGEMANN, A., L. A. PARDO, W. STUHMER and O. PONGS, 1993 Ether-a-go-go encodes a voltage-gated channel permeable to K+ and Ca2+ and modulated by cAMP. Nature **365:** 445-448.

BURG, M. B., 1995 Molecular basis of osmotic regulation. Am J Physiol **268:** F983-996.

BURG, M. G., C. GENG, Y. GUAN, G. KOLIANTZ and W. L. PAK, 1996 Drosophila rosA gene, which when mutant causes aberrant photoreceptor oscillation, encodes a novel neurotransmitter transporter homologue. J Neurogenet **11:** 59-79.

BUTLER, A., A. G. WEI, K. BAKER and L. SALKOFF, 1989 A family of putative potassium channel genes in Drosophila. Science **243:** 943-947.

CARDNELL, R. J. G., D. E. DALLE NOGARE, B. GANETZKY and M. STERN, 2006 *In vivo* analysis of a gain-of-function mutation in the Drosophila *eag*-encoded K^+ channel. Genetics **172:** 2351-2358.

CASTONGUAY, A., and R. ROBITAILLE, 2001 Differential regulation of transmitter release by presynaptic and glial Ca2+ internal stores at the neuromuscular synapse. J Neurosci **21:** 1911-1922.

CASTONGUAY, A., and R. ROBITAILLE, 2002 Xestospongin C is a potent inhibitor of SERCA at a vertebrate synapse. Cell Calcium **32:** 39-47.

CHEN, M. L., T. HOSHI and C. F. WU, 1996 Heteromultimeric interactions among K+ channel subunits from Shaker and eag families in Xenopus oocytes. Neuron **17:** 535-542.

CHEN, M. L., T. HOSHI and C. F. WU, 2000 Sh and eag K(+) channel subunit interaction in frog oocytes depends on level and time of expression. Biophys J **79:** 1358-1368.

CHEN, Y. H., S. J. XU, S. BENDAHHOU, X. L. WANG, Y. WANG *et al.*, 2003 KCNQ1 gain-of-function mutation in familial atrial fibrillation. Science **299:** 251-254.

CIRELLI, C., D. BUSHEY, S. HILL, R. HUBER, R. KREBER *et al.*, 2005 Reduced sleep in Drosophila Shaker mutants. Nature **434:** 1087-1092.

D'ADAMO, M. C., P. IMBRICI, F. SPONCICHETTI and M. PESSIA, 1999 Mutations in the KCNA1 gene associated with episodic ataxia type-1 syndrome impair heteromeric voltage-gated K(+) channel function. Faseb J **13:** 1335-1345.

DARBOUX, I., E. LINGUEGLIA, D. PAURON, P. BARBRY and M. LAZDUNSKI, 1998 A new member of the amiloride-sensitive sodium channel family in Drosophila

melanogaster peripheral nervous system. Biochem Biophys Res Commun **246:** 210-216.

DEDEK, K., B. KUNATH, C. KANANURA, U. REUNER, T. J. JENTSCH *et al.*, 2001 Myokymia and neonatal epilepsy caused by a mutation in the voltage sensor of the KCNQ2 K+ channel. Proc Natl Acad Sci U S A **98:** 12272-12277.

EDWARDS, J. S., L. S. SWALES and M. BATE, 1993 The Differentiation Between Neuroglia and Conective Tissue Sheath in Insect Ganglia Revisited: The Neural Lamella and Perineural Sheath Cells are Absent in a Mesodermless Mutant of *Drosophila*. J Comp Neurol **333:** 301-308.

ELKINS, T., B. GANETZKY and C. F. WU, 1986 A Drosophila mutation that eliminates a calcium-dependent potassium current. Proc Natl Acad Sci U S A **83:** 8415-8419.

EVANS, P. D., V. REALE, R. M. MERZON and J. VILLEGAS, 1992a The effect of a glutamate uptake inhibitor on axon-Schwann cell signalling in the squid giant nerve fibre. J Exp Biol **173:** 251-260.

EVANS, P. D., V. REALE, R. M. MERZON and J. VILLEGAS, 1992b N-methyl-D-aspartate (NMDA) and non-NMDA (metabotropic) type glutamate receptors modulate the membrane potential of the Schwann cell of the squid giant nerve fibre. J Exp Biol **173:** 229-249.

EVANS, P. D., V. REALE and J. VILLEGAS, 1985 The role of cyclic nucleotides in modulation of the membrane potential of the Schwann cell of squid giant nerve fibre. J Physiol **363:** 151-167.

EVANS, P. D., V. REALE and J. VILLEGAS, 1986 Peptidergic modulation of the membrane potential of the Schwann cell of the squid giant nerve fibre. J Physiol **379:** 61-82.

EVANS, P. D., and J. VILLEGAS, 1988 The action of vasoactive intestinal peptide antagonists on peptidergic modulation of the squid Schwann cell. J Exp Biol **138:** 259-269.

FERNANDEZ-FERNANDEZ, J. M., M. TOMAS, E. VAZQUEZ, P. ORIO, R. LATORRE *et al.*, 2004 Gain-of-function mutation in the KCNMB1 potassium channel subunit is associated with low prevalence of diastolic hypertension. J Clin Invest **113:** 1032-1039.

FRINGS, S., N. BRULL, C. DZEJA, A. ANGELE, V. HAGEN *et al.*, 1998 Characterization of ether-a-go-go channels present in photoreceptors reveals similarity to IKx, a K+ current in rod inner segments. J Gen Physiol **111:** 583-599.

GANETZKY, B., 1984 Genetic studies of membrane excitability in Drosophila: lethal interaction between two temperature-sensitive paralytic mutations. Genetics **108:** 897-911.

GANETZKY, B., 2000 Genetic analysis of ion channel dysfunction in Drosophila. Kidney Int **57:** 766-771.

GANETZKY, B., and C. F. WU, 1982 Drosophila mutants with opposing effects on nerve excitability: genetic and spatial interactions in repetitive firing. J Neurophysiol **47:** 501-514.

GANETZKY, B., and C. F. WU, 1983 Neurogenetic analysis of potassium currents in Drosophila: synergistic effects on neuromuscular transmission in double mutants. J Neurogenet **1:** 17-28.

GANETZKY, B., and C. F. WU, 1985 Genes and membrane excitability in *Drosophila.* TINS **8:** 322-326.

GESSNER, G., M. ZACHARIAS, S. BECHSTEDT, R. SCHONHERR and S. H. HEINEMANN, 2004 Molecular determinants for high-affinity block of human EAG potassium channels by antiarrhythmic agents. Mol Pharmacol **65:** 1120-1129.

GHO, M., and A. MALLART, 1986 Two distinct calcium-activated potassium currents in larval muscle fibres of Drosophila melanogaster. Pflugers Arch **407:** 526-533.

GIORDANO, E., R. RENDINA, I. PELUSO and M. FURIA, 2002 RNAi triggered by symmetrically transcribed transgenes in Drosophila melanogaster. Genetics **160:** 637-648.

GOLDSTEIN, S. A., L. A. PRICE, D. N. ROSENTHAL and M. H. PAUSCH, 1996 ORK1, a potassium-selective leak channel with two pore domains cloned from Drosophila melanogaster by expression in Saccharomyces cerevisiae. Proc Natl Acad Sci U S A **93:** 13256-13261.

GREENSPAN, R. J., 1997 *Fly Pushing: The Theory and Practice of Drosophila Genetics.* Cold Spring Harbor Laboratory Press.

GRIFFITH, L. C., J. WANG, Y. ZHONG, C. F. WU and R. J. GREENSPAN, 1994 Calcium/calmodulin-dependent protein kinase II and potassium channel subunit eag similarly affect plasticity in Drosophila. Proc Natl Acad Sci U S A **91:** 10044-10048.

GUY, H. R., S. R. DURELL, J. WARMKE, R. DRYSDALE and B. GANETZKY, 1991 Similarities in amino acid sequences of Drosophila eag and cyclic nucleotide-gated channels. Science **254:** 730.

HARIHARAN, I. K., R. W. CARTHEW and G. M. RUBIN, 1991 The Drosophila roughened mutation: activation of a rap homolog disrupts eye development and interferes with cell determination. Cell **67:** 717-722.

HUANG, X., Y. HUANG, R. CHINNAPPAN, C. BOCCHINI, M. C. GUSTIN *et al.*, 2002 The Drosophila inebriated-encoded neurotransmitter/osmolyte transporter: dual roles

in the control of neuronal excitability and the osmotic stress response. Genetics **160:** 561-569.

HUANG, Y., and M. STERN, 2002 In vivo properties of the Drosophila inebriated-encoded neurotransmitter transporter. J Neurosci **22:** 1698-1708.

ISHIHARA, K., T. MITSUIYE, A. NOMA and M. TAKANO, 1989 The Mg2+ block and intrinsic gating underlying inward rectification of the K+ current in guinea-pig cardiac myocytes. J Physiol **419:** 297-320.

ITO, K., J. URBAN and G. M. TECHNAU, 1995 Distribution, classification, and development of Drosophila glial cells in the late embryonic and early larval ventral nerve cord. Roux's Archives of Devleopmental Biology **204:** 284-307.

JACKSON, F. R., S. D. WILSON, G. R. STRICHARTZ and L. M. HALL, 1984 Two types of mutants affecting voltage-sensitive sodium channels in Drosophila melanogaster. Nature **308:** 189-191.

JAHROMI, B. S., R. ROBITAILLE and M. P. CHARLTON, 1992 Transmitter release increases intracellular calcium in perisynaptic Schwann cells in situ. Neuron **8:** 1069-1077.

JAN, L. Y., and Y. N. JAN, 1976 Properties of the larval neuromuscular junction in Drosophila melanogaster. J Physiol **262:** 189-214.

JAN, Y. N., and L. Y. JAN, 1978 Genetic dissection of short-term and long-term facilitation at the Drosophila neuromuscular junction. Proc Natl Acad Sci U S A **75:** 515-519.

JAN, Y. N., L. Y. JAN and M. J. DENNIS, 1977 Two mutations of synaptic transmission in Drosophila. Proc R Soc Lond B Biol Sci **198:** 87-108.

JIANG, Y., A. LEE, J. CHEN, V. RUTA, M. CADENE *et al.*, 2003a X-ray structure of a voltage-dependent K+ channel. Nature **423:** 33-41.

JIANG, Y., V. RUTA, J. CHEN, A. LEE and R. MACKINNON, 2003b The principle of gating charge movement in a voltage-dependent K+ channel. Nature **423:** 42-48.

KALIDAS, S., and D. P. SMITH, 2002 Novel genomic cDNA hybrids produce effective RNA interference in adult Drosophila. Neuron **33:** 177-184.

KAPLAN, W. D., and W. E. TROUT, 3RD, 1969 The behavior of four neurological mutants of Drosophila. Genetics **61:** 399-409.

KENNERDELL, J. R., and R. W. CARTHEW, 2000 Heritable gene silencing in Drosophila using double-stranded RNA. Nat Biotechnol **18:** 896-898.

KITAMOTO, T., X. XIE, C. F. WU and P. M. SALVATERRA, 2000 Isolation and characterization of mutants for the vesicular acetylcholine transporter gene in Drosophila melanogaster. J Neurobiol **42:** 161-171.

LANSMAN, J. B., P. HESS and R. W. TSIEN, 1986 Blockade of current through single calcium channels by Cd2+, Mg2+, and Ca2+. Voltage and concentration dependence of calcium entry into the pore. J Gen Physiol **88:** 321-347.

LEE, S. Y., A. LEE, J. CHEN and R. MACKINNON, 2005 Structure of the KvAP voltage-dependent K+ channel and its dependence on the lipid membrane. Proc Natl Acad Sci U S A **102:** 15441-15446.

LIEBERMAN, E. M., P. T. HARGITTAI and R. M. GROSSFELD, 1994 Electrophysiological and metabolic interactions between axons and glia in crayfish and squid. Prog Neurobiol **44:** 333-376.

LIEBERMAN, E. M., J. VILLEGAS and G. M. VILLEGAS, 1981 The nature of the membrane potential of glial cells associated with the medial giant axon of the crayfish. Neuroscience **6:** 261-271.

LONG, S. B., E. B. CAMPBELL and R. MACKINNON, 2005 Crystal structure of a mammalian voltage-dependent Shaker family K+ channel. Science **309:** 897-903.

LUDEWIG, U., C. LORRA, O. PONGS and S. H. HEINEMANN, 1993 A site accessible to extracellular TEA+ and K+ influences intracellular Mg2+ block of cloned potassium channels. Eur Biophys J **22:** 237-247.

LUDWIG, J., D. OWEN and O. PONGS, 1997 Carboxy-terminal domain mediates assembly of the voltage-gated rat ether-a-go-go potassium channel. Embo J **16:** 6337-6345.

LUDWIG, J., H. TERLAU, F. WUNDER, A. BRUGGEMANN, L. A. PARDO *et al.*, 1994 Functional expression of a rat homologue of the voltage gated either a go-go potassium channel reveals differences in selectivity and activation kinetics between the Drosophila channel and its mammalian counterpart. Embo J **13:** 4451-4458.

MACLEAN, S. J., B. C. ANDREWS and E. M. VERHEYEN, 2002 Characterization of Dir: a putative potassium inward rectifying channel in Drosophila. Mech Dev **116:** 193-197.

MARBLE, D. D., A. P. HEGLE, E. D. SNYDER, 2ND, S. DIMITRATOS, P. J. BRYANT *et al.*, 2005 Camguk/CASK enhances Ether-a-go-go potassium current by a phosphorylation-dependent mechanism. J Neurosci **25:** 4898-4907.

MATSUDA, H., A. SAIGUSA and H. IRISAWA, 1987 Ohmic conductance through the inwardly rectifying K channel and blocking by internal Mg2+. Nature **325:** 156-159.

MAYER, M. L., G. L. WESTBROOK and P. B. GUTHRIE, 1984 Voltage-dependent block by Mg2+ of NMDA responses in spinal cord neurones. Nature **309:** 261-263.

MEYER, R., and S. H. HEINEMANN, 1998 Characterization of an eag-like potassium channel in human neuroblastoma cells. J Physiol **508 (Pt 1):** 49-56.

MEYER, R., R. SCHONHERR, O. GAVRILOVA-RUCH, W. WOHLRAB and S. H. HEINEMANN, 1999 Identification of ether a go-go and calcium-activated potassium channels in human melanoma cells. J Membr Biol **171:** 107-115.

MONGIN, E., C. LOUIS, R. A. HOLT, E. BIRNEY and F. H. COLLINS, 2004 The Anopheles gambiae genome: an update. Trends Parasitol **20:** 49-52.

MORI, Y., T. FRIEDRICH, M. S. KIM, A. MIKAMI, J. NAKAI *et al.*, 1991 Primary structure and functional expression from complementary DNA of a brain calcium channel. Nature **350:** 398-402.

NOWAK, L., P. BREGESTOVSKI, P. ASCHER, A. HERBET and A. PROCHIANTZ, 1984 Magnesium gates glutamate-activated channels in mouse central neurones. Nature **307:** 462-465.

PARDO, L. A., D. DEL CAMINO, A. SANCHEZ, F. ALVES, A. BRUGGEMANN *et al.*, 1999 Oncogenic potential of EAG K(+) channels. Embo J **18:** 5540-5547.

PIGNONI, F., and S. L. ZIPURSKY, 1997 Induction of Drosophila eye development by decapentaplegic. Development **124:** 271-278.

PITTENDRIGH, B., R. REENAN, R. H. FFRENCH-CONSTANT and B. GANETZKY, 1997 Point mutations in the Drosophila sodium channel gene para associated with resistance to DDT and pyrethroid insecticides. Mol Gen Genet **256:** 602-610.

PUSCH, M., 1990 Open-channel block of Na+ channels by intracellular Mg2+. Eur Biophys J **18:** 317-326.

RICHARDS, S., T. HILLMAN and M. STERN, 1996 Mutations in the Drosophila pushover gene confer increased neuronal excitability and spontaneous synaptic vesicle fusion. Genetics **142:** 1215-1223.

RICHARDS, S., Y. LIU, B. R. BETTENCOURT, P. HRADECKY, S. LETOVSKY *et al.*, 2005 Comparative genome sequencing of Drosophila pseudoobscura: chromosomal, gene, and cis-element evolution. Genome Res **15:** 1-18.

RIVOSECCHI, R., O. PONGS, T. THEIL and A. MALLART, 1994 Implication of frequenin in the facilitation of transmitter release in Drosophila. J Physiol **474:** 223-232.

ROBERTSON, G. A., J. M. WARMKE and B. GANETZKY, 1996 Potassium currents expressed from Drosophila and mouse eag cDNAs in Xenopus oocytes. Neuropharmacology **35:** 841-850.

SALKOFF, L., A. BUTLER, N. SCAVARDA and A. WEI, 1987a Nucleotide sequence of the putative sodium channel gene from Drosophila: the four homologous domains. Nucleic Acids Res **15:** 8569-8572.

SALKOFF, L., A. BUTLER, A. WEI, N. SCAVARDA, K. GIFFEN *et al.*, 1987b Genomic organization and deduced amino acid sequence of a putative sodium channel gene in Drosophila. Science **237:** 744-749.

SANGUINETTI, M. C., 1999 Dysfunction of delayed rectifier potassium channels in an inherited cardiac arrhythmia. Ann N Y Acad Sci **868:** 406-413.

SCHONHERR, R., S. HEHL, H. TERLAU, A. BAUMANN and S. H. HEINEMANN, 1999 Individual subunits contribute independently to slow gating of bovine EAG potassium channels. J Biol Chem **274:** 5362-5369.

SCHONHERR, R., L. M. MANNUZZU, E. Y. ISACOFF and S. H. HEINEMANN, 2002 Conformational switch between slow and fast gating modes: allosteric regulation of voltage sensor mobility in the EAG K+ channel. Neuron **35:** 935-949.

SCHROEDER, B. C., C. KUBISCH, V. STEIN and T. J. JENTSCH, 1998 Moderate loss of function of cyclic-AMP-modulated KCNQ2/KCNQ3 K+ channels causes epilepsy. Nature **396:** 687-690.

SCHUSTER, C. M., G. W. DAVIS, R. D. FETTER and C. S. GOODMAN, 1996 Genetic dissection of structural and functional components of synaptic plasticity. II. Fasciclin II controls presynaptic structural plasticity. Neuron **17:** 655-667.

SCHWABE, T., R. J. BAINTON, R. D. FETTER, U. HEBERLEIN and U. GAUL, 2005 GPCR signaling is required for blood-brain barrier formation in drosophila. Cell **123:** 133-144.

SCHWEERS, B. A., K. J. WALTERS and M. STERN, 2002 The Drosophila melanogaster translational repressor pumilio regulates neuronal excitability. Genetics **161:** 1177-1185.

SEPP, K. J., and V. J. AULD, 1999 Conversion of lacZ enhancer trap lines to GAL4 lines using targeted transposition in Drosophila melanogaster. Genetics **151:** 1093-1101.

SEPP, K. J., J. SCHULTE and V. J. AULD, 2000 Developmental dynamics of peripheral glia in Drosophila melanogaster. Glia **30:** 122-133.

SILVERMAN, W. R., J. P. BANNISTER and D. M. PAPAZIAN, 2004 Binding site in eag voltage sensor accommodates a variety of ions and is accessible in closed channel. Biophys J **87:** 3110-3121.

SILVERMAN, W. R., C. Y. TANG, A. F. MOCK, K. B. HUH and D. M. PAPAZIAN, 2000 Mg(2+) modulates voltage-dependent activation in ether-a-go-go potassium channels by binding between transmembrane segments S2 and S3. J Gen Physiol **116:** 663-678.

SINGH, S., and C. F. WU, 1989 Complete separation of four potassium currents in Drosophila. Neuron **2:** 1325-1329.

SMITH, G. A., H. W. TSUI, E. W. NEWELL, X. JIANG, X. P. ZHU *et al.*, 2002 Functional up-regulation of HERG K+ channels in neoplastic hematopoietic cells. J Biol Chem **277:** 18528-18534.

SOEHNGE, H., X. HUANG, M. BECKER, P. WHITLEY, D. CONOVER *et al.*, 1996 A neurotransmitter transporter encoded by the *Drosophila* inebriated gene. Proc Natl Acad Sci U S A **93:** 13262-13267.

STERN, M., N. BLAKE, N. ZONDLO and K. WALTERS, 1995 Increased neuronal excitability conferred by a mutation in the Drosophila bemused gene. J Neurogenet **10:** 103-118.

STERN, M., and B. GANETZKY, 1989 Altered synaptic transmission in Drosophila hyperkinetic mutants. J Neurogenet **5:** 215-228.

STERN, M., and B. GANETZKY, 1992 Identification and characterization of inebriated, a gene affecting neuronal excitability in Drosophila. J Neurogenet **8:** 157-172.

STERN, M., R. KREBER and B. GANETZKY, 1990 Dosage effects of a Drosophila sodium channel gene on behavior and axonal excitability. Genetics **124:** 133-143.

STUHMER, W., M. STOCKER, B. SAKMANN, P. SEEBURG, A. BAUMANN *et al.*, 1988 Potassium channels expressed from rat brain cDNA have delayed rectifier properties. FEBS Lett **242:** 199-206.

SUN, X. X., J. J. HODGE, Y. ZHOU, M. NGUYEN and L. C. GRIFFITH, 2004 The eag potassium channel binds and locally activates calcium/calmodulin-dependent protein kinase II. J Biol Chem **279:** 10206-10214.

SUZUKI, D. T., T. GRIGLIATTI and R. WILLIAMSON, 1971 Temperature-sensitive mutations in Drosophila melanogaster. VII. A mutation (para-ts) causing reversible adult paralysis. Proc Natl Acad Sci U S A **68:** 890-893.

SUZUKI, T., and K. TAKIMOTO, 2004 Selective expression of HERG and Kv2 channels influences proliferation of uterine cancer cells. Int J Oncol **25:** 153-159.

TANG, C. Y., F. BEZANILLA and D. M. PAPAZIAN, 2000 Extracellular Mg(2+) modulates slow gating transitions and the opening of Drosophila ether-a-Go-Go potassium channels. J Gen Physiol **115:** 319-338.

TANG, C. Y., C. T. SCHULTEIS, R. M. JIMENEZ and D. M. PAPAZIAN, 1998 Shaker and ether-a-go-go K+ channel subunits fail to coassemble in Xenopus oocytes. Biophys J **75:** 1263-1270.

TERLAU, H., J. LUDWIG, R. STEFFAN, O. PONGS, W. STUHMER *et al.*, 1996 Extracellular Mg2+ regulates activation of rat eag potassium channel. Pflugers Arch **432:** 301-312.

TITUS, S. A., J. W. WARMKE and B. GANETZKY, 1997 The Drosophila erg K+ channel polypeptide is encoded by the seizure locus. J Neurosci **17:** 875-881.

VAN HAUWE, P., P. J. COUCKE, R. J. ENSINK, P. HUYGEN, C. W. CREMERS *et al.*, 2000 Mutations in the KCNQ4 K+ channel gene, responsible for autosomal dominant hearing loss, cluster in the channel pore region. Am J Med Genet **93:** 184-187.

VILLEGAS, J., 1974 Effects of acetylcholine and carbomylcholine on the axon and Schwann cell electrical potentials in the squid nerve fibre. J. Physiology **242:** 647-659.

WANG, J., J. J. RENGER, L. C. GRIFFITH, R. J. GREENSPAN and C. F. WU, 1994 Concomitant alterations of physiological and developmental plasticity in Drosophila CaM kinase II-inhibited synapses. Neuron **13:** 1373-1384.

WANG, M. H., S. P. YUSAF, D. J. ELLIOTT, D. WRAY and A. SIVAPRASADARAO, 1999 Effect of cysteine substitutions on the topology of the S4 segment of the Shaker potassium channel: implications for molecular models of gating. J Physiol **521 Pt 2:** 315-326.

WANG, X. J., E. R. REYNOLDS, P. DEAK and L. M. HALL, 1997 The seizure locus encodes the Drosophila homolog of the HERG potassium channel. J Neurosci **17:** 882-890.

WANG, Z., G. F. WILSON and L. C. GRIFFITH, 2002 Calcium/calmodulin-dependent protein kinase II phosphorylates and regulates the Drosophila eag potassium channel. J Biol Chem **277:** 24022-24029.

WARMKE, J., R. DRYSDALE and B. GANETZKY, 1991 A distinct potassium channel polypeptide encoded by the Drosophila eag locus. Science **252:** 1560-1562.

WARMKE, J. W., and B. GANETZKY, 1994 A family of potassium channel genes related to eag in Drosophila and mammals. Proc Natl Acad Sci U S A **91:** 3438-3442.

WU, C. F., and B. GANETZKY, 1986 Genes and Ionic Channels in *Drosophila*.

WU, C. F., B. GANETZKY, F. N. HAUGLAND and A. X. LIU, 1983 Potassium currents in Drosophila: different components affected by mutations of two genes. Science **220:** 1076-1078.

WU, C. F., and F. N. HAUGLAND, 1985 Voltage clamp analysis of membrane currents in larval muscle fibers of Drosophila: alteration of potassium currents in Shaker mutants. J Neurosci **5:** 2626-2640.

WU, C. F., M. C. TSAI, M. L. CHEN, Y. ZHONG, S. SINGH *et al.*, 1989 Actions of dendrotoxin on K+ channels and neuromuscular transmission in Drosophila melanogaster, and its effects in synergy with K+ channel-specific drugs and mutations. J Exp Biol **147:** 21-41.

YAGER, J., S. RICHARDS, D. S. HEKMAT-SCAFE, D. D. HURD, V. SUNDARESAN *et al.*, 2001 Control of Drosophila perineurial glial growth by interacting neurotransmitter-mediated signaling pathways. Proc Natl Acad Sci U S A **98:** 10445-10450.

YAMAMOTO, D., and N. SUZUKI, 1989 Two distinct mechanisms are responsible for single K channel block by internal tetraethylammonium ions. Am J Physiol **256:** C683-687.

YANG, N., A. L. GEORGE, JR. and R. HORN, 1996 Molecular basis of charge movement in voltage-gated sodium channels. Neuron **16:** 113-122.

YEH, E., K. GUSTAFSON and G. L. BOULIANNE, 1995 Green fluorescent protein as a vital marker and reporter of gene expression in Drosophila. Proc Natl Acad Sci U S A **92:** 7036-7040.

ZHONG, Y., and C. F. WU, 1991 Alteration of four identified K+ currents in Drosophila muscle by mutations in eag. Science **252:** 1562-1564.

ZHONG, Y., and C. F. WU, 1993 Modulation of different K+ currents in Drosophila: a hypothetical role for the Eag subunit in multimeric K+ channels. J Neurosci **13:** 4669-4679.

Chapter 7: Appendices

7.1 FlyBase Report: Alleles of Gene *eag*

Alleles

Symbol	Allele class	Phenotype includes	Mutagen	Stocks	Molec. info.
1	hypomorph	chemical sensitive	ethyl methanesulfonate	2	yes
24	--	behavioral	--	--	--
101	--	behavioral | conditional ts	ethyl methanesulfonate	--	--
102	--	hyperactive	ethyl methanesulfonate	--	--
4PM	--	neurophysiology defective	ethyl methanesulfonate	--	--
EY00714	--	--	P-element activity	1	--
f06369	--	--	piggyBac transposase	--	--
hd14	--	chemical sensitive | recessive	PM hybrid dysgenesis	--	yes
hd15	--	olfaction defective | recessive	PM hybrid dysgenesis	--	yes
hd15r1	--	--	PM hybrid dysgenesis	--	yes
hd15r2	--	--	PM hybrid dysgenesis	--	yes
hd15r3	--	--	PM hybrid dysgenesis	--	yes
sc29	amorph	olfaction defective | recessive	--	1	--
unspecified	--	--	--	--	--
X6	amorph	olfaction defective | recessive	γ ray	--	--
Δ932.Scer\UAS	--	neurophysiology defective | conditional ts with Scer\GAL4$^{hs.PB}$	in vitro construct | deletion	--	yes

Sixteen mutant alleles in a addition to the wild-type allele of *eag* are recorded in the FlyBase database. All of the mutant alleles confer a decrease in Eag function. The mutant phenotypes are summarized below. Stocks refer to the number of stocks of that allele held in publicly available stock centers such as Bloomington.

Summary of Allele Phenotypes

Phenotype manifest in	Allele
leg	eag^1
neuromuscular junction, synapse	eag^1
synapse	eag^1

http://flybase.bio.indiana.edu/.bin/fbidq.html?content=allele-table&FBgn0000535

7.2 Amino acid translation sequence from *Sup*^{39}, *Sup*^{146}, *Sup*^{84}, *para*^{141} and *para*^{63}

Translation of sequence derived from genomic sequencing. Also shown is a consensus sequence for wild-type Eag (WARMKE and GANETZKY 1994).

```
                    10         20         30         40
                ....|....| ....|....| ....|....| ....|....|
consensus       MPGGRRGLVA PQNTFLENII RRSNSQPDSS FLLANAQIVD
para141f        MPGGRRGLVA PQNTFLENII RRSNSQPDSS FLLANAQIVD
Sup39 Sh133     MPGGRRGLVA PQNTFLENII RRSNSQPDSS FLLANAQIVD
Sup146 Sh133    MPGGRRGLVA PQNTFLENII RRSNSQPDSS FLLANAQIVD
Sup84           MPGGRRGLVA PQNTFLENII RRSNSQPDSS FLLANAQIVD
para63          ~~~~~~~~~~ ~~~~~~~~~~ ~~~~~~~~~~ ~~~~~~~~~~

                    50         60         70         80
                ....|....| ....|....| ....|....| ....|....|
consensus       FPIVYCNESF CKISGYNRAE VMQKSCRYVC GFMYGELTDK
para141f        FPIVYCNESF CKISGYNRAE VMQKSCRYVC GFMYGELTNK
Sup39 Sh133     FPIVYCNESF CKISGYNRAE VMQKSCRYVC GFMYGELTDK
Sup146 Sh133    FPIVYCNESF CKISGYNRAE VMQKSCRYVC GFMYGELTDK
Sup84           FPIVYCNESF CKISGYNRAE VMQKSCRYVC GFMYGELTNK
para63          ~~~~~~~~~~ ~~~~~~~~~~ ~~~~~~~~~~ ~~~~~~~~~~

                    90        100        110        120
                ....|....| ....|....| ....|....| ....|....|
consensus       ETVGRLEYTL ENQQQDQFEI LLYKKNNLQC GCALSQFGKA
para141f        ETVGRLEYTL ENQQQDQFKI LLYKKNNLQC GCALSQFGKA
Sup39 Sh133     ETVGRLEYTL ENQQQDQFEI LLYKKNNLQC GCALSQFGKA
Sup146 Sh133    ETVGRLEYTL ENQQQDQFEI LLYKKNNLQC GCALSQFGKA
Sup84           ETVGRLEYTL ENQQQDQFKI LLYKKNNLQC GCALSQFGKA
para63          ~~~~~~~~~~ ~~~~~~~~~~ ~~~~~~~~~~ ~~~~~~~~~~

                   130        140        150        160
                ....|....| ....|....| ....|....| ....|....|
consensus       QTQETPLWLL LQVAPIRNER DLVVLFLLTF RDITALKQPI
para141f        QTQETPLWLL LQVAPIRNER DLVVLFLLTF RDITALKQPI
Sup39 Sh133     QTQETPLWLL LQVAPIRNER DLVVLFLLTF RDITALKQPI
Sup146 Sh133    QTQETPLWLL LQVAPIRNER DLVVLFLLTF RDITALKQPI
Sup84           QTQETPLWLL LQVAPIRNER DLVVLFLLTF RDITALKQPI
para63          ~~~~~~~~~~ ~~~~~~~~~~ ~~~~~~~~~~ ~~~~~~~~~~


                   170        180        190        200
                ....|....| ....|....| ....|....| ....|....|
consensus       DSEDTKGVLG LSKFAKLARS VTRSRQFSAH LPTLKDPTKQ
para141f        DSEDTKGVLG LSKFAKLARS VTRSRQFSAH LPTLKDPTKQ
Sup39 Sh133     DSEDTKGVLG LSKFAKLARS VTRSRQFSAH LPTLKDPTKQ
Sup146 Sh133    DSEDTKGVLG LSKFAKLARS VTRSRQFSAH LPTLKDPTKQ
Sup84           DSEDTKGVLG LSKFAKLARS VTRSRQFSAH LPTLKDPTKQ
para63          ~~~~~~~~~~ ~~~~~~~~~~ ~~~~~~~~~~ ~~~~~~~~~~
```

```
                    210         220         230         240
                .....|....| ....|....| ....|....| ....|....|
consensus       SNLAHMMSLS ADIMPQYRQE APKTPPHILL HYCAFKAIWD
para141f        SNLAHVMSLS ADIMPQYRQE APKTPPHILL HYCAFKAIWD
Sup39 Sh133     SNLAHVMSLS ADIMPQYRQE APKTPPHILL HYCAFKAIWD
Sup146 Sh133    SNLAHVMSLS ADIMPQYRQE APKTPPHILL HYCAFKAIWD
Sup84           SNLAHVMSLS ADIMPQYRQE APKTPPHILL HYCAFKAIWD
para63          ~~~~~~~~~~ ~~~~~~~~~~ ~~~~~~~~~~ ~~~~~~~~~~

                    250         260         270         280
                .....|....| ....|....| ....|....| ....|....|
consensus       WVILCLTFYT AIMVPYNVAF KNKTSEDVSL LVVDSIVDVI
para141f        WVILCLTFYT AIMVPYNVAF KNKTSEDVSL LVVDSIVDVI
Sup39 Sh133     WVILCLTFYT AIMVPYNVAF KNKTSEDVSL LVVDSIVDVI
Sup146 Sh133    WVILCLTFYT AIMVPYNVAF KNKTSEDVSL LVVDSIVDVI
Sup84           WVILCLTFYT AIMVPYNVVF KNKTSEDVSL LVVDSIVDVI
para63          ~~~~~~~~~~ ~~~VPYNVAF KNKTSEDVSL LVVDSIVDVI

                    290         300         310         320
                .....|....| ....|....| ....|....| ....|....|
consensus       FFIDIVLNFH TTFVGPGGEV VSDPKVIRMN YLKSWFIIDL
para141f        FFIDIVLNFH TTFVGPGGEV VSDPKVIRMN YLKSWFIIDL
Sup39 Sh133     FFIDIVLNFH TTFVGPEGEV VSDPKVIRMN YLKSWFIIDL
Sup146 Sh133    FFIDIVLNFH TTFVGPEGEV VSDPKVIRMN YLKSWFIIDL
Sup84           FFIDIVLNFH TTFVGPGGEV VSDPKVIRMN YLKSWFIIDL
para63          FFIDIVLNFH TTFVGPGGEV VSDPKVIRMN YLKSWFIIDL

                    330         340         350         360
                .....|....| ....|....| ....|....| ....|....|
consensus       LSCLPYDVFN AFDRDEDGIG SLFSALKVVR LLRLGRVVRK
para141f        LSCLPYDVFN AFDRDEDGIG SLFSALKVVR LLRLGRVVRK
Sup39 Sh133     LSCLPYDVFN AFDRDEDGIG SLFSALKVVR LLRLGRVVRK
Sup146 Sh133    LSCLPYDVFN AFDRDEDGIG SLFSALKVVR LLRLGRVVRK
Sup84           LSCLPYDVFN AFDRDEDGIG SLFSALKVVR LLRLGRVVRK
para63          LSCLPYDVFN AFDRDEDGIG SLFSALKVVR LLRLGRVVRK

                    370         380         390         400
                .....|....| ....|....| ....|....| ....|....|
consensus       LDRYLEYGAA MLILLLCFYM LVAHWLACIW YSIGRSDADN
para141f        LDRYLEYGAA MLILLLCFYM LVAHWLACIW YSIGRSDADN
Sup39 Sh133     LDRYLEYGAA MLILLLCFYM LVAHWLACIW YSIGRSDADN
Sup146 Sh133    LDRYLEYGAA MLILLLCFYM LVAHWLACIW YSIGRSDADN
Sup84           LDRYLEYGAA MLILLLCFYM LVAHWLACIW YSIGRSDADN
para63          LDRYLEYGAA MLILLLCFYM LVAHWLACIW YSIGRSDADN

                    410         420         430         440
                .....|....| ....|....| ....|....| ....|....|
consensus       GIQYSWLWKL ANVTQSPYSY IWSNDTGPEL VNGPSRKSMY
para141f        GIQYSWLWKL ANVTQSPYSY IWSNDTGPEL VNGPSRKSMY
Sup39 Sh133     GIQYSWLWKL ANVTQSPYSY IWSNDTGPEL VNGPSRKSMY
Sup146 Sh133    GIQYSWLWKL ANVTQSPYSY IWSNDTGPEL VNGPSRKSMY
Sup84           GIQYSWLWKL ANVTQSPYSY IWSNDTGPEL VNGPSRKSMY
para63          G~~~~~~~~~ ~~~~~~~~~~ ~~~~~~~~~~ ~~~~~~~~~~
```

```
                    450         460         470         480
                    ....|....| ....|....| ....|....| ....|....|
consensus           VTALYFTMTC MTSVGFGNVA AETDNEKVFT ICMMIIAALL
para141f            VTALYFTMTC MTSVGFGNVA AETDNEKVFT ICMMIIAALL
Sup39 Sh133         VTALYFTMTC MTSVGFGNVA AETDNEKVFT ICMMIIAALL
Sup146 Sh133        VTALYFTMTC MTSVGFGNVA AETDNEKVFT ICMMIIAALL
Sup84               VTALYFTMTC MTSVGFGNVA AETDNEKVFT ICMMIIAALL
para63              ~~~~~~~~~~ ~~~~~~~~~~ ~~~~~~~~~~ ~~~~~~~~~~

                    490         500         510         520
                    ....|....| ....|....| ....|....| ....|....|
consensus           YATIFGHVTT IIQQMTSATA KYHDMLNNVR EFMKLHEVPK
para141f            YATIFGHVTT IIQQMTSATA KYHDMLNNVR EFMKLHEVPK
Sup39 Sh133         YATIFGHVTT IIQQMTSATA KYHDMLNNVR EFMKLHEVPK
Sup146 Sh133        YATIFGHVTT IIQQMTSATA KYHDMLNNVR EFMKLHEVPK
Sup84               YATIFGHVTT IIQQMTSATA KYHDMLNNVR EFMKLHEVPK
para63              ~~~~~~~~~~ ~~~~~~~~~~ ~~~~~~~~~~ ~~~~~~~~~~

                    530         540         550         560
                    ....|....| ....|....| ....|....| ....|....|
consensus           ALSERVMDYV VSTWAMTKGL DTEKVLNYCP KDMKADICVH
para141f            ALSERVMDYV VSTWAMTKGL DTEKVLNYCP KDMKADICVH
Sup39 Sh133         ALSERVMDYV VSTWAMTKGL DTEKVLNYCP KDMKADICVH
Sup146 Sh133        ALSERVMDYV VSTWAMTKGL DTEKVLNYCP KDMKADICVH
Sup84               ALSERVMDYV VSTWAMTKGL DTEKVLNYCP KDMKADICVH
para63              ~~~~~~~~~~ ~~~~~~~~~~ ~~~~~~~~~~ ~~~~ADICVH

                    570         580         590         600
                    ....|....| ....|....| ....|....| ....|....|
consensus           LNRKVFNEHP AFRLASDGCL RALAMHFMMS HSAPGDLLYH
para141f            LNRKVFNEHP AFRLASDGCL RALAMHFMMS HSAPGDLLYH
Sup39 Sh133         LNRKVFNEHP AFRLASDGCL RALAMHFMMS HSAPGDLLYH
Sup146 Sh133        LNRKVFNEHP AFRLASDGCL RALAMHFMMS HSAPGDLLYH
Sup84               LNRKVFNEHP AFRLASDGCL RALAMHFMMS HSAPGDLLYH
para63              LNRKVFNEHP AFRLASDGCL RALAMHFMMS HSAPGDLLYH

                    610         620         630         640
                    ....|....| ....|....| ....|....| ....|....|
consensus           TGESIDSLCF IVTGSLEVIQ DDEVVAILGK GDVFGDQFWK
para141f            TGESIDSLCF IVTGSLEVIQ DDEVVAILGK GDVFGDQFWK
Sup39 Sh133         TGESIDSLCF IVTGSLEVIQ DDEVVAILGK GDVFGDQFWK
Sup146 Sh133        TGESIDSLCF IVTGSLEVIQ DDEVVAILGK GDVFGDQFWK
Sup84               TGESIDSLCF IVTGSLEVIQ DDEVVAILGK GDVFGDQFWK
para63              TGESIDSLCF IVTGSLEVIQ DDEVVAIL~~ ~~~~~~~~~~

                    650         660         670         680
                    ....|....| ....|....| ....|....| ....|....|
consensus           DSAVGQSAAN VRALTYCDLH AIKRDKLLEV LDFYSAFANS
para141f            DSAVGQSAAN VRALTYCDLH AIKRDKLLEV LDFYSAFANS
Sup39 Sh133         DSAVGQSAAN VRALTYCDLH AIKRDKLLEV LDFYSAFANS
Sup146 Sh133        DSAVGQSAAN VRALTYCDLH AIKRDKLLEV LDFYSAFANS
Sup84               DSAVGQSAAN VRALTYCDLH AIKRDKLLEV LDFYSAFANS
para63              DSAVGQSAXN VRALTYCDLH AIKRDKLLEV LDFYSAFANS
```

```
                    690         700         710         720
                   ....|....| ....|....| ....|....| ....|....|
consensus          FARNLVLTYN LRHRLIFRKV ADVKREKELA ERRKNEPQLP
para141f           FARNLVLTYN LRHRLIFRKV ADVKREKELA ERRKNEPQLP
Sup39 Sh133        FARNLVLTYN LRHRLIFRKV ADVKREKELA ERRKNEPQLP
Sup146 Sh133       FARNLVLTYN LRHRLIFRKV ADVKREKELA ERRKNEPQLP
Sup84              FARNLVLTYN LRHRLIFRKV ADVKREKELA ERRKNEPQLP
para63             FARNLVLTYN LRHRLIFRKV ADVKREKELA ERRKNEPQLP

                    730         740         750         760
                   ....|....| ....|....| ....|....| ....|....|
consensus          QNQDHLVRKI FSKFRRTPQV QAGSKELVGG SGQSDVEKGD
para141f           QNQDHLVRKI FSKFRRTPQV QAGSKELVGG SGQSDVEKGD
Sup39 Sh133        QNQDHLVRKI FSKFRRTPQV QAGSKELVGG SGQSDVEKGD
Sup146 Sh133       QNQDHLVRKI FSKFRRTPQV QAGSKELVGG SGQSDVEKGD
Sup84              QNQDHLVRKI FSKFRRTPQV QAGSKELVGG SGQSDVEKGD
para63             QNQDHLVRKI FSKFRRTPQV QAGSKELVGG SGQSDVEKGD

                    770         780         790         800
                   ....|....| ....|....| ....|....| ....|....|
consensus          GEVERTKVFP KAPKLQASQA TLARQDTIDE GGEVDSSPPS
para141f           GEVERTKVFP KAPKLQASQA TLARQDTIDE GGEVDSSPPS
Sup39 Sh133        GEVERTKVFP KAPKLQASQA TLARQDTIDE GGEVDSSPPS
Sup146 Sh133       GEVERTKVFP KAPKLQASQA TLARQDTIDE GGEVDSSPPS
Sup84              GEVERTKVFP KAPKLQASQA TLARQDTIDE GGEVDSSPPS
para63             GEVERTK~~P KAPKLQASQA TLARQDTIDE GGEVDSSPPS

                    810         820         830         840
                   ....|....| ....|....| ....|....| ....|....|
consensus          RDSRVVIEGA AVSSATVGPS PPVATTSSAA AGAGVSGGPG
para141f           RDSRVVIEGA AVSSATVGPS PPVATTSSAA AGAGVSGGPG
Sup39 Sh133        RDSRVVIEGA AVSSATVGPS PPVATTSSAA AGAGVSGGPG
Sup146 Sh133       RDSRVVIEGA AVSSATVGPS PPVATTSSAA AGAGVSGGPG
Sup84              RDSRVVIEGA AVSSATVGPS PPVATTSSAA AGAGVSGGPG
para63             RDSRVVIEGA AVSSATVGPS PPVATTSSAA AGAGVSGGPG

                    850         860         870         880
                   ....|....| ....|....| ....|....| ....|....|
consensus          SGGTVVAIVT KADRNLALER ERQIEMASSR ATTSDTYDTG
para141f           SGGTVVAIVT KADRNLALER ERQIEMASSR ATTSDTYDTG
Sup39 Sh133        SGGTVVAIVT KADRNLALER ERQIEMASSR ATTSDTYDTG
Sup146 Sh133       SGGTVVAIVT KADRNLALER ERQIEMASSR ATTSDTYDTG
Sup84              SGGTVVAIVT KADRNLALER ERQIEMASSR ATTSDTYDTG
para63             SGGTVVAIVT KADRNLALER ERQIEMASSR ATTSDTYDTG

                    890         900         910         920
                   ....|....| ....|....| ....|....| ....|....|
consensus          LRETPPTLAQ RDLIATVLDM KVDVRLELQR MQQRIGRIED
para141f           LRETPPTLAQ RDLIATVLDM KVDVRLELQR MQQRIGRIED
Sup39 Sh133        LRETPPTLAQ RDLIATVLDM KVDVRLELQR MQQRIGRIED
Sup146 Sh133       LRETPPTLAQ RDLIATVLDM KVDVRLELQR MQQRIGRIED
Sup84              LRETPPTLAQ RDLIATVLDM KVDVRLELQR MQQRIGRIED
para63             LRETPPTLAQ RDLIATVLDM KVDVRLELQR MQQRIGRIED
```

```
                    930         940         950         960
                ....|....| ....|....| ....|....| ....|....|
consensus       LLGELVKRLA PGAGSGGNAP DNSSGQTTPG DEICAGCGAG
para141f        LLGELVKRLA PGAGSGGNAP DNSSGQTTPG DEICAGCGAG
Sup39 Sh133     LLGELVKRLA PGAGSGGNAP DNSSGQTTPG DEICAGCGAG
Sup146 Sh133    LLGELVKRLA PGAGSGGNAP DNSSGQTTPG DEICAGCGAG
Sup84           LLGELVKRLA PGAGSGGNAP DNSSGQTTPG DEICAGCGAG
para63          LLGELVKRLA PGAGSGGNAP DNSSGXTXPG DXICAGCGAG

                    970         980         990         1000
                ....|....| ....|....| ....|....| ....|....|
consensus       GGGTPTTQAP PTSAVTSPVD TVITISSPGA SGSGSGTGAG
para141f        GGGTPTTQAP PTSAVTSPVD TVITISSQGT SGSGSGTGAG
Sup39 Sh133     GGGTPTTQAP PTSAVTSPVD TVITISSPGA SGSGSGTGAG
Sup146 Sh133    GGGTPTTQAP PTSAVTSPVD TVITISSPGA SGSGSGTGAG
Sup84           GGGTPTTQAP PTSAVTSPVD TVITISSPGA SGSGSGTGAG
para63          GGGTPTTXAP PTSAVTSPVD TVITISSPGA SGSGSGTGAG

                    1010        1020        1030        1040
                ....|....| ....|....| ....|....| ....|....|
consensus       AGSAVAGAGG AGLLNPGATV VSSAGGNGLG PLMLKKRRSK
para141f        AGSAVAGAGG AGLLNPGATV VSSAGGNGLG PLMLKKRRSK
Sup39 Sh133     AGSAVAGAGG AGLLNPGATV VSSAGGNGLG PLMLKKRRSK
Sup146 Sh133    AGSAVAGAGG AGLLNPGATV VSSAGGNGLG PLMLKKRRSK
Sup84           AGSAVAGAGG AGLLNPGATV VSSAGGNGLG PLMLKKRRSK
para63          AGSAVAGAGG AGLLNPGATV VSSAGGNGLG PLMLKKRRSK

                    1050        1060        1070        1080
                ....|....| ....|....| ....|....| ....|....|
consensus       SRKAPAPPKQ TLASTAGTAT AAPAGVAGSG MTSSAPASAD
para141f        SRKAPAPPKQ TLASTAGTAT AAPAGVAGSG MTSSAPASAD
Sup39 Sh133     SRKAPAPPKQ TLASTAGTAT AAPAGVAGSG MTSSAPASAD
Sup146 Sh133    SRKAPAPPKQ TLASTAGTAT AAPAGVAGSG MTSSAPASAD
Sup84           SRKAPAPPKQ TLASTAGTAT AAPAGVAGSG MTSSAPASAD
para63          SRKAPAPPKQ TLASTAGTAT AAPAGVAGSG MTSSAPASAD

                    1090        1100        1110        1120
                ....|....| ....|....| ....|....| ....|....|
consensus       QQQQHQSTAD QSPTTPGAEL LHLRLLEEDF TAAQLPSTSS
para141f        QQQQHQSAAD QSPTTPGAEL LHLRLLEEDF TAAQLPSTSS
Sup39 Sh133     QQQQHQSAAD QSPTTPGAEL LHLRLLEEDF TAAQLPSTSS
Sup146 Sh133    QQQQHQSTAD QSPTTPGAEL LHLRLLEEDF TAAQLPSTSS
Sup84           QQQQHQSAAD QSPTTPGAEL LHLRLLEEDF TAAQLPSTSS
para63          QQQQHQSAAD QSPTTPGAEL LHLRLLEEDF TAAQLPSTSS

                    1130        1140        1150        1160
                ....|....| ....|....| ....|....| ....|....|
consensus       GGAGGGGGSG SGATPTTPPP TTAGGSGSGT PTSTTATTTP
para141f        GGAGGGGGSG SGATPTTPPP TIAGGSGSGT PTSTTATTTP
Sup39 Sh133     GGAGGGGGSG SGATPTTPPP TIAGGSGSGT PTSTTATTTP
Sup146 Sh133    GGAGGGGGSG SGATPTTPPP TTAGGSGSGT PTSTTATTTP
Sup84           GGAGGGGGSG SGATPTTPPP TIAGGSGSGT PTSTTATTTP
para63          GGAGGGGGSG SGATPTTPPP TIAGGSGSGT PTTPQPXHPT
```

```
                    1170        1180        1190        1200
                ....|....| ....|....| ....|....| ....|....|
consensus       TGSGTATRGK LDFL
para141f        TGSGTATRGK LDFL*PTTIG KERRGEGDTS SQEQ*YKNWG
Sup39 Sh133     TGSGTATRGK LDFL*PTTIG KERRGEGDTS SQEQ*YKNWG
Sup146 Sh133    TGSGTATRGK LDFL*PTTIG KERRGEGDTS SQEQ*YKNWG
Sup84           TGSGTATRGK LDFL*PTTIG KERRGEGDTS SQEQ*YKNWG
para63          GSG

                    1210        1220        1230        1240
                ....|....| ....|....| ....|....| ....|....|
consensus
para141f        K*GPSHAHSQ AYAYA*LVYI LKIQL*PQLD TETRSSISNT
Sup39 Sh133     K*GPSHAHSQ AYXYA*LVYI LKIQL*PQLD TETRSSISNT
Sup146 Sh133    K*GPXHAHSQ AYAYA*LVYI LKIQL*PQLD TETXSSISNT
Sup84           K*GPSHAHSQ AYAYA*LVYI LKIQL*PQLD TETRSSISNT
para63

                    1250        1260        1270        1280
                ....|....| ....|....| ....|....| ....|....|
consensus
para141f        LKVHCNVFIR R*RKAFRKKI V*KRF*KSDF *KFKSRVQRE
Sup39 Sh133     LKVHCNVFIR R*RKAFRKKI V*KRF*KSDF *KFKSRVQRE
Sup146 Sh133    LKVHCNVFIR R*RKAFRKKI V*KRF*KXDF *KFISRVQRE
Sup84           LKVHCNVFIR R*RKAFRKKI V*KRF*KSDF *KFKSRVQRE
para63

                    1290        1300        1310        1320
                ....|....| ....|....| ....|....| ....|....|
consensus
para141f        TFKYS*YGTQ SI*DCN*LKI MN*YLI*RLE NMNIIYLHLS
Sup39 Sh133     TFKYS*YGTQ SI*DCN*LKI MN*YLI*RLE NMNIIYLHLS
Sup146 Sh133    TFKYS*YGTQ SI*DCN*LKI MN*YLI*RLE NMNIIYLHLS
Sup84           TFKYS*YGTQ SI*DCN*LKI MN*YLI*RLE NMNIIYLHLS
para63

                    1330        1340        1350        1360
                ....|....| ....|....| ....|....| ....|....|
consensus
para141f        SIQILFS*YL *ALW*YS*YL YITNN*FMIF FKGKRLLLSF
Sup39 Sh133     SIQILFS*YL *ALW*YS*YL YITNN*FMIF FKGKRLLLSF
Sup146 Sh133    SIQILFS*YL *ALW*YS*YL YITNN*FMIF FKGKRLLLSF
Sup84           SIQILFS*YL *ALW*YS*YL YITNN*FMIF FKGKRLLLSF
para63

                    1370
                ....|....|
consensus
para141f        VSLNH
Sup39 Sh133     VSLNH
Sup146 Sh133    VSLNH
Sup84           VSLNH
para63
```

7.3 Amino acid alignment of Dm-Eag, Dp-Eag, M-Eag, R-EAG1, B-EAG, Ag-Eag, H-Erg and Elk

Amino acid sequence alignment Dm-Eag, *Drosophila melanogaster* (WARMKE *et al.* 1991); Dp-Eag, *Drosophila pseudobscura* (RICHARDS *et al.* 2005); M-Eag, Mouse (WARMKE and GANETZKY 1994); R-EAG1 (LUDWIG *et al.* 1994), Rat; B-EAG, *Bos Taurus* (Bovine) (FRINGS *et al.* 1998); Ag-Eag, *Anopheles gambiae* (mosquito) (MONGIN *et al.* 2004), H-Erg, Human Eag related gene (WARMKE and GANETZKY 1994); Elk, Human Eag like K^+ channel (WARMKE and GANETZKY 1994).

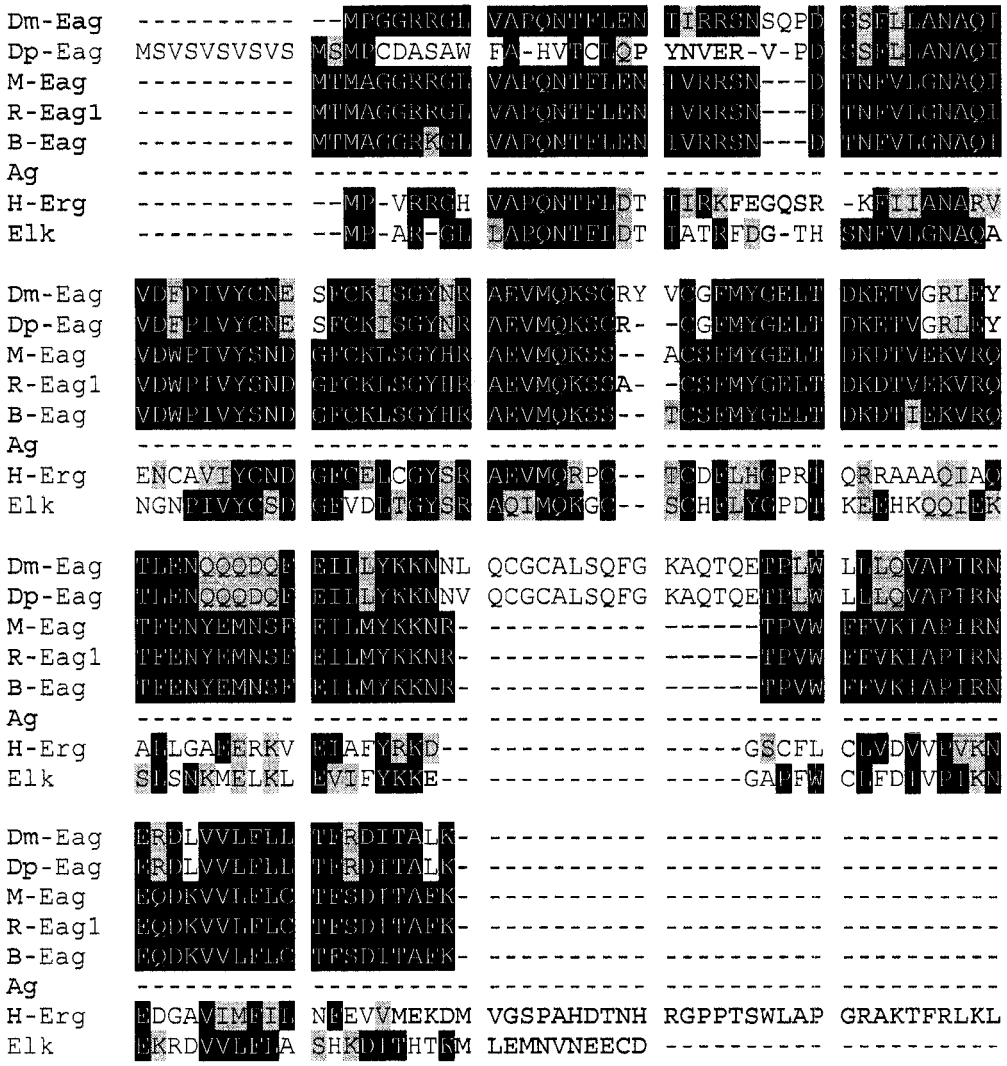

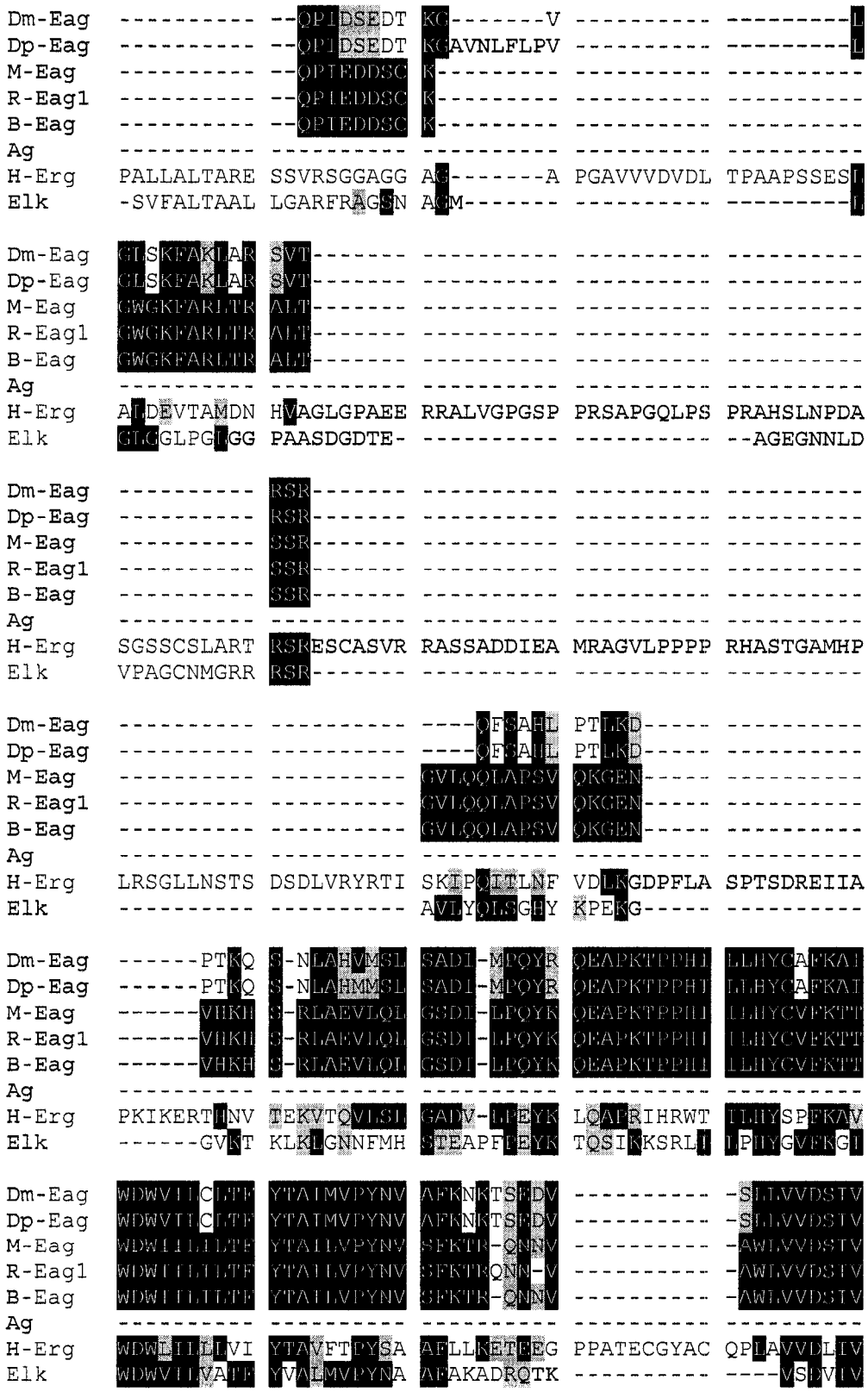
Dm-Eag
Dp-Eag
M-Eag
R-Eag1
B-Eag
Ag
H-Erg
Elk

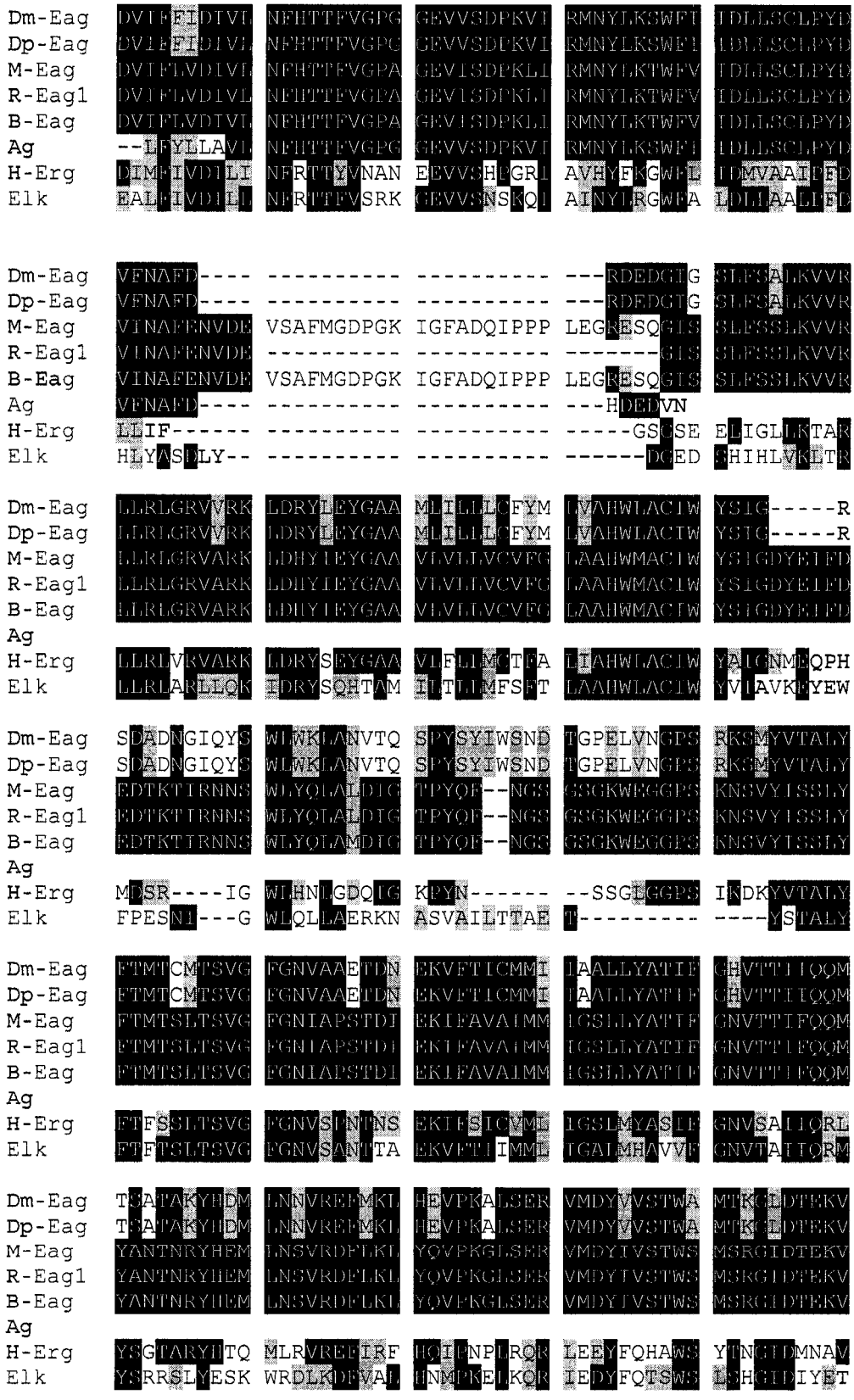
Dm-Eag
Dp-Eag
M-Eag
R-Eag1
B-Eag
Ag
H-Erg
Elk

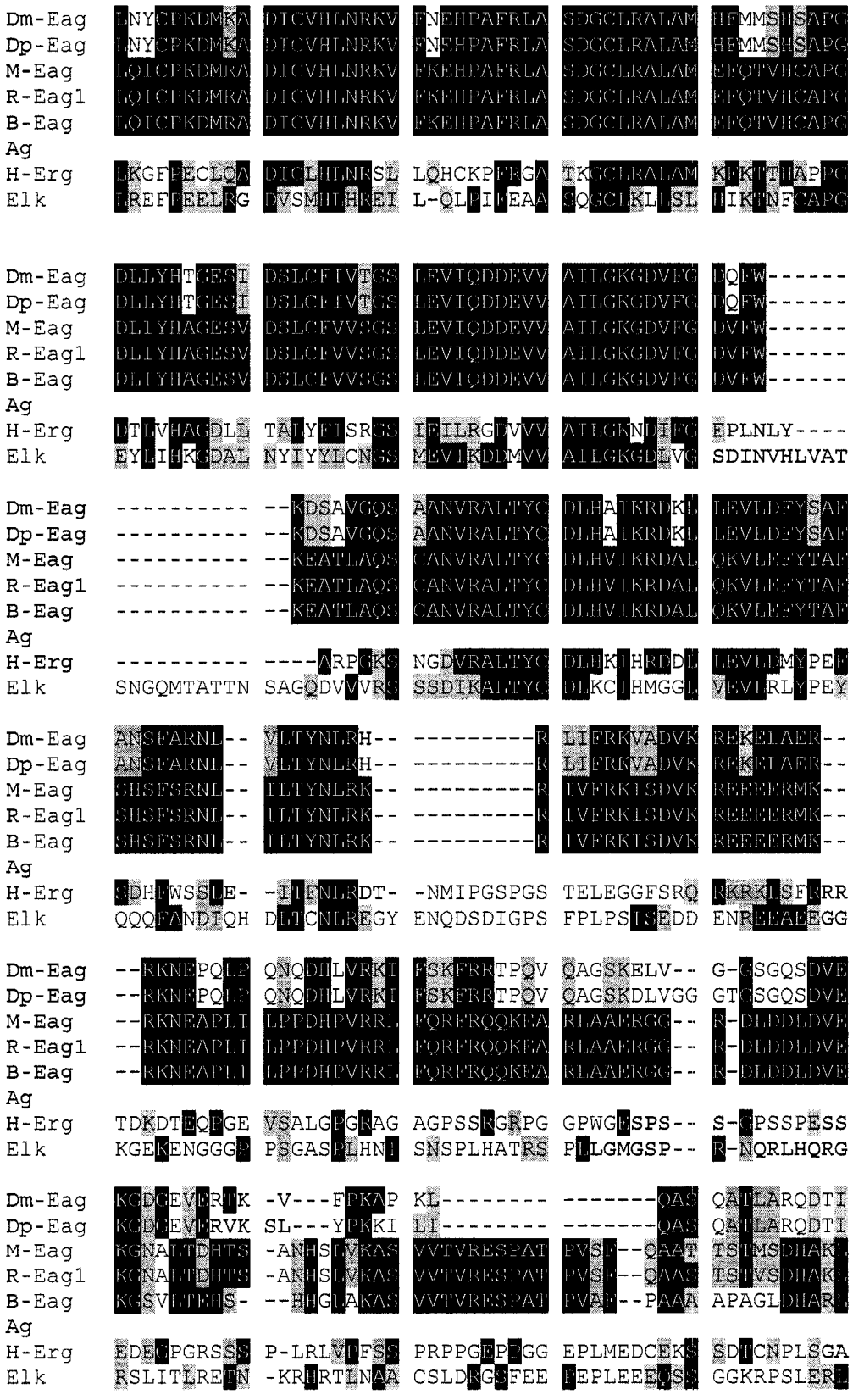
Dm-Eag
Dp-Eag
M-Eag
R-Eag1
B-Eag
Ag
H-Erg
Elk

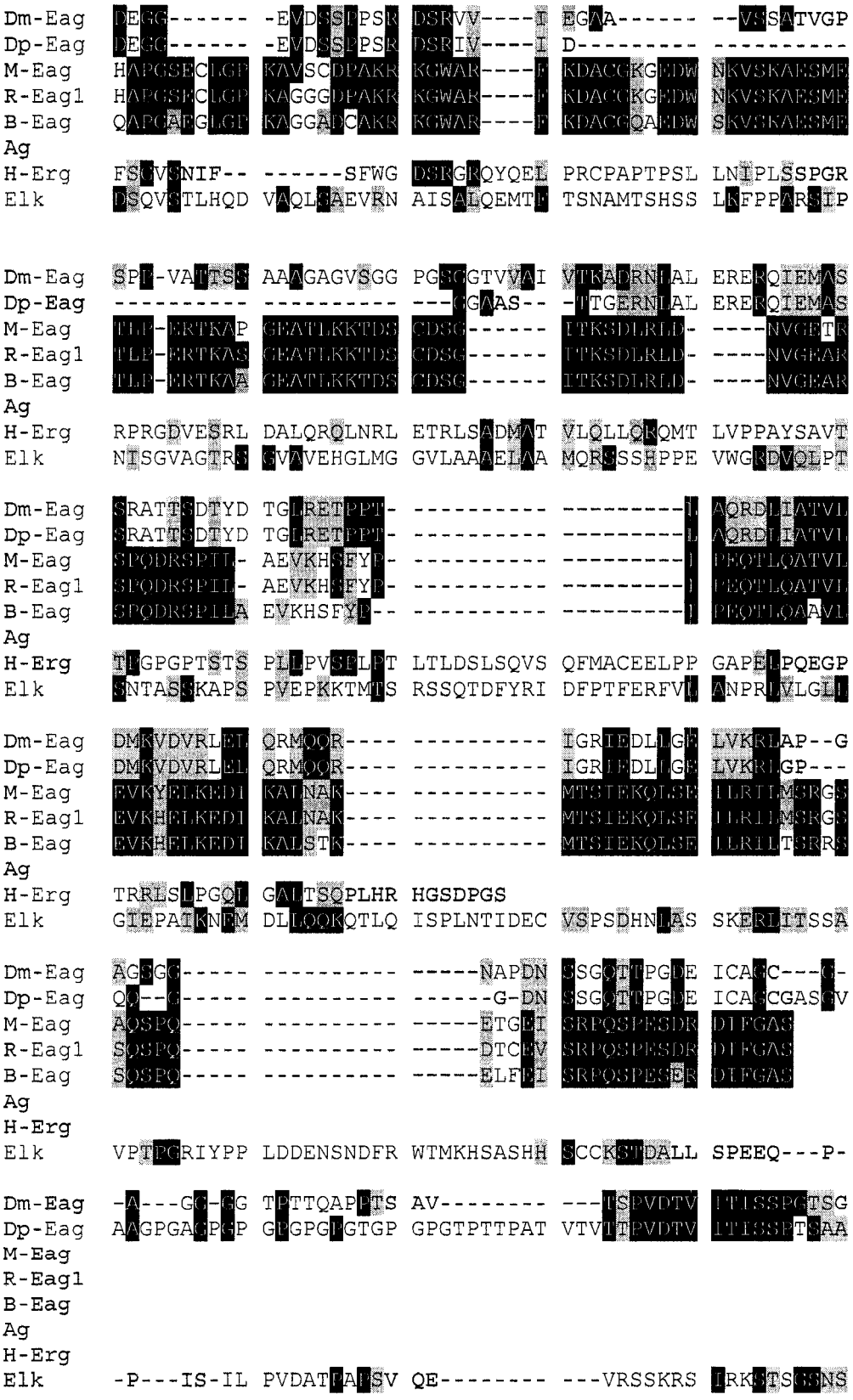
Dm-Eag
Dp-Eag
M-Eag
R-Eag1
B-Eag
Ag
H-Erg
Elk
Dm-Eag
Dp-Eag
M-Eag
R-Eag1
B-Eag
Ag
H-Erg
Elk
Dm-Eag
Dp-Eag
M-Eag
R-Eag1
B-Eag
Ag
H-Erg
Elk
Dm-Eag
Dp-Eag
M-Eag
R-Eag1
B-Eag
Ag
H-Erg
Elk
Dm-Eag
Dp-Eag
M-Eag
R-Eag1
B-Eag
Ag
H-Erg
Elk
Dm-Eag
Dp-Eag
M-Eag
R-Eag1
B-Eag
Ag
H-Erg
Elk

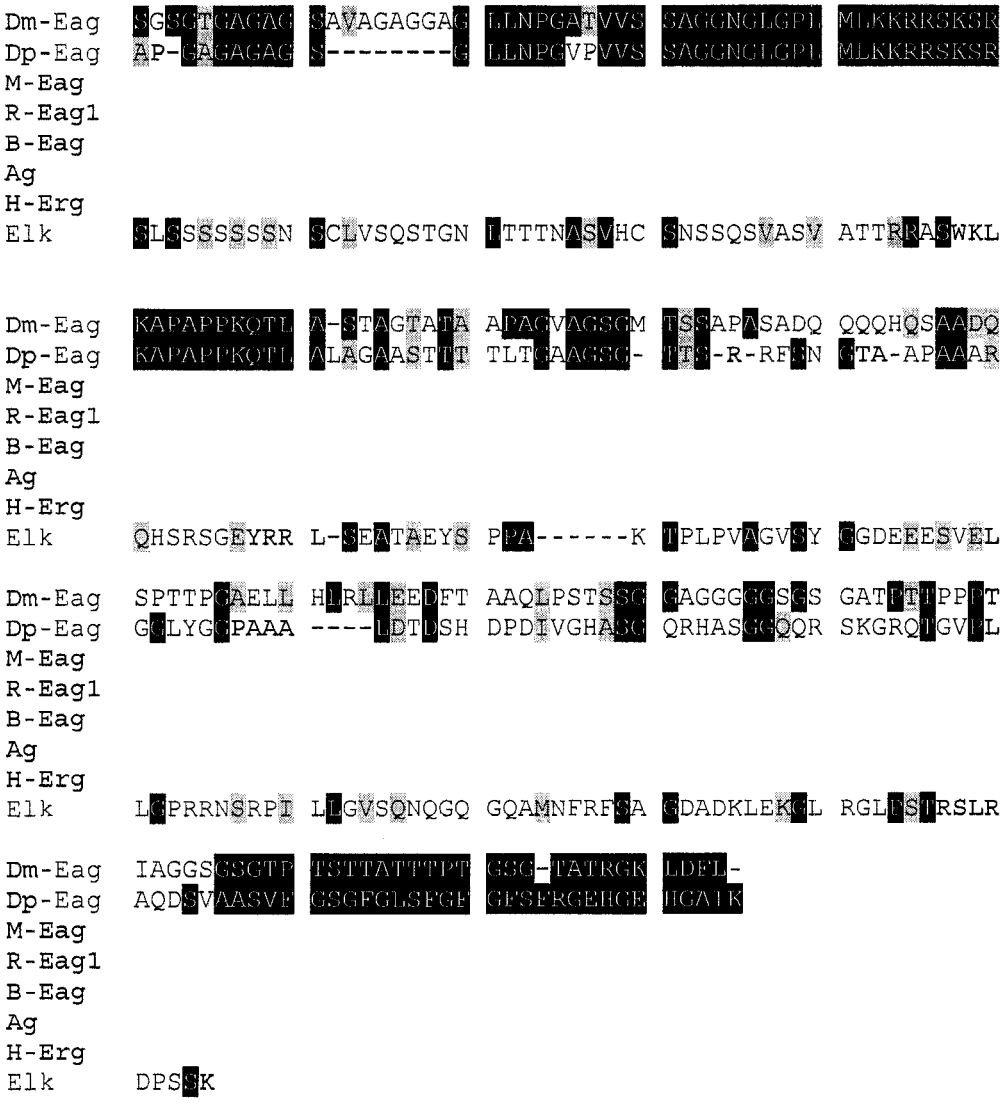
Dm-Eag
Dp-Eag
M-Eag
R-Eag1
B-Eag
Ag
H-Erg
Elk

7.4 Control of perineural glial growth and neuronal excitability: axon-glia signalling

Communication between the axon and the glia (or Schwann cell) has been studied in many systems other than Drosophila, such as squid, frog and crayfish. For example, in response to 100Hz stimulation of the squid giant axon, the surrounding Schwann cell exhibits a hyper-polarization of its membrane potential (VILLEGAS 1974).

Like the Drosophila motor axon, the squid giant axon is glutamatergic. A series of pharmacological experiments identified the mechanism that underlies the hyper-polarization. The principal components are acetylcholine (ACh), a neuropeptide related to VIP and PACAP, octopamine (a stress hormone) and the intracellular messengers IP3, PLC and cAMP, all of which are produced in the Schwann cell (EVANS *et al.* 1992a; EVANS *et al.* 1992b; EVANS *et al.* 1985; EVANS *et al.* 1986; EVANS and VILLEGAS 1988). These molecules act either as internal messengers or are released to feedback onto other Schwann cells further along the axon. The hyper-polarization is associated with an increase in K^+ selectivity by the Schwann cell membrane that most likely results from the activation of K^+ channels (VILLEGAS 1974).

Experiments using crayfish satellite cells, which are analogous to glia or Schwann cells, have shown that membrane hyper-polarization can be achieved by exogenous addition of ACh, carbachol or nicotine (LIEBERMAN *et al.* 1981). These results suggest that the hyper-polarization is mediated by ACh acting upon a nicotinic ACh receptor.

Additional experiments using the crayfish medial giant axon have shown that electrical stimulation of the nerve results in a change in the membrane potential of the periaxonal glia (LIEBERMAN *et al.* 1994). Furthermore, this change in the membrane potential is blocked by a non-NMDA glutamate receptor antagonist and is enhanced by a non-specific glutamate transporter inhibitor indicating that the signal from the axon to the glia is glutamatergic (LIEBERMAN *et al.* 1994).

Electrical stimulation of the Rana pipiens frog motor nerve, or the application of exogenous ACh to the perisynaptic Schwann cell (PSC) results in an increase in intracellular calcium concentration in the Schwann cell (JAHROMI *et al.* 1992). Further analysis in the absence of extracellular Ca^{2+} or presence of extracellular EGTA failed to eliminate the PSC response to ACh suggesting that the calcium is released from intracellular stores (JAHROMI *et al.* 1992). More recently experiments using immunoflouresence to label IP3 receptors and Xestospongin C (an IP3 receptor blocker) have indicated that IP3 is involved in the liberation of the Ca^{2+} in the PSC (CASTONGUAY and ROBITAILLE 2001; CASTONGUAY and ROBITAILLE 2002).

The conclusions about axon-glia communication that can be drawn from these other systems are that the initial signal from the neuron to the glia is glutamatergic; the glia may feedback onto itself using ACh; the release of intracellular Ca^{2+} stores is key; IP3 probably mediates the release of intracellular Ca^{2+}; and that the glial response is also affected by a neuropeptide.

Considering the evidence from these non-Drosophila systems and the intracellular signaling pathways the Stern lab has elucidated in the Drosophila peripheral nerve, I decided to explore the roles of a number of genes in axon-glia signaling, neuronal excitability and perineural glial growth.

To address these questions I created a number of transgenic lines carrying RNAi constructs targeting a number of genes. *Ras1* and *push* were chosen for their proven roles in perineural glial growth (YAGER *et al.* 2001). *VAChT, PLC* and *itpr* were chosen as they have been implicated in axon-glia signalling in other species. *Rap1* was chosen as it is suspected to antagonize *Ras1* in intracellular signalling (HARIHARAN *et al.* 1991). *RyR* was chosen as this is an alternative to IP3 signaling for the release of intracellular Ca^{2+} stores.

7.3.1 RNAi vectors

RNAi vectors were created in a similar manner to that targeting *eag* (described in Chapter 2). Details of the trigger fragment introduced into the *sym-p*UAST vector are listed below.

sym-p*UAST-*itpr.

RNAi trigger fragment targeting *itrp* of 336nt created using forward primer: AGATCTACATAACGAGGTCGAC, reverse: GAATTCAGTGTGCTCAAGAAACC.

sym-p*UAST-*PLC.

RNAi trigger fragment targeting *PLC* of 251nt created using forward primer: GCATAGATCTCGTCAAATTCTCGACAAGGAGG, reverse: GGAATTCGAAAAA-CCTATACGGGCGTGGC.

sym-p*UAST-*Push.

RNAi trigger fragment targeting *push* of 316nt created using forward primer: GCATAGATCTACCATTTCGCTGTCTTCGC, reverse: GAATTCTGCTATCCGTG-GACTTG.

sym-p*UAST-*Ras1.

RNAi trigger fragment of 310nt targeting *Ras1* created using forward primer: TAAGAATTCACCGACCAACACGCTCCCAC, reverse: TAAGAATTCATACATTG-AGACATCCGCC.

sym-p*UAST-*VAChT.

RNAi trigger fragment of 260nt targeting *VAChT* created using forward primer: GGAATTCGTTGACTCTATGTGCGTAT, reverse: GGAATTCCGATATGACGGA-GCTTAGGTCCGAC.

sym-p*UAST-*Rap1.

RNAi trigger fragment of 271nt targeting *Rap1* created using forward primer: ATTTAGAATTCATACCAGCCACATCCCACACAC, reverse: ATTAGATCTTGGG-ATTGACACGACAGTTTAG.

sym-p*UAST-*RyR.

RNAi trigger fragment of 309nt targeting *RyR* created using forward primer: TATTGAATTCTGCCACGACGACGACTTTCTGC, reverse: AAATTAGATCTAGG-CTGCTGCACTTGCGG.

7.3.2 Preliminary data

***itpr* hypomorph.**

To determine if larvae from a hypomorphic allele of *itpr* could affect perineural glial growth, larvae from the hypomorphic line ($itpr^{5616}$) (1.81μm ±0.12), from a line

carrying a rescue construct (*Insp3R Cosmid*) (1.72μm ±0.07), and from a rescue cross (*Insp3R Cosmid;itpr*^{5616}) (1.690μm ±0.08) were measured. All these perineural glial thicknesses are similar to that of the *amn*^{x8} mutant (Figure 7.1). None of these values are statistically significantly different from each other, all of them being at around 1.7μm, which is significantly thicker than wild type (1.3μm).

To determine of the *itpr*^{5616} hypomorph has an effect upon neuronal excitability, the rate of onset of LTF was also determined for *itpr*^{5616}, *Insp3R Cosmid*, and from *Insp3R Cosmid;itpr*^{5616} (Figure 7.2). It appears that both the hypomorphs and the rescue are moderately hypoexcitable, whereas the cosmid alone has a similar excitability to wild-type.

Ras signaling is involved in the regulation of perineural glial growth. To determine if there is a relationship between Ras and IP3, the perineural glial thickness of the genotype *gli*-GAL4/UAS-Ras^{v12}(II); *itpr*^{5616}/*itpr*$^{90B.0}$ was measured and shown to be 2.083μm ±0.135. This may be showing an enhancement of *gli*-GAL4/UAS-Ras^{v12}(II) which has been previously shown to be 1.4μm ±0.069. This value also thicker than that of *itpr*^{5616} which is 1.81μm ±0.12. These enhancements are, however, most likely not meaningful.

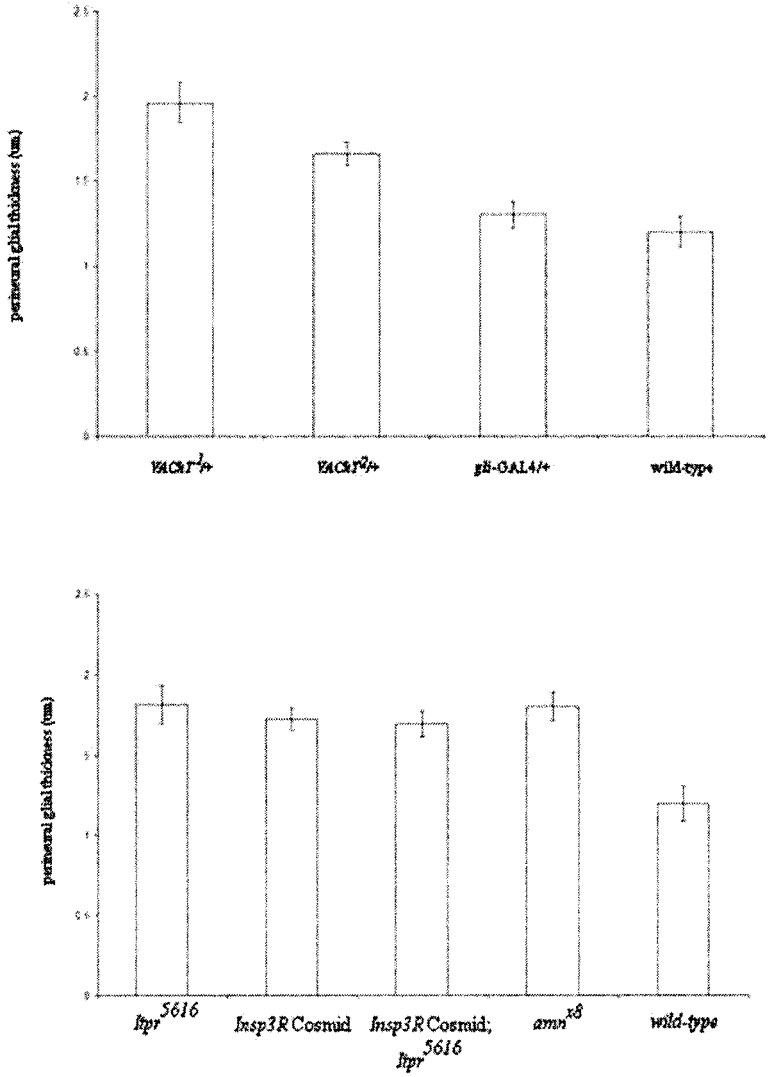

Figure 7.1 Preliminary perineural glial thickness data

Perineural glia thickness data from two *VAChT* hypomorphs an IP3 receptor hypomorph and a rescue of the IP3 hypomorph. Nerves from larvae carrying the IP3-R hypomorphic (*itpr*^{5616}) allele, larvae carrying only the rescue cosmid (*Insp3R Cosmid*), and larvae from a rescue cross (*Insp3R Cosmid ; itpr*^{5616}) were photographed using electron microscopy. *VAChT*^{1}/+ and *VAChT*^{2}/+ heterozygote larvae were also measured. Values for *amn*^{x8}, and *wt* (YAGER *et al.* 2001), *gli*-GAL4/+ (MIKE STERN, UNPUBLISHED DATA).

***VAChT* hypomorphs.**

Two hypomorphic alleles of *VAChT* were acquired from Paul Salvaterra (KITAMOTO *et al.* 2000). Theses are each lethal when homozygous. Similar to the homozygotes, the trans-heterozygote ($VAChT^{1}/VAChT^{2}$) fails to mature to third instar larvae. As such I was only able to collect heterozygote 3rd instar larvae.

To determine if the the *VAChT* alleles affected perineural glial growth we measured the perineural glial thickness in $VAChT^{1}/+$ and $VAChT^{2}/+$. The data collected showed a slight, but not significant, thickening of the perineural glial (Figure 7.1) that was greater in $VAChT^{1}/+$ (1.957μm ±0.117) than $VAChT^{2}/+$ (1.661μm ±0.122). This fits with previous characterizations of these *VAChT* hypomorphs, where $VAChT^{1}$ had a stronger mutant phenotype than $VAChT^{2}$ (KITAMOTO *et al.* 2000).

VAChT RNAi.

Cha-GAL4 is a GAL4 insertion in the *Choline acetyltransferase* gene that is essential for the production of Acetyl Choline (Ach). As *VAChT* is an essential gene, we crossed the *VAChT* RNAi construct to *Cha*-GAL4. The heterozygous combination of the *Cha*-GAL4 driver and the RNAi construct produced adult flies. As *VAChT* is known to be an essential gene, no adult survivors were expected to be seen. As with eag^{RNAi}, it is possible that a single copy of the RNAi transgene is not sufficient to produce a phenotype.

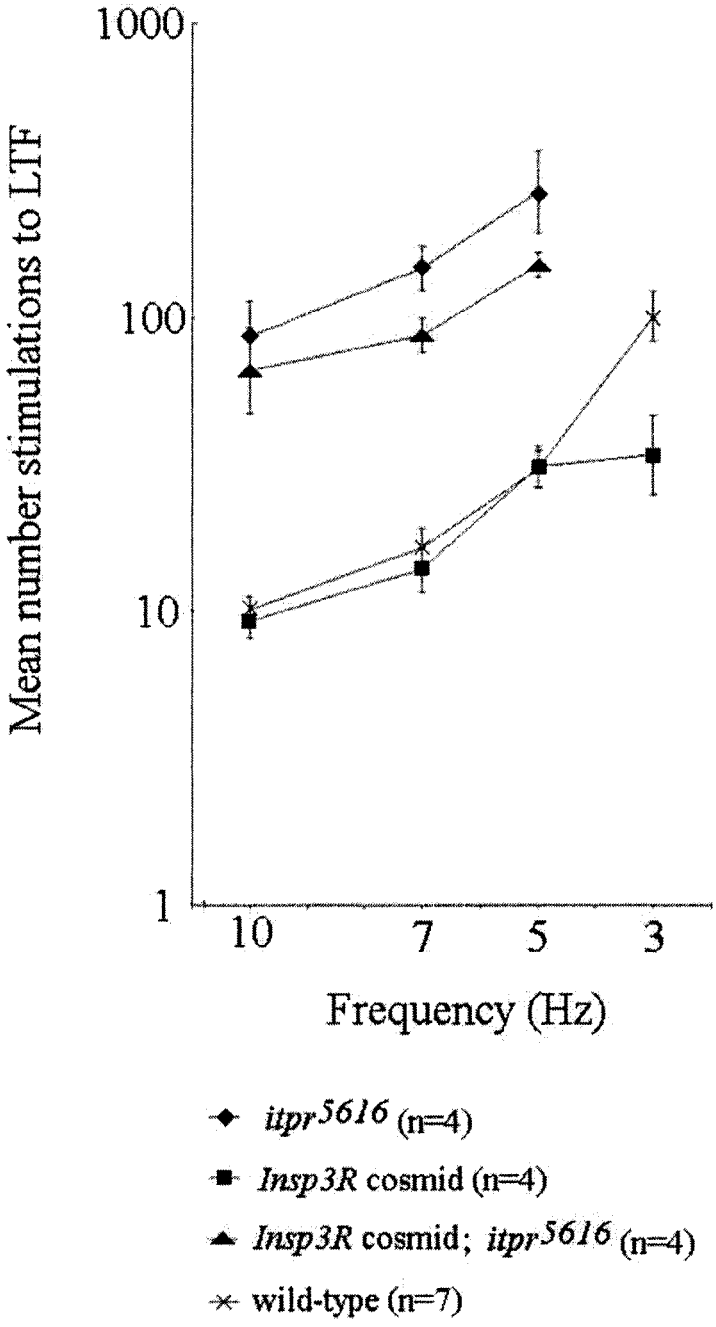

Figure 7.2 *itpr* hypomorphs may confer neuronal hypoexcitability

Average number of stimulations required to elicit the facilitative response at the stimulation frequencies tested (10, 7, 5 and 3 Hz). Values presented as mean ± SEM, n-values as indicated. Wild-type is $Sup^{+}f$, as used in Figure 3.10.

Ras1 RNAi.

To determine if the loss of *Ras1* can affect perineural glial thickness, we tested perineural glial thickness of UAS-$Ras1^{RNAi}$/y; *gli*-GAL4/+ and determined the thickness to be 1.77μm ±0.068. This value is not significantly different from *gli*-GAL4/+. Again, it may be necessary for there to be two copies of the transgene for a *Ras1* loss of function phenotype.

Unexpectedly, F1 flies from the cross UAS-$Ras1^{RNAi}$ x *gli*-GAL4 did not produce an equal number of male and female progeny; there were approximately twice as many females (UAS-$Ras1^{RNAi}$/X; *gli*-GAL4/+) than males (UAS-$Ras1^{RNAi}$/y; *gli*-GAL4/+). This observation suggests that there may be a reduction in viability when the RNAi construct is homozygous. This is not unexpected as null alleles of *Ras1* are lethal, as is gli-GAL4 driven UAS-Ras^{v12} (a constitutively active transgene). An alternative hypothesis is that the effect of the loss of *Ras1* is more profound in males than in females.

UAS-$Ras1^{RNAi}$/y; *gli*-GAL4/+ larvae were also examined for an electrophysiological phenotype; there did not appear to be an LTF phenotype.

PLC RNAi.

To determine if PLC plays a role in the control of perineural glial growth, nerves from larvae of the genotype UAS-PLC^{RNAi}/*gli*-GAL4 were measured. Larvae of the genotype UAS-PLC^{RNAi}/*gli*-GAL4 have a perineural glial thickness of 1.844μm ±0.126.